United States Weather Bureau
Contract No. Cwb-10763

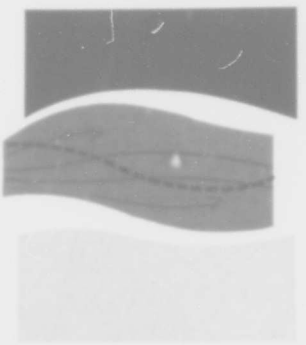

FINAL REPORT

GENERAL CIRCULATION RESEARCH

7462-122
October 1964

Principal Investigators:
BARRY SALTZMAN
M. SANKAR RAO

THE TRAVELERS RESEARCH CENTER, INC.
250 CONSTITUTION PLAZA / HARTFORD, CONNECTICUT

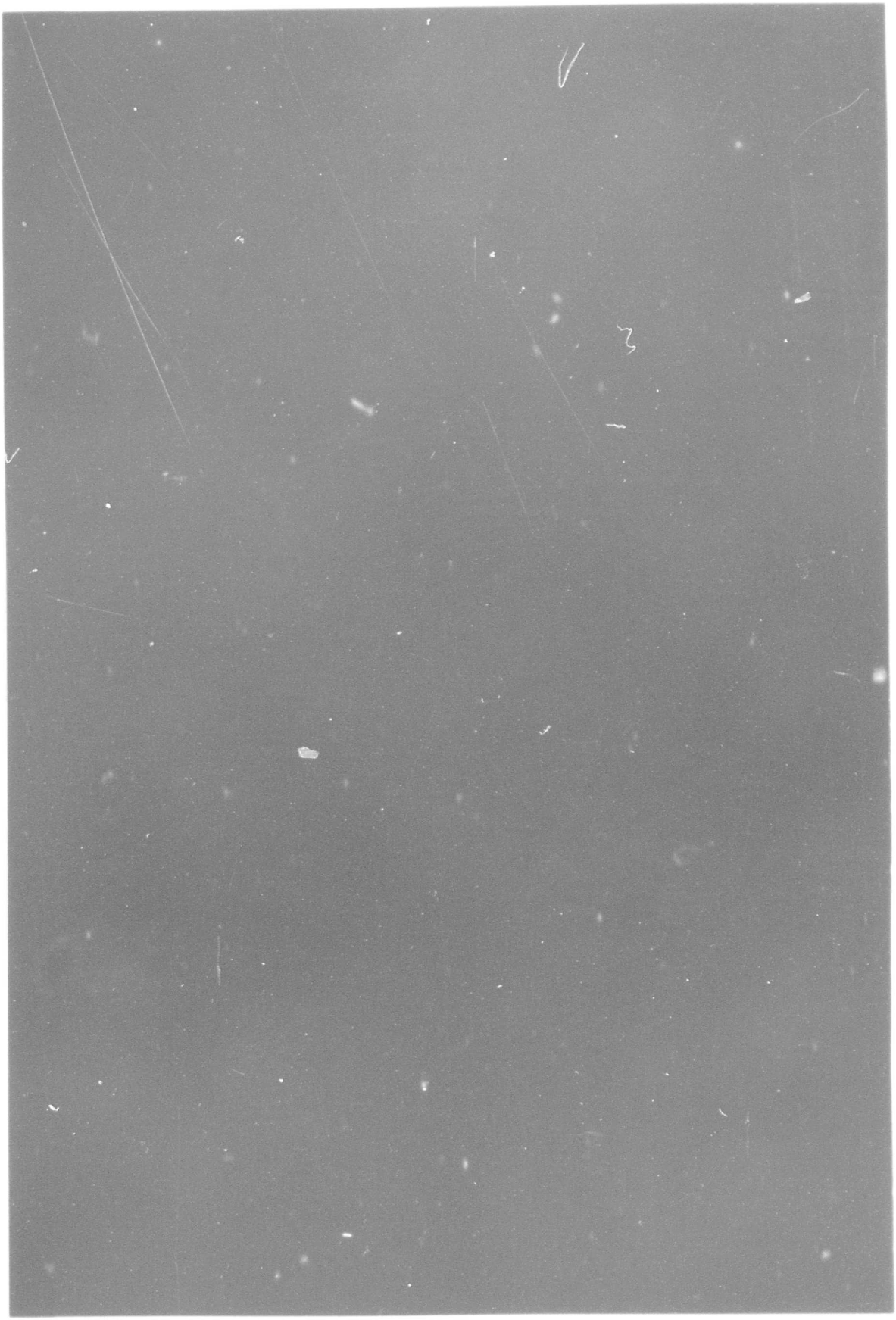

FINAL REPORT

to

THE UNITED STATES DEPARTMENT OF COMMERCE

WEATHER BUREAU

WASHINGTON 25, D. C.

CONTRACT NO. Cwb-10763

(GENERAL CIRCULATION RESEARCH)

Principal Investigators: Barry Saltzman

M. Sankar Rao

October 1964

THE TRAVELERS RESEARCH CENTER, INC.

250 Constitution Plaza Hartford, Connecticut 06103

TABLE OF CONTENTS

LIST OF ILLUSTRATIONS

LIST OF TABLES

INTRODUCTION

This Final Report describes the work completed under Contract Cwb-10763 during the period 1 November 1963 to 31 October 1964.

The results are presented in the form of four papers, the first three of which (A,B, and C) deal with the theory of the time-average (i.e., normal) motions of the atmosphere, and the fourth (D) dealing with the observed mean energetical properties of the 500-mb waves.

In an appendix we include an article dealing with the harmonic representation of surface topography. This article was not written under contract auspices, but is of great relevance to the overall program of the contract research (especially to the first two papers included in this report).

Further work, not completed as yet and hence not reported on here, deals with the reformulation of the problems treated in papers A and B in a more realistic spherical geometry rather than a Cartesian β-plane.

PAPER A

ON THE THEORY OF THE MEAN PERTURBATIONS IN THE ATMOSPHERE

Barry Saltzman

ABSTRACT

A general solution is obtained for forced, stationary, quasi-geostrophic perturbations in an atmosphere having the main zonal-average characteristics of the real troposphere and stratophere. Special solutions for winter conditions along 45° N latitude are obtained for idealized representations of forcing due to internal sources and sinks of heat and due to lower boundary airflow over topography. The results show how the solutions depend on the spatial scale of the disturbances. For example, on the longwave side of a critical vector wave number corresponding to quasi-resonance, the disturbances forced by internal heating tilt eastward with height thereby transporting heat southward, and tend to increase in amplitude above the tropopause into the high stratosphere. The reverse is true for waves smaller than critical. Comparisons with observations suggest that the real atmospheric mean waves are combinations of modes from the two regimes.

1. Introduction

This work is an extension of two previous studies by the writer (1961, 1963) concerning the linear theory of the time-average perturbations in the westerlies, a subject considered earlier by Charney and Eliassen (1949), Smagorinsky (1953), and Gilchrist (1953), for example, and more recently by the Staff Members of the Academia Sinica (1958), Barrett (1961), and Döös (1962), for example. As in the previous studies, we base the theory on a quasi-geostrophic, β-plane representation of the atmosphere and apply it only to winter conditions along 45 deg N latitude. Our aim here is 1) to improve upon the representation of the basic zonal-average state by adopting a more realistic vertical profile of the basic zonal wind and static stability, including a stratosphere, 2) to extend the calculations to a broader spectrum of harmonic components, and 3) to examine the energetical properties of the solutions.

The extension of the calculation to lower wave numbers is made in spite of the realization that there may be a deterioration of the validity of the quasi-geostrophic and β-plane approximations for very long waves (c.f., Burger, 1958; Phillips, 1963). This was done in order to obtain a basis for measuring the importance of removing these restrictive assumptions.

Moreover, we also recognize that the linear equations used here and previously are valid only as a first approximation, and cannot be expected to be capable of accounting for all of the details of the observed mean perturbations, especially in higher latitudes (c.f., Saltzman and Rao, 1963).

2. The Mathematical Model

The linearised potential vorticity equation governing the time-average perturbations of the meridional geostrophic wind speed, can be written as follows for a β - plane with no latitudinal variation of the basic state (c.f., Saltzman 1961),

$$\frac{\partial^2 v_1}{\partial x^{*2}} + \frac{\partial^2 v_1}{\partial y^{*2}} - \frac{f^2 p^2}{R\Gamma_0}\frac{\partial^2 v_1}{\partial p^2} - \frac{f^2}{R}\frac{\partial}{\partial p}\left(\frac{p^2}{\Gamma_0}\right)\frac{\partial v_1}{\partial p} + \left[\frac{\beta}{u_0} + \frac{f^2}{u_0 R}\frac{\partial}{\partial p}\left(\frac{p^2}{\Gamma_0}\frac{\partial u_0}{\partial p}\right)\right] v_1 = \frac{F_1}{u_0} \quad (1)$$

where

x^* = distance eastward

y^* = distance northward

p = pressure

t = time

u = eastward wind speed

v = northward wind speed

$\omega = dp/dt$

T = temperature

$\dot{q}$ = rate of heat addition, per unit mass, due to radiation conduction, water phase changes, and friction

g = acceleration of gravity

R = gas constant for air

C_p = specific heat at constant pressure

f = Coriolis parameter

$\beta = \partial f/\partial y^*$

X = eastward component of viscous force per unit mass

Y = northward component of viscous force per unit mass

$\Gamma = (\partial T/\partial p - RT/c_p p)$ = static stability

$\bar{()} = \Delta t^{-1} \int_0^{\Delta t} () dt$ (time mean over interval or ensemble Δt, such that $\partial \bar{()}/\partial t = 0$)

$()' = () - \bar{()}$ = transient departure from time mean

$()_0 = K^{*-1} \int_0^{K^*} \bar{()} dx^*$ = zonal average of time mean variable

$()_1 = \bar{()} - ()_0$ = departure of time mean variable from zonal average

$F = H + M$

$H = f \partial (Q/\Gamma_0)/\partial p$

$$Q = \left[\frac{\dot{q}}{c_p} - \left(\frac{\partial \overline{u'T'}}{\partial x^*} + \frac{\partial \overline{v'T'}}{\partial y^*} + \frac{\partial \overline{\omega'T'}}{\partial p} + \frac{R}{c_p p} \overline{\omega'T'} \right) \right]$$

$$M = \left\{ \frac{\partial}{\partial x^*} \left[Y - \left(\frac{\partial \overline{u'v'}}{\partial x^*} + \frac{\partial \overline{v'^2}}{\partial y^*} + \frac{\partial \overline{v'\omega'}}{\partial p} \right) \right] + \frac{\partial}{\partial y^*} \left[X - \left(\frac{\partial \overline{u'^2}}{\partial x^*} + \frac{\partial \overline{u'v'}}{\partial y^*} + \frac{\partial \overline{u'\omega'}}{\partial p} \right) \right] \right\}$$

At the lower boundary (which we take as the top of a shallow friction layer, designated by the subscript s) we assume that the mean ω - perturbations can be expressed as the sum of effects due to forced motion over topography and forced vertical motion due to friction (Charney and Eliassen, 1949). Thus, defining h as the height of the ground surface above sea level and C as the lower boundary friction coefficient, we have

$$\omega_{1,s} = -\rho_s g \left[\left(\bar{u} \frac{\partial h}{\partial x^*} + \bar{v} \frac{\partial h}{\partial y^*} \right)_1 + C \left(\frac{\partial v_1}{\partial x^*} - \frac{\partial u_1}{\partial y^*} \right) \right]_s$$

(ρ = density)

which leads to the following form of the thermodynamical energy equation,

$$\frac{u_0 \cos\varphi}{R} \frac{\partial v_1}{\partial p} - \frac{\partial T_0}{\partial y^*} v_1 + \rho_s g \Gamma_0 \left[\left(\bar{u} \frac{\partial h}{\partial x^*} + \bar{v} \frac{\partial h}{\partial y^*} \right) + C \left(\frac{\partial v_1}{\partial x^*} - \frac{\partial u_1}{\partial y^*} \right) \right] + Q_1 = 0 \qquad (2)$$

($p = p_s$)

Although C and ϕ_s are really functions of x^* and y^*, we shall assume the effects of their variability in (2) are small enough that we can adopt some constant average value. Some justification for this is given by Smagorinsky (1953).

At the tropopause (which we designate by the subscript R) we assume σ_1 is continuous—i.e., $(\sigma_1)_{RI} = (\sigma_1)_{RII}$, which I denotes the value on the troposphere side and II the value on the stratosphere side. We can thus write the energy equation governing σ_{1R} in the form,

$$\left(\frac{\partial \sigma_1}{\partial \phi}\right)_I - \left[\frac{1}{\alpha}\left(\frac{1}{u_1}\frac{\partial u_1}{\partial \phi}\right)_{II} + \frac{R(\alpha-1)}{u_0 f \phi a}\frac{\partial T_0}{\partial y^*}\right]\sigma_1 + \frac{R(\alpha-1)}{u_0 f \phi a} Q_1 = 0 \,, \quad (\phi = \phi_R) \qquad (3)$$

where $\alpha = \Gamma_{0II}/\Gamma_{0I}$.

At the "top" of the atmosphere (which we designate by the subscript T), taken to correspond to some arbitrarily small pressure, we require (c.f., Smagorinsky 1953) that

$$\sigma_1 = 0 \,, \quad (\phi = \phi_T) \,. \qquad (4)$$

This upper boundary condition is consistent with the requirement that $\omega_1 \to 0$ as $\phi_T \to 0$ providing $\partial \sigma_1/\partial \phi$ remains finite and $Q_{1T} \to 0$ (c.f., Saltzman 1961, Eq. 26), and is also consistent with the requirement that the system be energetically "closed" at the upper boundary (see Section 5).

We now specify the basic zonal average state to consist of 1) a troposphere ($\phi_S > \phi > \phi_R$) in which the vertical profile of the geostrophic zonal wind is given by

$$u_0(\phi) = a J_0(c\phi^{*}) + b N_0(c\phi^{*}) - \frac{\Gamma_0 R \beta}{f^2 c} \qquad (5)$$

$$(c^2 > 0)$$

where J_0 and N_0 are the zero order Bessel and Neumann functions, a, b and c are constants, and the static stability is given by a constant, $\Gamma_0 = -A_I$, and 2) a stratosphere ($p_R > p > p_T$) in which $u_0(p)$ is a constant, (i.e., $\partial T_0/\partial y^*_{II} = 0$), and the static stability is given by another constant, $\Gamma_{0II} = \alpha\Gamma_{0I} = -A_{II} < -A_I$. With suitably choices of a, b, and c, (5) can give a very good fit to the observed winter profile of u_0 (see Figure 1a) and has the important additional property that it makes the coefficient of the first order term of (1) a constant (c.f., Döös, 1962). The representation of Γ_0 is most valid in the troposphere, and is least valid in the stratosphere where a representation of the form $\Gamma_{0II} = -A/p$ corresponding to isothermal conditions would be better (c.f., e.g., Gates, 1961; Saltzman and Rao, 1963). However, the main feature of the static stability variation with height (i.e., a very stable stratospheric layer overlying a less stable troposphere is adequately represented (see Figure 1b).

If, furthermore, we introduce the coordinate transformations,

$$(x, y) = f(RA_I p_s)^{-\frac{1}{2}} \cdot (x^*, y^*)$$

$$\xi = 2\left(\frac{p}{p_s}\right)^{\frac{1}{2}}$$

where s denotes the value at sea level, we can write the governing equations for our system in the form,

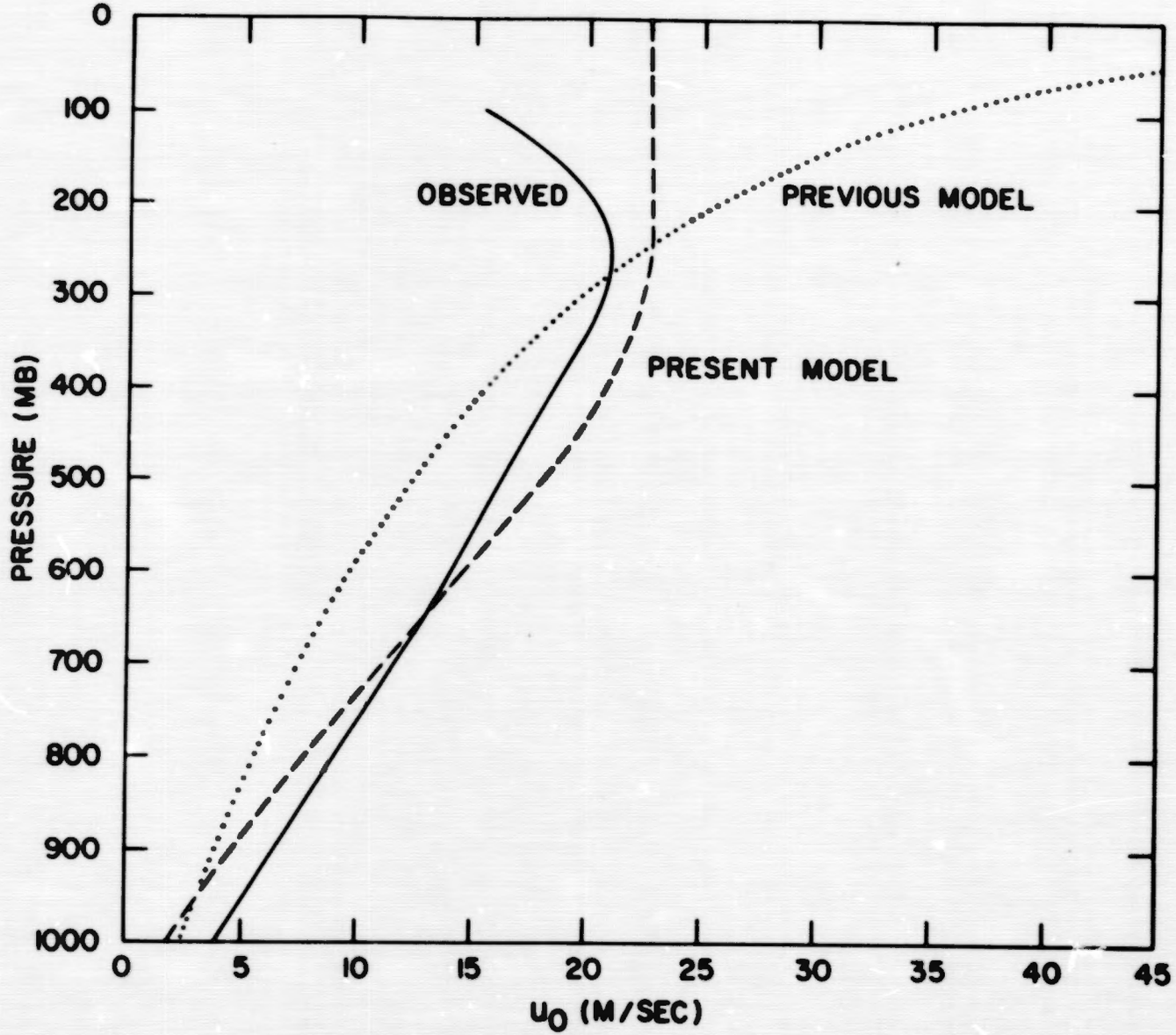

Fig. 1a. Winter profile of u_0 at 45°N used in the present study (dashed line); in the previous study [Saltzman, 1963] (dotted line); and actually observed according to Döös (1962) and Crutcher (1959), (solid line).

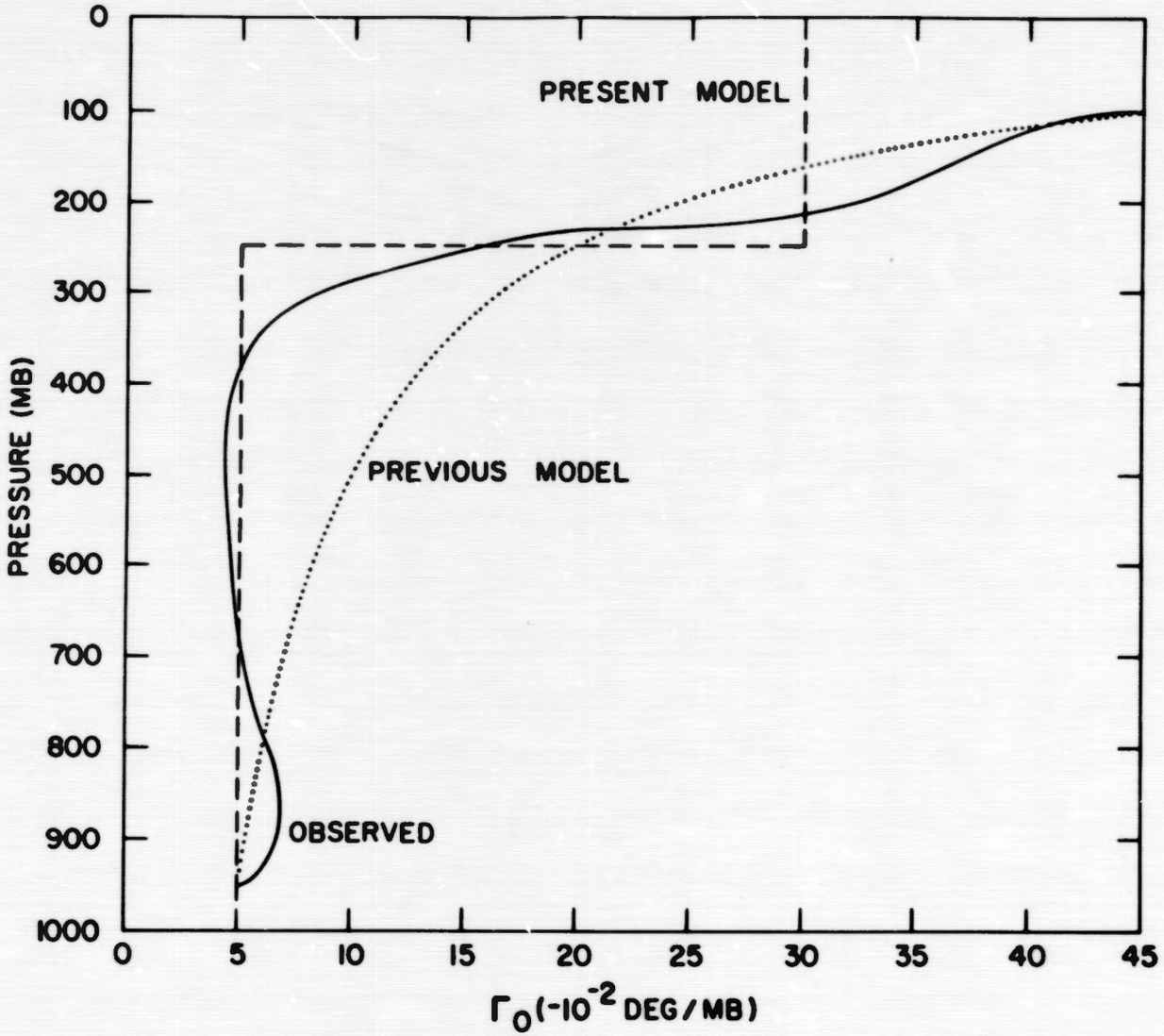

Fig. 1b. Winter profile of Γ_0 at 45°N used in the present study (dashed line); in the previous (1963) study (dotted line); and actually observed according to Gates (1961), (solid line).

$$\frac{\partial^2 v_1}{\partial x^2} + \frac{\partial^2 v_1}{\partial y^2} + \frac{\partial^2 v_1}{\partial \xi^2} + \frac{1}{\xi}\frac{\partial v_1}{\partial \xi} + k_I^2 v_1 = \left(\frac{RA_I p_2}{\xi^2 \mu_0}\right) F_1 \quad , \qquad (6)$$

$$(\xi_s > \xi > \xi_R)$$

$$\alpha\left(\frac{\partial^2 v_1}{\partial x^2} + \frac{\partial^2 v_1}{\partial y^2}\right) + \frac{\partial^2 v_1}{\partial \xi^2} + \frac{1}{\xi}\frac{\partial v_1}{\partial \xi} + k_{II}^2 v_1 = \left(\frac{RA_{II} p_2}{\xi^2 \mu_0}\right) F_1 \quad , \qquad (7)$$

$$(\xi_R > \xi > \xi_T)$$

$$\frac{\partial v_1}{\partial \xi} + k_s v_1 - \lambda\left(\frac{\partial v_1}{\partial x} - \frac{\partial u_1}{\partial y}\right) = -\frac{2R}{\mu_0 \xi \xi} S_1 \quad , \qquad (8)$$

$$(\xi = \xi_s)$$

$$\frac{\partial v_1}{\partial \xi} + \lambda v_1 = -\frac{2R(\alpha-1)}{\mu_{0R} \xi \xi \alpha} Q_1 \quad , \quad (\xi = \xi_R) \qquad (9)$$

$$v_1 = 0 \quad , \quad (\xi = \xi_T) \qquad (10)$$

where

$$K_I^2 = \rho_s c^2 > 0$$

$$K_s^2 = \frac{R A_I \rho_s \beta}{f^2 u_{os}}$$

$$\kappa = -\frac{2R(\partial T_o/\partial y^*)}{u_o f \xi}$$

$$\lambda = \frac{2\rho_s g (A_I R/\rho_s)^{1/2} C}{\xi u_{os}}$$

$$\nu = -\frac{1}{\alpha}\left(\frac{1}{v_1}\frac{\partial v_1}{\partial \xi}\right)_{RII}$$

$$S_1 = S_1^{(h)} + Q_{1s}$$

$$S_1^{(h)} = -\rho_s g f (A_I/R\rho_s)^{\frac{1}{2}}\left(\bar{u}\frac{\partial h}{\partial x} + \bar{v}\frac{\partial h}{\partial y}\right)$$

$$\approx -\rho_s g f (A_I/R\rho_s)^{\frac{1}{2}} u_{os}\frac{\partial h}{\partial x}$$

Notice that the effect of forced airflow over mountains represented by $S_1^{(h)}$ as it appears in the lower boundary condition used here and also previously (1963), is that of an equivalent surface heating. This is therefore the converse of the approach used by Stern and Malkus (1953) in their treatment of the problem of airflow over a heated surface.

3. The Solution

We assume that the variations of the forcing functions F_1 , Q_1 , and S_1 near a given latitude circle can be represented by a double Fourier series over a region formed by the length of the latitude circle and an arbitrary meridional width (let us say, 40 degrees of latitude) centered on the latitude circle. That is,

$$\begin{Bmatrix} F_1 \\ Q_1 \\ S_1 \end{Bmatrix} = \sum_{m=-\infty}^{\infty} \sum_{n=-\infty}^{\infty} \begin{Bmatrix} \mathcal{F}_{m,n} \\ \mathcal{Q}_{m,n} \\ \mathcal{S}_{m,n} \end{Bmatrix} \exp\left[i(k_m x + l_n y)\right] \tag{11}$$

where

$i = \sqrt{-1}$

$k = 2\pi (RA_I \phi_s)^{-1} / 5 K^*$

$l = 2\pi (RA_I \phi_s)^{-1} / 5 L^*$

K^* = length of the fundamental region corresponding roughly to the distance around a latitude circle

L^* = zonal width of the fundamental region

m = wave number in the x-direction

n = wave number in the y-direction

Then we can write the solution of the system (5) - (9) in the form,

$$v_1(x,y,\xi) = \sum_{m=-\infty}^{\infty} \sum_{n=-\infty}^{\infty} V_{m,n}(\xi) \exp\left[i(k_m x + l_n y)\right] \tag{12}$$

where, for the <u>troposphere</u>:

$$V_{m,n}(\xi) = \int_{\xi_s}^{\xi_R} G_{m,n}(\epsilon;\xi)\, \mathcal{F}_{m,n}(\epsilon)\, d\epsilon + I_{m,n}(\xi)\, \mathcal{S}_{m,n}(\xi_s) + J_{m,n}(\xi)\, \mathcal{Q}_{m,n}(\xi_R) , \tag{13}$$

in which G, I, and J are the complex influence functions for the effects of heat and momentum sources in the interior of the troposphere, at the lower boundary, and at the tropopause, respectively. These are given by

$$G_{m,n}(\epsilon;\xi) = -\frac{\pi R A_I p_s \Phi \epsilon}{2 f^2 u_0(\epsilon)} \times \begin{cases} g(\xi;\epsilon) & \epsilon < \xi \\ g(\epsilon;\xi) & \epsilon > \xi \end{cases} \tag{14}$$

$$= G^{(r)}_{m,n} + i\, G^{(i)}_{m,n}$$

$$I_{m,n}(\xi) = -\frac{2R\Phi}{u_{0s} f \xi_s}\left[c_3 \psi_2(\lambda\xi) - c_4 \psi_1(\lambda\xi)\right] \tag{15}$$

$$= I^{(r)}_{m,n} + i\, I^{(i)}_{m,n}$$

$$J_{m,n}(\xi) = \frac{2R\Phi}{u_{0a} f \xi_a}\left[c_2 \psi_1(\lambda\xi) - c_1 \psi_2(\lambda\xi)\right] \tag{16}$$

$$= J^{(r)}_{m,n} + i\, J^{(i)}_{m,n}$$

where

$$g(a;b) = \left[c_3 \psi_2(b) - c_4 \psi_1(b)\right] \times \left[c_2 \psi_1(a) - c_1 \psi_2(a)\right]$$

$$c_1 = \left[\psi_1'(\lambda\xi_s) + (k_s - i\gamma)\psi_1(\lambda\xi_s)\right]$$

$$c_2 = \left[\psi_2'(\lambda\xi_s) + (k_s - i\gamma)\psi_2(\lambda\xi_s)\right]$$

$$c_3 = \left[\psi_1'(\lambda\xi_a) + \nu\,\psi_1(\lambda\xi_a)\right]$$

$$c_4 = \left[\psi_2'(\lambda\xi_a) + \nu\,\psi_2(\lambda\xi_a)\right]$$

$$\psi' = d\psi/d\xi$$

$$\lambda^2 = \left(k^2 - \frac{\Gamma_0}{\Gamma_{0I}}\mu^2\right), \quad \left[\lambda_I^2 = \left(k_I^2 - \mu^2\right), \ \lambda_{II}^2 = \left(k_{II}^2 - \alpha\mu^2\right)\right]$$

$$\mu^2 = \left(k^2 m^2 + l^2 n^2\right)$$

$$\Phi = \left(c_2 c_3 - c_1 c_4\right)^{-1}$$

$$\gamma = \mu^2 \lambda / k m$$

and the functions $\psi_1(\lambda\xi)$ and $\psi_2(\lambda\xi)$ are given by,

$$\psi_1 = J_0(\lambda\xi), \quad \lambda^2 > 0$$

$$\psi_2 = N_0(\lambda\xi), \quad \lambda^2 > 0$$

$$\psi_1 = J_0(i\lambda'\xi), \quad \lambda^2 = (i\lambda')^2 < 0$$

$$\psi_2 = i H_0^{(1)}(i\lambda'\xi), \quad \lambda^2 = (i\lambda')^2 < 0$$

$$\psi_1 = 1, \quad \lambda^2 = 0$$

$$\psi_2 = \log\xi, \quad \lambda^2 = 0$$

where J_0, N_0, and H_0 are the zero order Bessel, Neumann, and Hankel functions, respectively. Note that for the previous model studies by the writer (1963), as well as for the models studied earlier by Smagorinsky (1953) and the Staff Members (1958), the homogeneous solutions, in terms of which the complete solutions were expressed, were the confluent hypergeometric functions rather than Bessel functions.

Assuming all the forcing is confined below the tropopause (i.e., $F_1 = 0$ for $\xi < \xi_R$), we have for the stratosphere:

$$V_{m,n}(\xi) = \chi_{m,n}(\xi) \cdot V_{m,n}(\xi_R), \quad (\xi_R > \xi > \xi_T) \tag{17}$$

where

$$\chi_{m,n}(\xi) = \left[\frac{a\psi_1(\lambda_{II}\xi) + \psi_2(\lambda_{II}\xi)}{a\psi_1(\lambda_{II}\xi_R) + \psi_2(\lambda_{II}\xi_R)}\right], \quad a = -\frac{\psi_2(\lambda_{II}\xi_T)}{\psi_1(\lambda_{II}\xi_T)}.$$

In the sense that both damping and amplification of the mean tropopause perturbations into the stratosphere are permitted, this solution is more general than the stratosphere solution of Smagorinsky (1953) which requires exponential damping in all cases.

Some of the general properties of the solution regarding the positions and slopes of troughs and ridges of the pressure field are readily deducible from the differential equations:

Case I) Forcing due to mountains or equivalent boundary heating ($F_1 = Q_{1R} = 0$, $S_1^{(1)} \neq 0$) - Assuming an harmonic form for v_1 we have by applying (6) at the trough or ridge ($v_1 = 0$),

$$\frac{d}{d\xi}\left(\frac{dv_1}{d\xi}\right) + \frac{1}{\xi}\left(\frac{dv_1}{d\xi}\right) = 0$$

which has the general solution

$$\left(\frac{dv_1}{d\xi}\right) = \frac{A}{\xi} \quad , \quad (A \text{ is a constant}) .$$

In order to satisfy the tropopause condition (9), for $Q_{1R} = 0$, we must set $A = 0$ which means that $dv_1/d\xi = 0$ for all ξ along a trough or ridge line. Thus we conclude that in this model <u>trough and ridge lines associated with a boundary-induced perturbation of a given wave number has no slope and height.</u>

Furthermore, at the intersection of a trough or ridge with the lower boundary, we have from (8)

$$\kappa\left(\frac{\partial v_1}{\partial x} - \frac{\partial u_1}{\partial y}\right) = \frac{2RS_1}{u_{0.6}\, \xi_6} .$$

Thus, in the case of a pure mountain effect, for example, we have the approximate relation

$$C\left(\frac{\partial v_1}{\partial x} - \frac{\partial u_1}{\partial y}\right) \approx -u_{0s}\frac{\partial h}{\partial x}$$

which implies that <u>the center of cyclonic vorticity must be on the downslope (heated) side of the mountain and the center of anticyclonic vorticity on the upslope (cooled) side</u>. In the absence of friction (i.e., $C = 0$) we would have $\partial h/\partial x = 0$ at $v_1 = 0$, which would mean that troughs and ridges coincide with the valleys and peaks of the topographic harmonics, (c.f., Barrett, 1961).

Case II) Forcing due to internal sources of heat and momentum ($F_1 \neq 0, S_1 = 0$) - For the intersection of a trough or ridge line with the lower boundary in this case, we can write (8) in the form

$$\frac{\partial v_1}{\partial \xi} = \lambda\left(\frac{\partial v_1}{\partial x} - \frac{\partial u_1}{\partial y}\right) ,$$

which means

$$\frac{\partial v_1}{\partial \xi} \begin{cases} > 0 & \text{for a trough} \\ < 0 & \text{for a ridge} \end{cases}$$

since $\lambda > 0$. Thus, <u>at the lower boundary all troughs and ridges induced by internal sources of heat and momentum must tilt EASTWARD with height.</u> In the absence of the surface friction ($C = 0$), we have $\lambda = 0$ and hence $\partial v_1/\partial \xi = 0$ which would imply no tilt of the troughs and ridges with height at the lower boundary. From (13) and (14) we can show that in the absence of friction we

have $q^{(i)} = 0$ and, hence, the troughs and ridges would continue to show no tilt with height throughout the entire atmosphere if the vertical model surfaces of the forcing function have no tilt with height (c.f., Smagorinsky, 1953).

As can be seen in the following section (and also in the previous calculations by the writer, 1963), when friction is included, the slopes of the troughs and ridges some distance above the lower boundary display systematic variations depending on the wave number of the perturbation. These appear to be in accord with the results of Gilchrist (1953).

From (3) or (9), we can also deduce some of the properties which the solution must display at the tropopause. If, for example, $Q_{1R} = 0$ we must have $\frac{\partial v_1}{\partial p} = 0$ at a trough or ridge, which means that the trough and ridge lines are vertical. More generally, we must have at all points along the tropopause,

$$\left(\frac{\partial v_1}{\partial p}\right)_{RT} = \alpha \left(\frac{\partial v_1}{\partial p}\right)_{RI}$$

or

$$\left(\frac{\partial T_1}{\partial x}\right)_{RT} = \alpha \left(\frac{\partial T_1}{\partial x}\right)_{RI}$$

which implies an increase of the amplitude of the mean temperature waves as we pass from the troposphere side to the stratosphere side.

4. Special Solutions Corresponding to Winter Normal Conditions at 45°N Latitude

a) Parameters - The following constants defining the physical system are chosen,

$K^* = 3 \times 10^9$ cm

$L^* = 4.5 \times 10^8$ cm

$f = 10^{-4}$ sec^{-1}

$\beta = 1.7 \times 10^{-13}$ cm^{-1} sec^{-1}

$p_s = 1000$ mb

$\xi_3 = 1.8974$ (900 mb)

$\xi_R = 1.0000$ (250 mb)

$\varrho_s = 1.2 \times 10^{-3}$ gm cm^{-3}

$C = 1.6 \times 10^4$ cm

and the following constants are taken to describe the mean zonal state,

$a = 0$

$b = 33$ m sec^{-1}

$c = 0.067$ mb$^{-\frac{1}{2}}$

$A_2 = 5 \times 10^{-2}$ deg mb^{-1}

$A_R = 3 \times 10^{-1}$ deg mb^{-1} $(\alpha = 6)$

$U_{oS}(45) = 4.68$ m sec^{-1}

The profiles of $U_o(p)$ and $\Gamma_o(p)$ implied by these constants are shown in Figure 1a and 1b along with the profiles used in the previous study (Saltzman, 1963) and the observed January normal values at 45°N.

Forcing due to two physical effects will be considered: 1) lower boundary heating and cooling due to adiabatic airflow over topography and 2) internal

heating and cooling with an assumed maximum near 700 mb due to a combination of diabatic effects and transient eddy heat fluxes. From previous studies by the writer (1962, 1963) it appears that forcing due to internal sources of momentum, measured by M_1, is smaller than the above effects, but perhaps is not unimportant if one wishes to account for a small residual percentage of the total variance of the mean map. (Better determinations of M_1 should be possible now with the use of data presented by Crutcher, 1959.)

b) Influence functions and resonance - Before discussing these forcing functions, let us first consider the influence functions $I_{m,n}$, $J_{m,n}$, and $G_{m,n}$, and, also, the quantity $\chi_{m,n}$ which represents the magnification factor for the amplitude of the perturbations above the tropopause. These quantities depend only on the wave number and the physical constants given above.

In Table 1 we present some of the derived parameters which depend on wave number, for $m = 1$ through 6 and $n = 0$ and 1, (i.e., for twelve vector wave numbers, measured by μ^2) and in Figure 2 we show the stratosphere amplitude function $\chi_{m,n}$ for these same wave numbers. We can see from this figure that only the perturbations having the lowest vector wave numbers can amplify above the tropopause in this model. This seems to be in agreement with observations (c.f., Arctic Meteorology Research Group, 1963).

The influence functions $I\ (= I^{(r)} + i\, I^{(i)})$, $J\ (= J^{(r)} + i\, J^{(i)})$, and $G\ (= G^{(r)} + i\, G^{(i)})$ from which one can compute the troposphere solution, given the forcing functions, are tabulated in Tables 2 and 3 at every 100 mb although actual calculations were made at every 50 mb. In the case of G tabulations for only four reference levels (900, 700, 500, and 300 mb) are given although actual calculations were made for every 50 mb between 900 and 250 mb.

Table 1. Parameters dependent on wave number.

m	n	μ^2	Λ_I^2	Λ_{II}^2	γ	r	$\xi^{(r)}$	$\xi^{(i)}$
1	0	0.0630	4.4261	6.1663	0.1273	0.5011	0.5463	0.0061
2	0	0.2518	4.2372	5.0332	0.2547	0.3775	0.6272	0.0117
3	0	0.5666	3.9225	3.1447	0.3820	0.1542	0.8811	0.0102
4	0	1.0072	3.4818	0.5008	0.5093	-0.0394	1.8466	-0.1117
5	0	1.5738	2.9153	- 2.8985	0.6368	-0.0478	-0.6451	-10.9261
6	0	2.6620	2.2228	- 7.0532	0.8975	-0.3600	-0.7300	- 0.0700
1	1	2.8606	1.6285	-10.6193	5.7863	-0.4533	-0.1785	- 0.2153
2	1	3.0494	1.4396	-11.7524	3.0842	-0.4812	-0.2773	- 0.1702
3	1	3.3642	1.1249	-13.6409	2.2683	-0.5252	-0.2643	- 0.1122
4	1	3.8048	0.6842	-16.2848	1.9241	-0.5828	-0.2199	- 0.0741
5	1	4.3714	0.1177	-19.6841	1.7685	-0.6502	-0.1735	- 0.0505
6	1	5.0638	-0.5748	-23.8388	1.7072	-0.7252	—	—

Table 2. Influence functions, $I_{m,n}$ and $J_{m,n}$ in units of 10^{4} cm deg^{-1}.

$I^{(r)}$ (p)

p(mb) (m,n)	(1,0)	(2,0)	(3,0)	(4,0)	(5,0)	(6,0)	(1,1)	(2,1)	(3,1)	(4,1)	(5,1)
300	-2,103	-2,445	-3,513	-7,511	2,633	3,074	760	1,184	1,134	950	757
400	-1,682	-2,017	-3,049	-6,826	2,437	3,038	773	1,215	1,181	1,008	821
500	-1,188	-1,492	-2,421	-5,761	2,126	2,860	755	1,200	1,187	1,037	869
600	- 688	- 948	-1,733	-4,524	1,758	2,597	718	1,156	1,168	1,048	906
700	- 217	- 425	-1,047	-3,235	1,368	2,287	669	1,094	1,131	1,046	936
800	204	53	- 396	-1,966	976	1,950	611	1,018	1,083	1,035	960
900	565	472	1,967	- 765	597	1,601	549	935	1,025	1,017	980

$I^{(1)}$ (p)

300	- 23	- 45	- 41	454	44,587	721	916	727	481	320	220
400	- 19	- 38	- 35	413	41,269	712	932	746	501	340	239
500	- 13	- 28	- 28	349	36.000	670	911	737	504	350	253
600	- 8	- 18	- 20	274	29,776	609	866	710	496	353	263
700	- 2	- 8	- 12	196	23,168	536	806	671	480	353	272
800	2	1	- 5	119	16,537	457	737	625	459	349	279
900	6	9	2	46	10,118	375	662	574	435	343	285

$J^{(r)}$ (p)

300	-1,269	-1,519	-2,279	-5,186	5,702	2,687	1,471	1,456	1,295	1,104	930
400	-1,334	-1,567	-2,286	-5,015	4,975	2,363	1,285	1,284	1,058	883	723
500	-1,252	-1,457	-2,091	-4,492	4,086	1,992	954	969	848	697	560
600	-1,085	-1,254	-1,783	-3,779	3,141	1,609	720	751	658	537	425
700	- 869	-1,001	-1,414	-2,973	2,200	1,229	505	55[illegible]	486	395	311
800	- 631	- 725	-1,020	-2,136	1,298	863	307	363	330	269	211
900	- 387	- 445	- 625	-1,310	457	518	127	197	187	156	123

$J^{(1)}$ (p)

300	16	43	130	778	34,147	233	211	153	88	49	28
400	13	35	113	707	31,605	230	215	157	92	52	30
500	9	26	89	596	27,570	217	210	155	92	54	32
600	5	17	64	468	22,804	197	200	149	91	54	33
700	2	7	39	335	17,743	173	186	141	88	54	34
800	- 2	- 1	15	204	12,665	148	170	132	84	53	35
900	- 4	- 8	- 73	79	7,749	121	153	121	80	53	36

Table 3. Influence functions, $G_{m,n}$, in units of 10^{10} cm sec.

$G^{(r)}$ (p ; 900 mb)

p(mb) (m,n)	(1,0)	(2,0)	(3,0)	(4,0)	(5,0)	(6,0)	(1,1)	(2,1)	(3,1)	(4,1)	(5,1)
300	- 119	- 139	- 200	- 427	150	175	43	67	64	54	43
400	- 119	- 143	- 216	- 484	173	215	54	86	84	71	58
500	- 110	- 138	- 223	- 532	196	264	70	111	110	96	80
600	- 85	- 117	- 215	- 561	218	322	89	143	145	130	112
700	- 38	- 75	- 185	- 572	242	405	118	193	200	185	166
800	55	14	- 107	- 530	263	526	165	275	292	279	259
900	268	224	93	- 363	283	759	260	443	486	482	465

$G^{(i)}$ (p ; 900 mb)

300	- 1	- 3	- 2	25	2,532	40	52	41	27	18	12
400	- 1	- 3	- 2	29	2,927	50	66	52	35	24	16
500	- 1	- 3	- 3	32	3,321	61	84	68	46	32	23
600	- 1	- 2	- 2	33	3,689	75	107	88	61	43	32
700	0	- 1	- 2	34	4,098	94	142	118	84	62	48
800	1	0	- 1	32	4,462	123	198	168	124	94	75
900	3	4	1	22	4,798	178	314	272	206	162	135

$G^{(r)}$ (p ; 700 mb)

300	- 268	- 313	- 451	- 969	719	414	172	188	167	137	109
400	- 268	- 322	- 489	-1,099	831	511	219	241	217	181	147
500	- 246	- 310	- 505	-1,207	943	626	278	310	284	243	203
600	- 191	- 264	- 486	-1,273	1,047	764	355	401	375	329	284
700	- 86	- 169	- 419	-1,299	1,163	960	472	542	519	449	418
800	- 96	- 147	- 461	-1,424	1,047	1,029	437	549	537	487	434
900	- 103	- 202	- 496	-1,534	649	1,085	317	519	537	496	444

$G^{(i)}$ (p ; 700 mb)

300	1	2	12	109	5,799	58	63	48	30	18	11
400	1	2	13	123	6,702	72	80	61	39	24	16
500	0	2	13	136	7,606	88	10	79	51	33	22
600	0	2	13	143	8,448	107	13	102	67	45	31
700	0	1	11	146	9,383	135	17	139	93	64	45
800	0	0	6	135	10,217	176	24	197	136	96	71
900	- 1	- 4	- 5	92	10,988	254	38	318	227	167	12

Table 3. Influence functions, $G_{m,n}$, in units of 10^{10} cm sec (Continued).

$G^{(r)}$ (p ; 500 mb)

p(mb) (m,n)	(1,0)	(2,0)	(3,0)	(4,0)	(5,0)	(6,0)	(1,1)	(2,1)	(3,1)	(4,1)	(5,1)
300	- 386	- 455	- 668	-1,464	1,335	672	325	331	291	241	196
400	- 386	- 468	- 724	-1,661	1,543	829	413	425	379	320	265
500	- 354	- 451	- 748	-1,824	1,742	1,015	525	546	495	428	365
600	- 412	- 522	- 856	-2,060	1,808	1,101	532	568	516	442	372
700	- 471	- 594	- 969	-2,314	1,808	1,201	533	594	544	465	388
800	- 522	- 656	-1,066	-2,536	1,627	1,286	494	602	563	483	403
900	- 564	- 708	-1,148	-2,733	1,008	1,356	358	569	563	492	412

$G^{(1)}$ (p ; 500 mb)

300	3	- 8	28	194	9,011	73	71	53	31	18	11
400	3	8	30	220	10,414	90	91	67	41	24	15
500	3	8	32	242	11,819	110	115	87	53	32	20
600	2	7	30	255	13,127	134	145	112	71	44	28
700	0	4	26	260	14,581	169	196	152	98	63	42
800	- 1	- 1	15	241	15,876	220	273	216	143	96	66
900	- 6	- 1	- 13	165	17,075	318	431	349	239	165	119

$G^{(r)}$ (p ; 300 mb)

300	- 391	- 474	- 728	-1,689	1,864	906	501	498	445	382	325
400	- 513	- 611	- 911	-2,040	2,030	995	513	514	454	382	315
500	- 627	- 739	-1,085	-2,378	2,170	1,091	528	538	473	392	318
600	- 730	- 854	-1,242	-2,686	2,239	1,183	536	561	493	405	324
700	- 834	- 974	-1,406	-3,017	2,239	1,291	536	586	520	426	338
800	- 924	-1,075	-1,547	-3,306	2,015	1,383	497	594	538	443	351
900	- 997	-1,160	-1,666	-3,562	1,249	1,458	360	561	538	451	359

$G^{(1)}$ (p ; 300 mb)

300	5	13	41	253	11,161	78	72	52	30	17	9
400	5	13	44	287	12,898	97	91	67	39	22	13
500	4	13	46	315	14,639	118	116	86	51	30	18
600	3	11	44	332	16,258	144	148	111	67	40	25
700	1	7	38	339	18,059	182	197	150	94	58	37
800	- 2	- 1	22	315	19,663	236	275	213	137	88	58
900	- 11	- 21	- 19	215	21,148	341	434	344	228	151	104

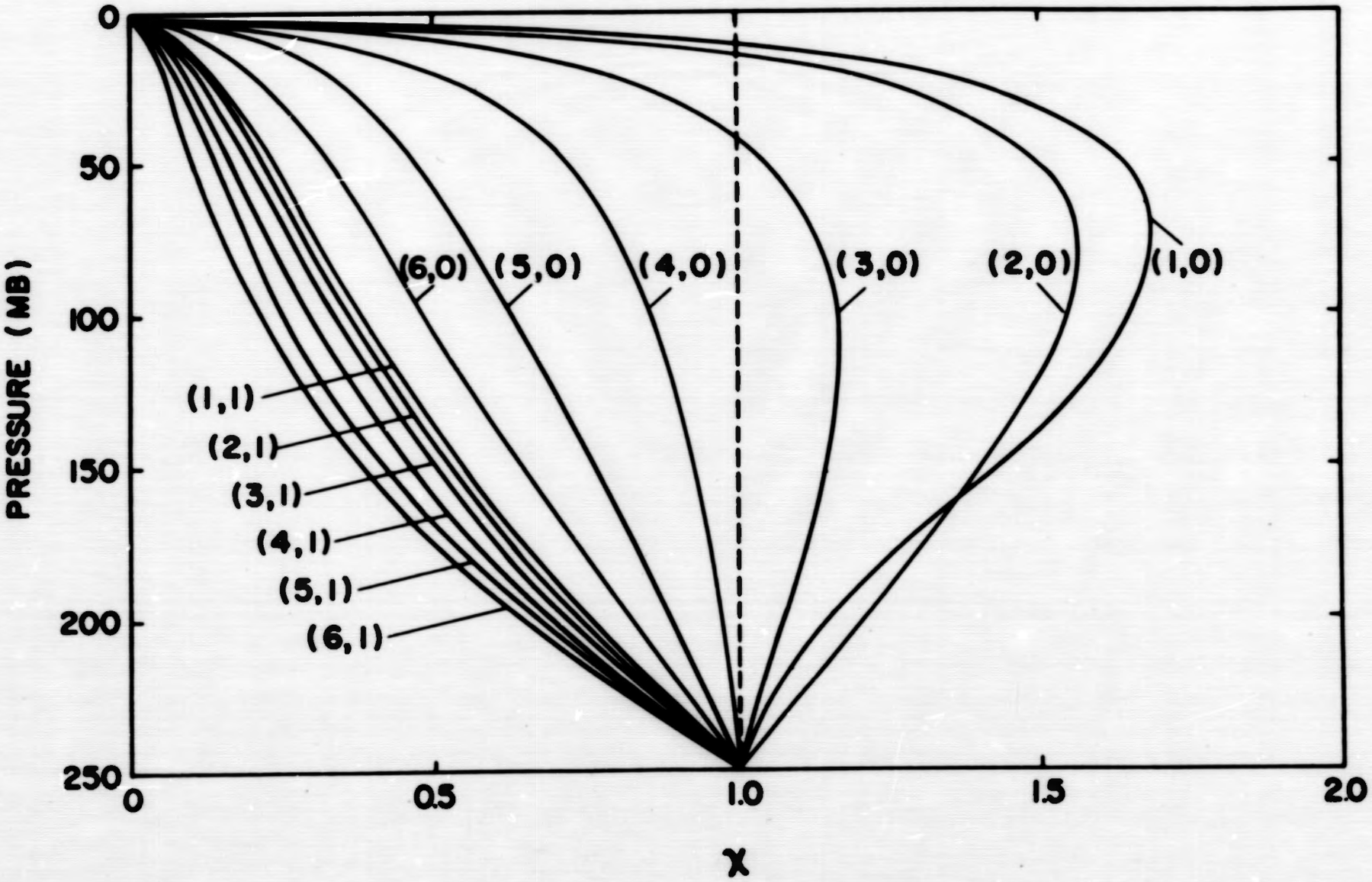

Fig. 2. Stratospheric amplification factor, $x_{m,n}$.

An obvious feature of these tabulated influence functions is the marked increase in magnitude, and the reversal of signs, in the vicinity of wave number (5,0), which imply high amplitude responses and changes of phase of the perturbations near this wave number. This is a reflection of the fact that the vector wave number $\mu^2_{5,0}$ is very close to the "quasi-resonant" vector wave number for the model treated (c.f., Gilchrist, 1953; Smagorinsky, 1953). The exact quasi-resonant vector wave number, which we call $\mu^2_{m^*,n^*}$ $(= k m^{*2} + l n^{*2})$ satisfies the condition

$$C_2^{(n)} C_3 - C_1^{(n)} C_4 = 0 \tag{18}$$

which in the absence of surface friction ($C=0$) would imply that $\Phi^{(n)}_{m^*,n^*}$ (and also $I^{(n)}_{m^*,n^*}$, $J^{(n)}_{m^*,n^*}$, and $G^{(n)}_{m^*,n^*}$) approaches infinity and $\Phi^{(i)}_{m^*,n^*}$ (and also, $I^{(i)}_{m^*,n^*}$, $J^{(i)}_{m^*,n^*}$, and $G^{(i)}_{m^*,n^*}$) equals zero. Hence, the responses would be of infinite amplitude. In the presence of surface friction, however, the condition (18) implies that $\Phi^{(n)}_{m^*,n^*}$ (and also $I^{(n)}_{m^*,n^*}$, $J^{(n)}_{m^*,n^*}$, and $G^{(n)}_{m^*,n^*}$) equals zero and $\Phi^{(i)}_{m^*,n^*}$ (and also $I^{(i)}_{m^*,n^*}$, $J^{(i)}_{m^*,n^*}$, and $G^{(i)}_{m^*,n^*}$) is a large but finite number. Thus, in our frictional case, internal sources and sinks of heat and momentum of scale (m^*, n^*) having no tilt with height will induce large amplitude perturbations also having no tilt with height.

One is tempted to speculate that if there happened to be some forcing on a scale near $\mu^2_{m^*,n^*}$ a very high amplitude response of the mean meteorological variables would be induced. In fact, we actually do observe a response on the scale $m = 5$ which is perhaps greater than might have been expected (c.f., Saltzman and Peixoto, 1957). For two main reasons, however, we must be cautious about discussing solutions near the quasi-resonant point. The first is that a very

high amplitude response would be inconsistent with the hypothesis of small perturbations—i.e., the appearance of strong non-linear effects may invalidate the theory near (m^2, ω^2). The second is that even if the solutions near (m^2, ω^2) are roughly correct, they are so sensitive to the choice of parameters that we cannot be sure of their correspondence to real atmosphere conditions. Needless to say, these questions concerning resonance can have important implications for the subject of global modification of climate.

c) Response to Topography - Let us represent the topographic surface in the neighborhood of 45°N by a double Fourier expansion of the form

$$
\begin{aligned}
h(x,y) &= \sum_{m=-\infty}^{\infty} \sum_{n=-\infty}^{\infty} E_{m,n} \exp\left[i(mkx + nly)\right] \\
&= \varepsilon_{0,0}^{(a)} + \sum_{n=1}^{\infty} \left[2\varepsilon_{0,n}^{(a)} \cos nly + 2\varepsilon_{0,n}^{(i)} \sin nly\right] \\
&\quad + \sum_{m=1}^{\infty} \frac{C_{m,0}}{2} \cos m(kx - \epsilon_{m,0}) \\
&\quad + \sum_{m=1}^{\infty} \sum_{n=1}^{\infty} \left[C_{m,n} \cos m(kx - \epsilon_{m,n}) \cos nly + D_{m,n} \cos m(kx - \theta_{m,n}) \sin nly\right.
\end{aligned}
\tag{19}
$$

where

$$
\begin{aligned}
E_{m,n} &= \frac{1}{KL} \int_0^K \int_0^L h(x,y) \exp\left[-i(kmx + lny)\right] dx\, dy \\
&= \varepsilon_{m,n}^{(a)} - i\,\varepsilon_{m,n}^{(i)}
\end{aligned}
$$

$$
C_{m,n} = 2\left[\left(\varepsilon_{m,n}^{(a)} + \varepsilon_{m,-n}^{(a)}\right)^2 + \left(\varepsilon_{m,n}^{(i)} + \varepsilon_{m,-n}^{(i)}\right)^2\right]^{\frac{1}{2}}
$$

$$
D_{m,n} = 2\left[\left(\varepsilon_{m,-n}^{(a)} - \varepsilon_{m,n}^{(a)}\right)^2 + \left(\varepsilon_{m,n}^{(i)} - \varepsilon_{m,-n}^{(i)}\right)^2\right]^{\frac{1}{2}}
$$

$$\epsilon_{m,n} = \frac{1}{m} \arctan\left[\frac{\mathcal{E}^{(i)}_{m,m} + \mathcal{E}^{(i)}_{m,-m}}{\mathcal{E}^{(r)}_{m,m} + \mathcal{E}^{(r)}_{m,-m}}\right]$$

$$\theta_{m,n} = \frac{1}{m} \arctan\left[\frac{\mathcal{E}^{(r)}_{m,-m} - \mathcal{E}^{(r)}_{m,m}}{\mathcal{E}^{(i)}_{m,m} - \mathcal{E}^{(i)}_{m,-m}}\right]$$

$E_{m,n}$ is the complex Fourier coefficient, and ϵ and θ are the phase angles of the harmonics along a latitude circle indicating the first longitude at which a maximum of h occurs. From (19) and the definition of $S_1^{(k)}$ we can now write the following expressions for the real and imaginary parts of the complex Fourier coefficients of the boundary forcing function, providing we take $u_0\delta$ as a constant,

$$\mathcal{S}_{m,n} = \mathcal{S}^{(r)}_{m,n} - i\,\mathcal{S}^{(i)}_{m,n}$$

where
$$\mathcal{S}^{(r)}_{m,n} = -\Xi\,\mathcal{E}^{(i)}_{m,n}$$
$$\mathcal{S}^{(i)}_{m,n} = \Xi\,\mathcal{E}^{(r)}_{m,n}$$

$$\Xi = \rho_0 g f u_0 \delta (A_I/R\rho_0)^{\frac{1}{2}} m k$$

It is instructive first to show the general effects of the <u>scale</u> of the topography only by computing the response U_1 on the assumption that all of

the topographic harmonics have equal amplitude and phase along a given latitude (45°N, in our case). We also assume that u_{os} is uniform with y. For this purpose, we consider all the wave numbers included by $m = 1$ through 6 and $= 0$ and 1 except $(m,n) = (6,1)$.

In particular, we shall set $C_{m,0}/2 = -C_{m,1} = 200$ meters, $D_{m,n} = 0$, and $\epsilon_{m,0} = \epsilon_{m,1} = 0$, which from (19) is equivalent to setting $\mathcal{E}^{(i)}_{m,0} = \mathcal{E}^{(i)}_{m,1} = \mathcal{E}^{(i)}_{m,-1} = 0$, $C_{m,0}/2 = 2\mathcal{E}^{(a)}_{m,0}$, and $C_{m,1} = 4\mathcal{E}^{(a)}_{m,1} = 4\mathcal{E}^{(a)}_{m,-1}$. Thus, we are considering all components except (6,1) included by the expansion

$$h(x,y) = \sum_{m=1}^{6} \left[h^{(m,0)} + h^{(m,1)} \right]$$

where

$$h^{(m,0)} = \frac{C_{m,0}}{2} \cos mkx$$

$$h^{(m,1)} = -C_{m,1} \cos mkx \cos ly$$

The values of $I_{m,n}$ from which the responses are easily obtained using (13) are given in Table 2. The solutions are shown in the form of cross-sections along 45°N in Figures 3 through 13, with the mountain profiles shown at the bottom. In Figures 14 and 15, the fields of ω_1 and T_1 associated with the solutions for $(m,n) = (2,0)$ and $(2,1)$ respectively are shown, as these are representative of the two regimes separated by the quasi-resonant wave number. It can be seen that in all cases $|\omega_1|_{max}$ coincides with $|v_1|_{max}$, and $|T_1|_{max}$ coincides with $v_1 = 0$ (in agreement with the fact that the troughs and ridges have no slope with height—c.f., Section 3).

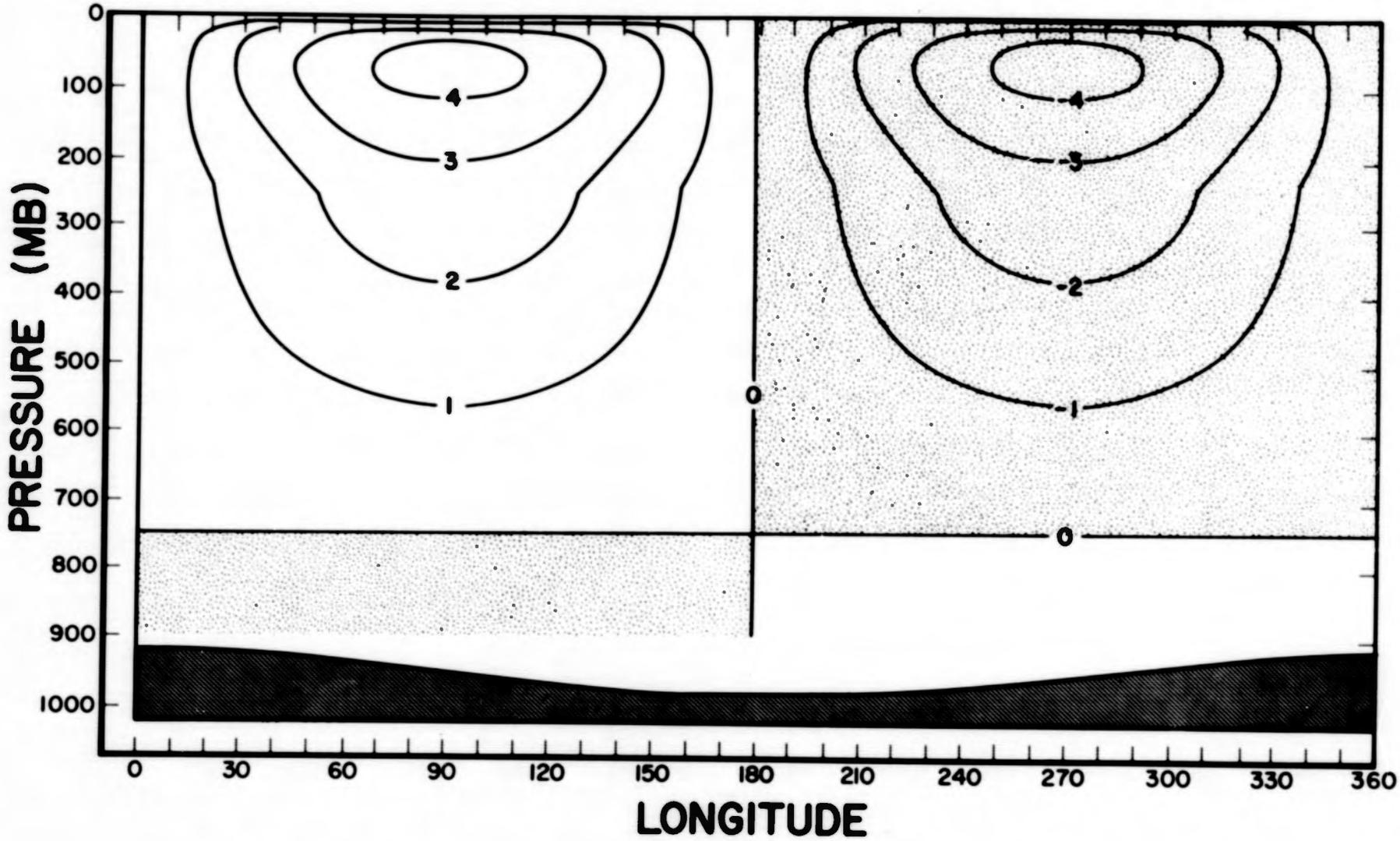

Fig. 3. Mean meridional wind response, v_1, to uniform airflow over topographic harmonic, $h^{(1,0)}$, along y=L/2 in units of 10^{-1} m sec^{-1}.

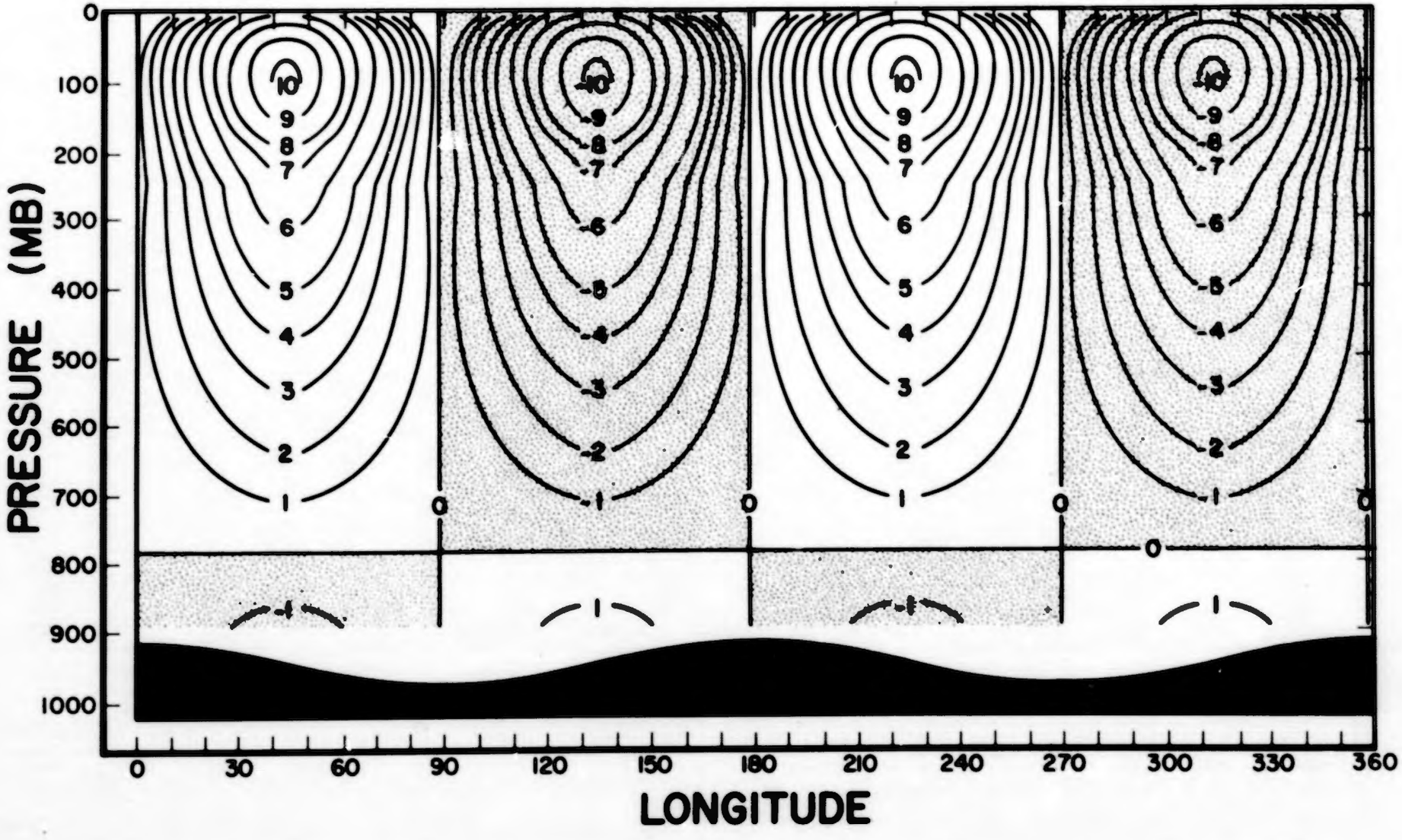

Fig. 4. Mean meridional wind response, v_1, to uniform airflow over topographic harmonic, $h^{(2,0)}$, along y=L/2 in units of 10^{-1} m sec^{-1}.

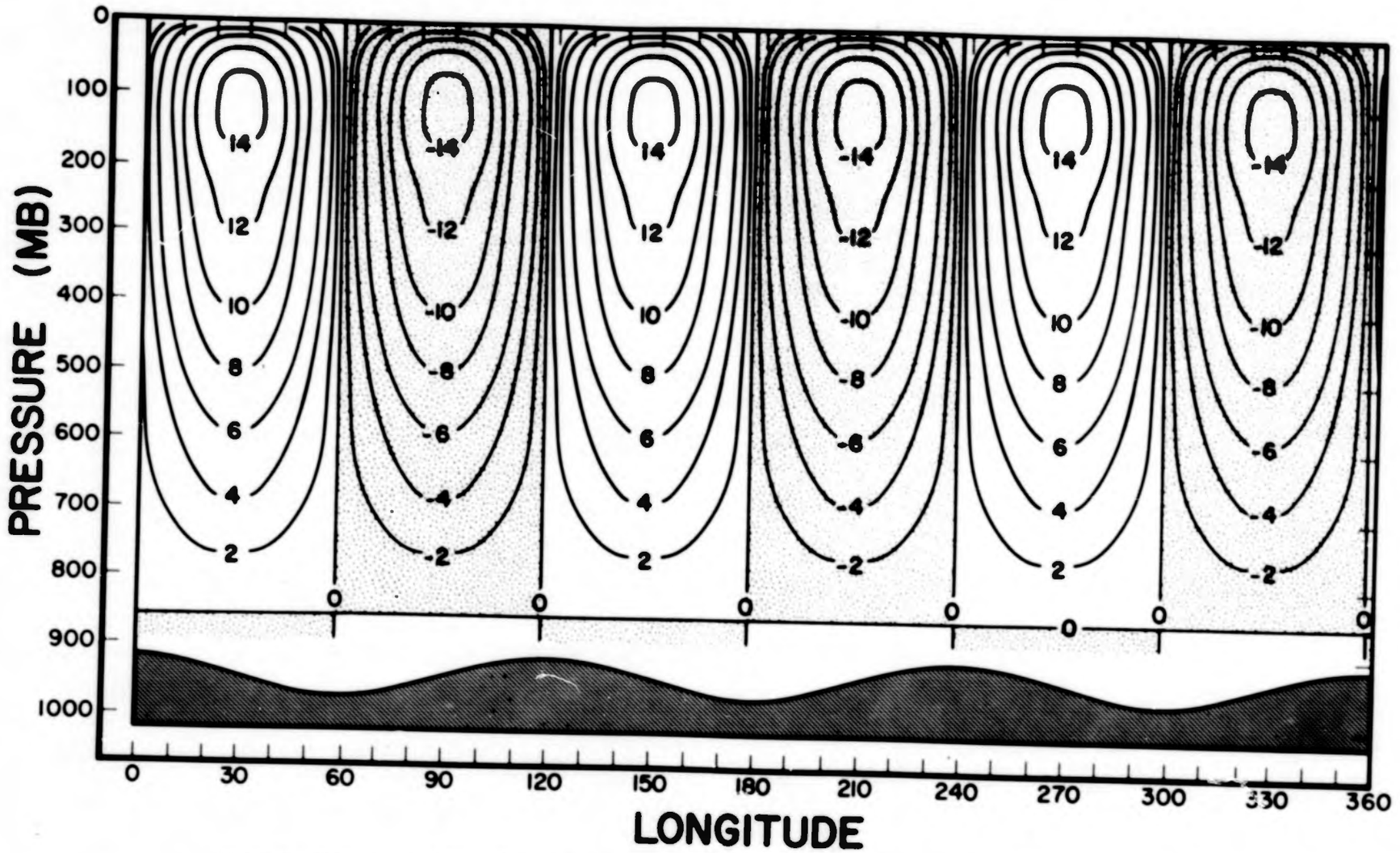

Fig. 5. Mean meridional wind response, v_1, to uniform airflow over topographic harmonic, $h^{(3,0)}$, along y=L/2 in units of 10^{-1} m sec^{-1}.

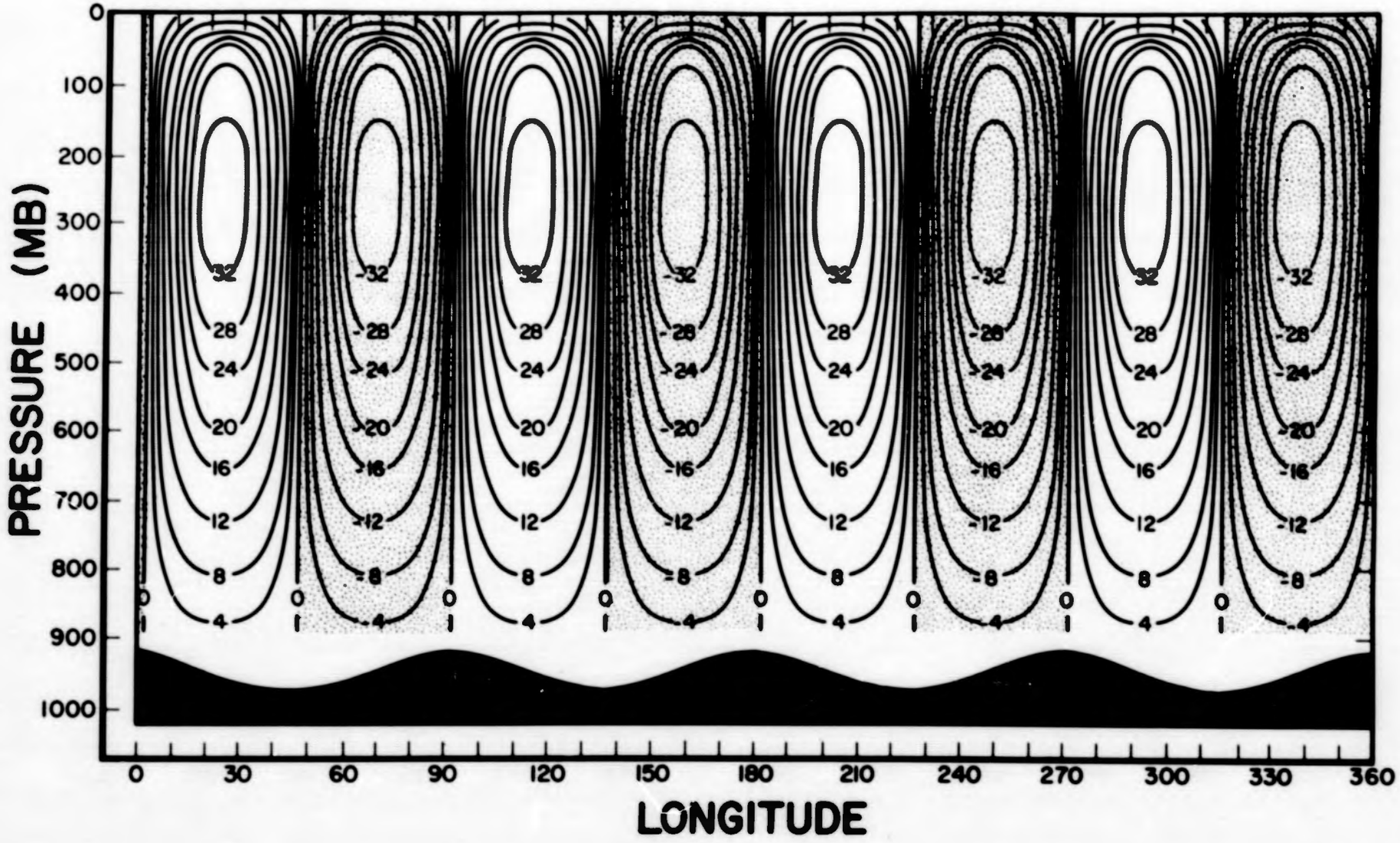

Fig. 6. Mean meridional wind response, v_1, to uniform airflow over topographic harmonic, $h^{(4,0)}$, along y=L/2 in units of 10^{-1}m sec^{-1}.

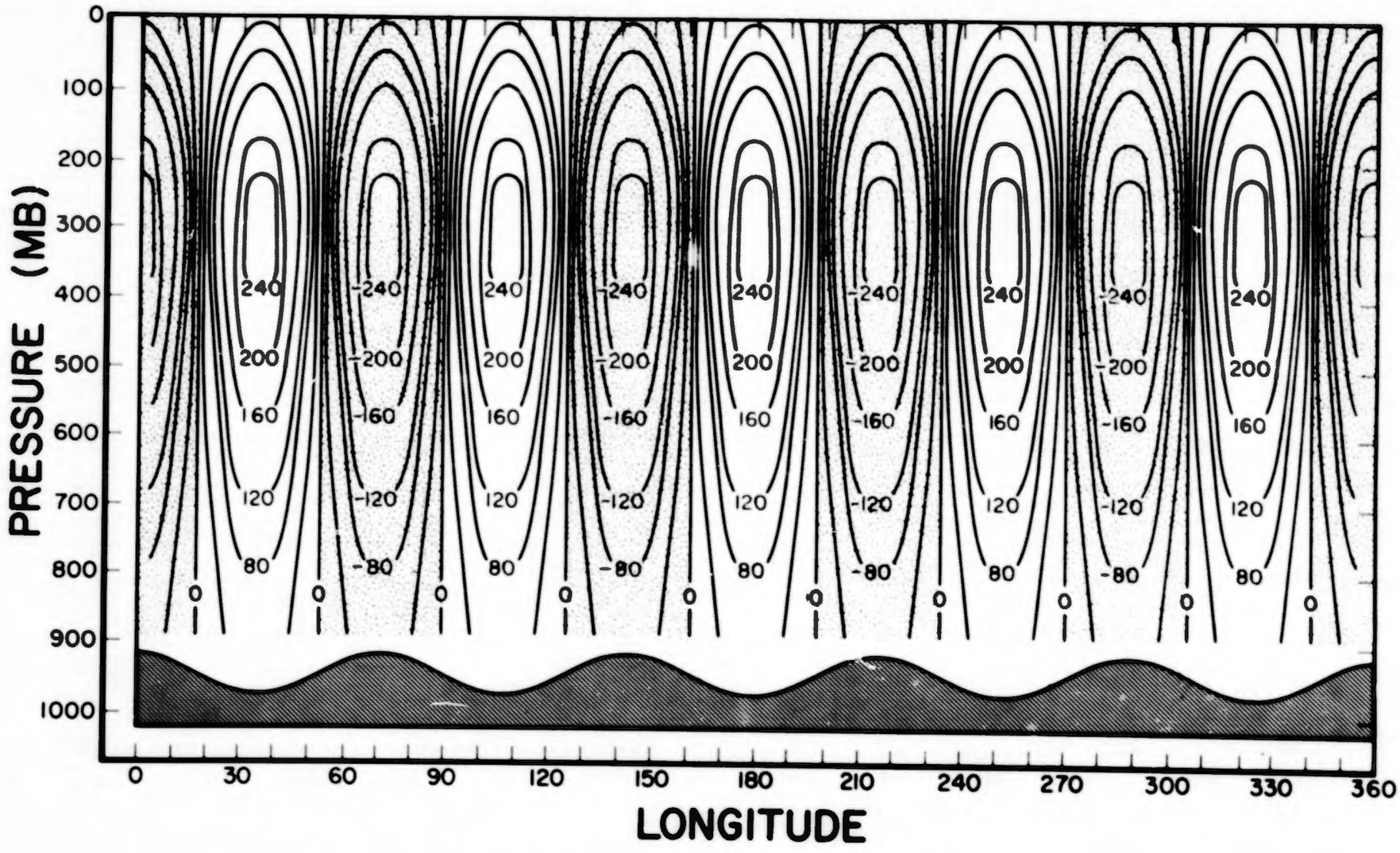

Fig. 7. Mean meridional wind response, v_1, to uniform airflow over topographic harmonic, $h(5,0)$, along $y=L/2$ in units of 10^{-1}m sec^{-1}.

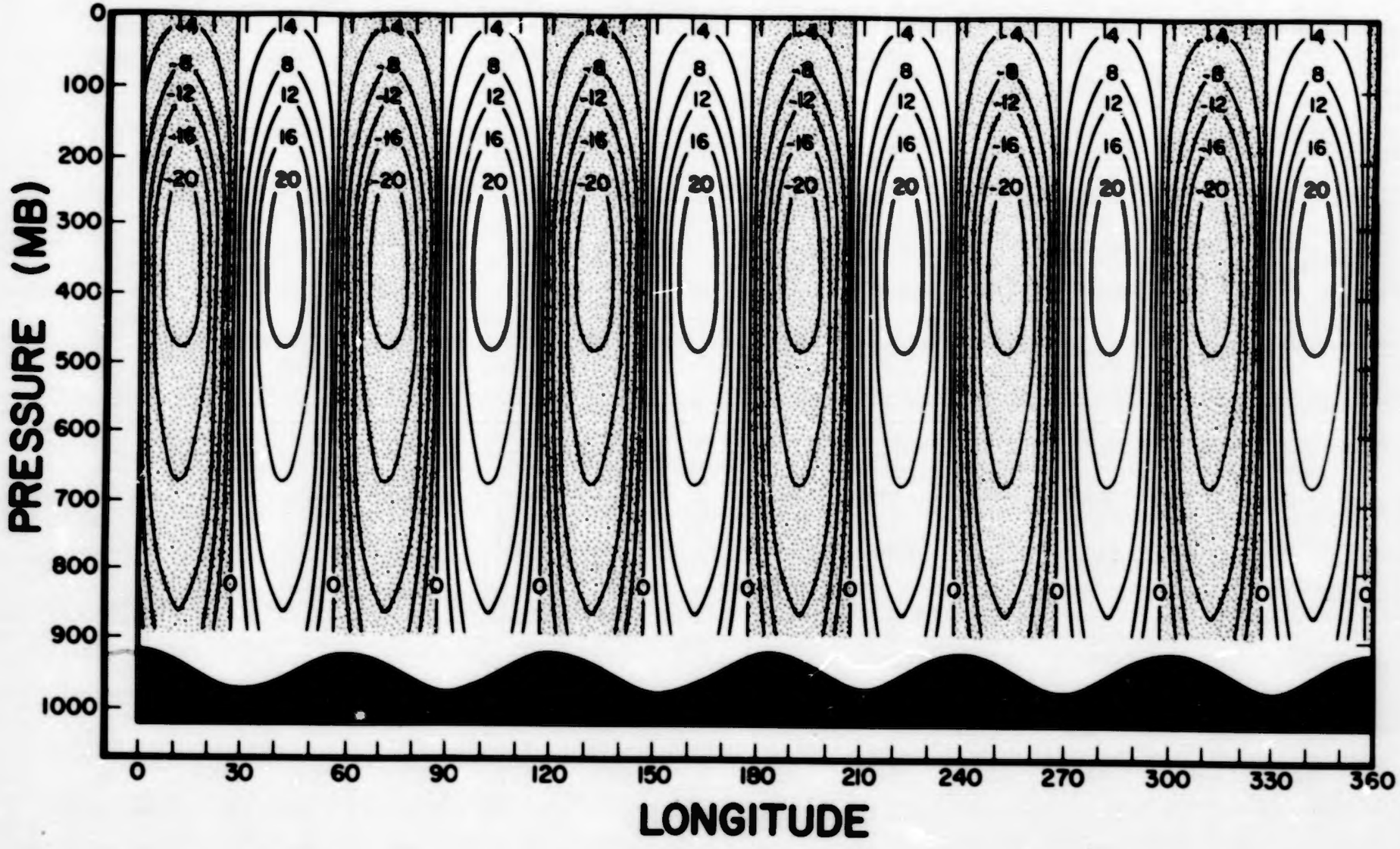

Fig. 8. Mean meridional wind response, v_1, to uniform airflow over topographic harmonic $h^{(6,0)}$, along y=L/2 in units of 10^{-1}m sec^{-1}.

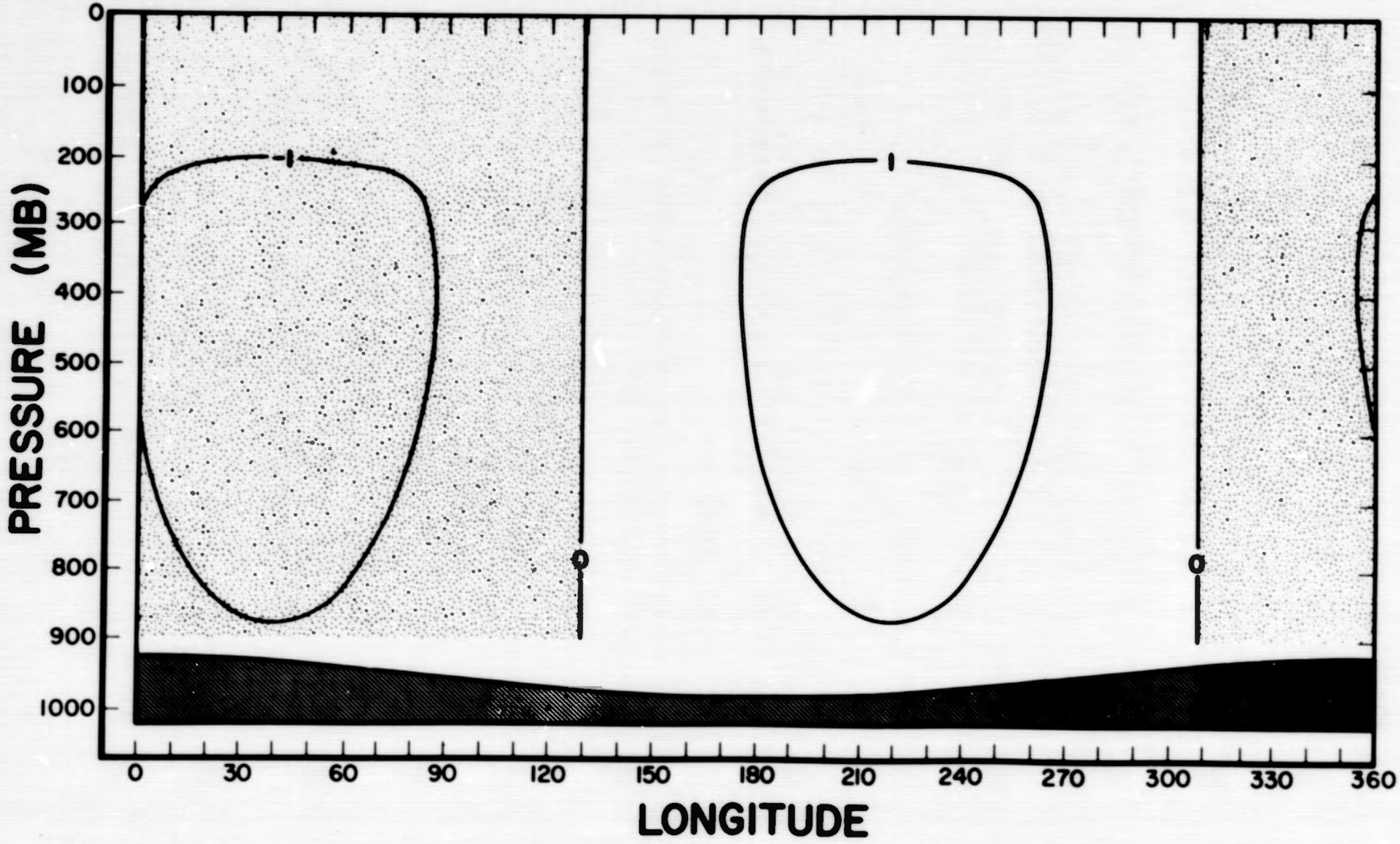

Fig. 9. Mean meridional wind response, v_1, to uniform airflow over topographic harmonic, $h^{(1,1)}$, along y=L/2 in units of 10^{-2}m sec^{-1}.

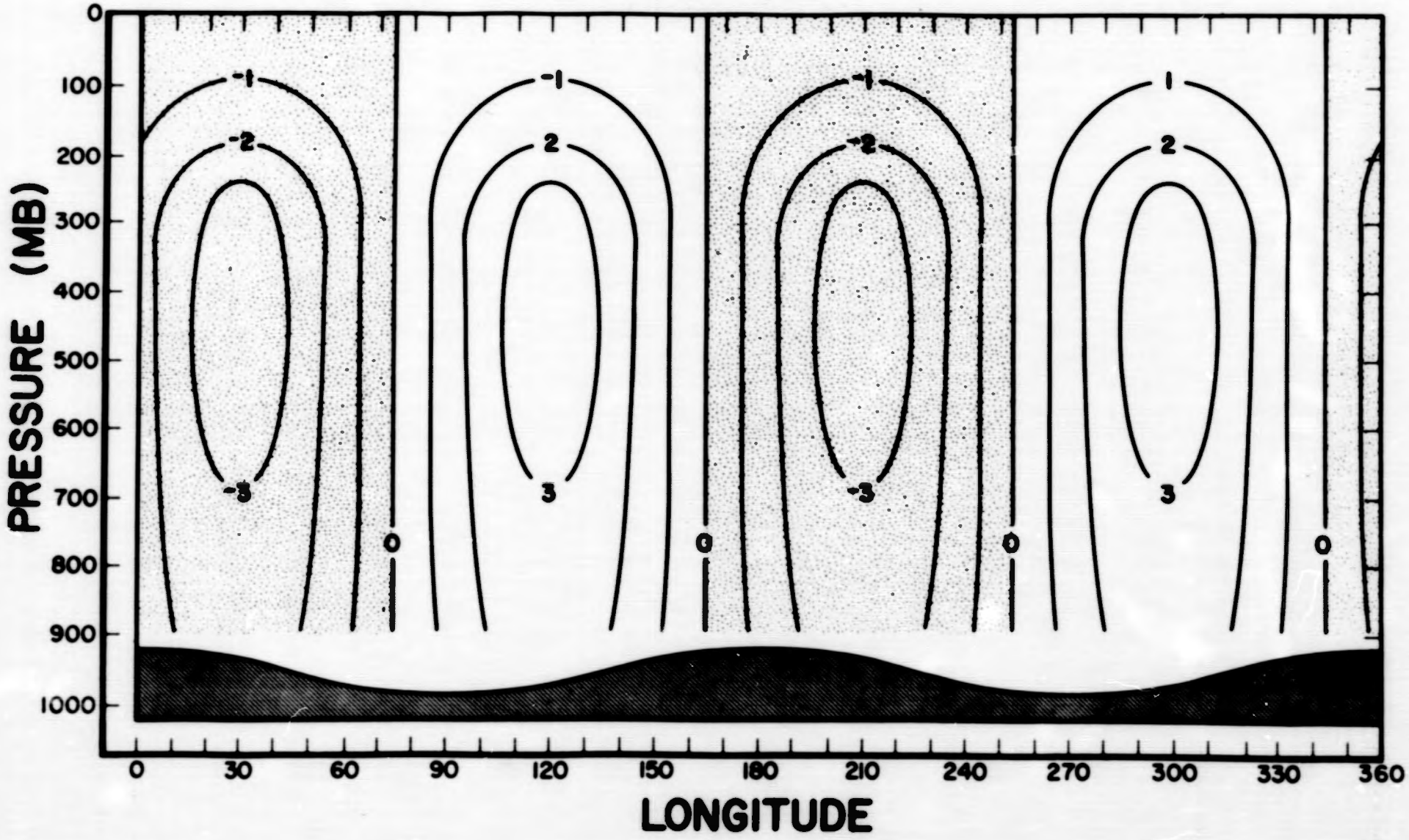

Fig. 10. Mean meridional wind response, v_1, to uniform airflow over topographic harmonic, $h^{(2,1)}$, along y=L/2 in units of 10^{-1}m sec^{-1}.

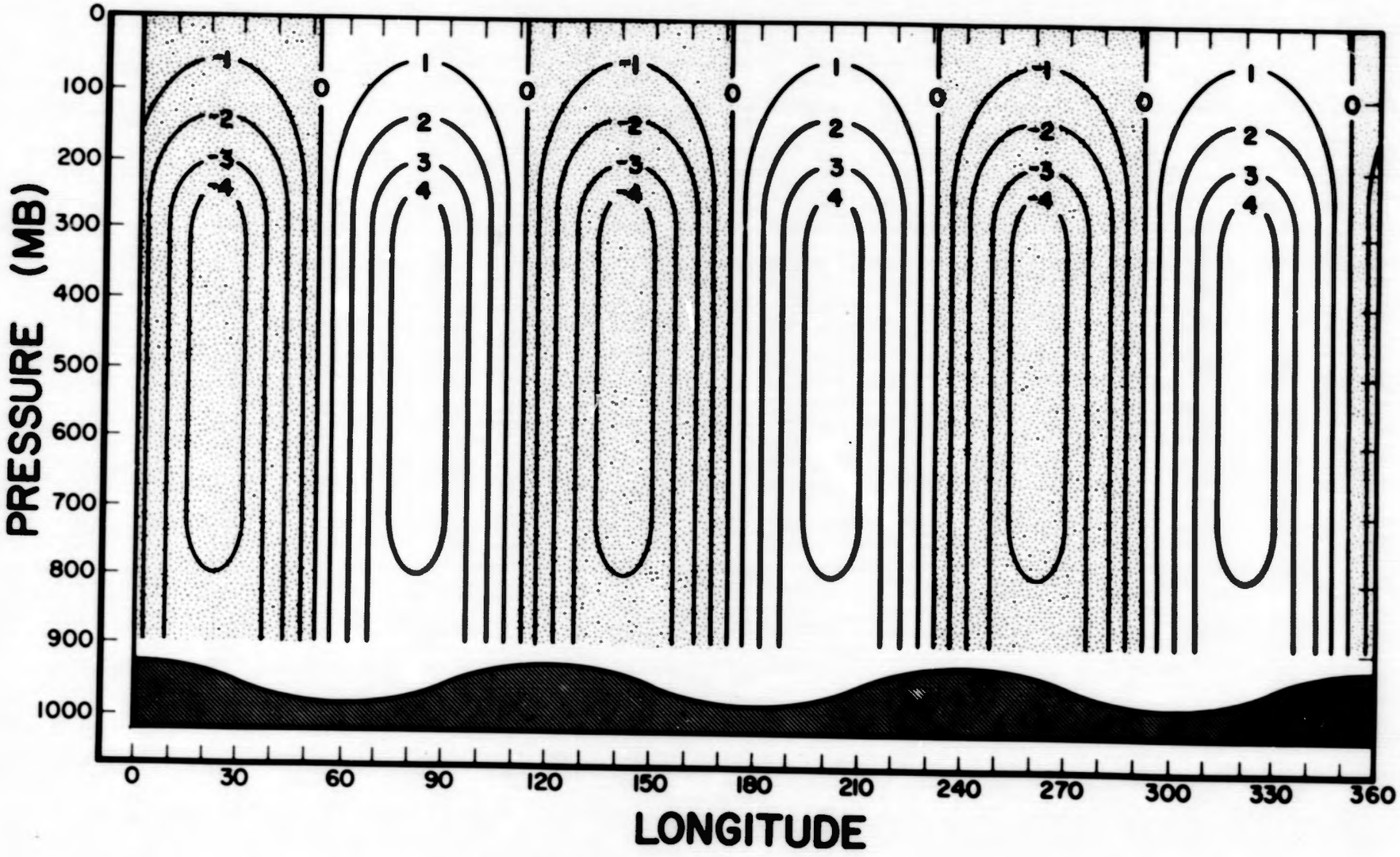

Fig. 11. Mean meridional wind response, v_1, to uniform airflow over topographic harmonic, $h^{(3,1)}$, along y=L/2 in units of 10^{-1}m sec^{-1}.

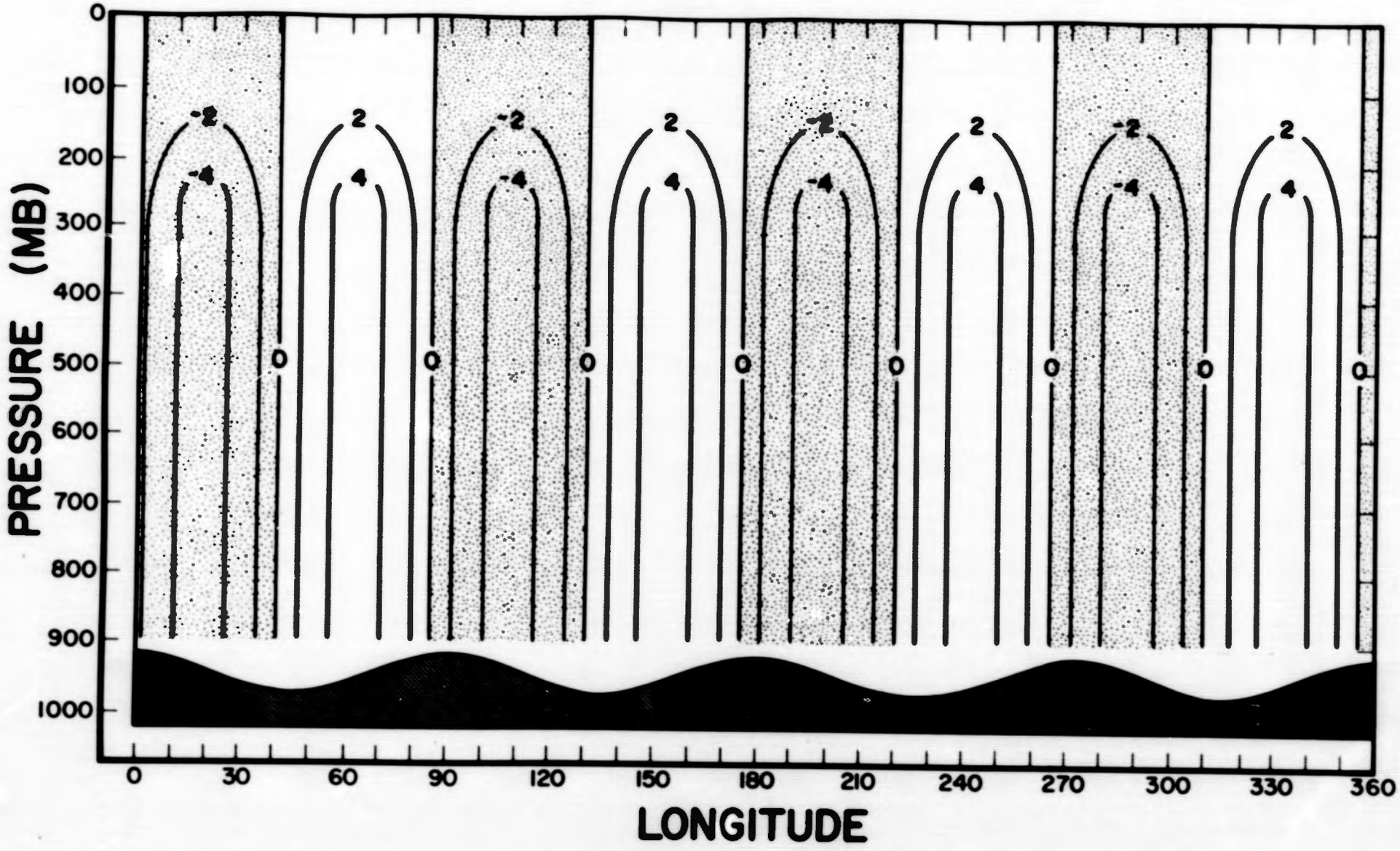

Fig. 12. Mean meridional wind response, v_1, to uniform airflow over topographic harmonic, $h^{(4,1)}$, along y=L/2 in units of 10^{-1}m sec^{-1}.

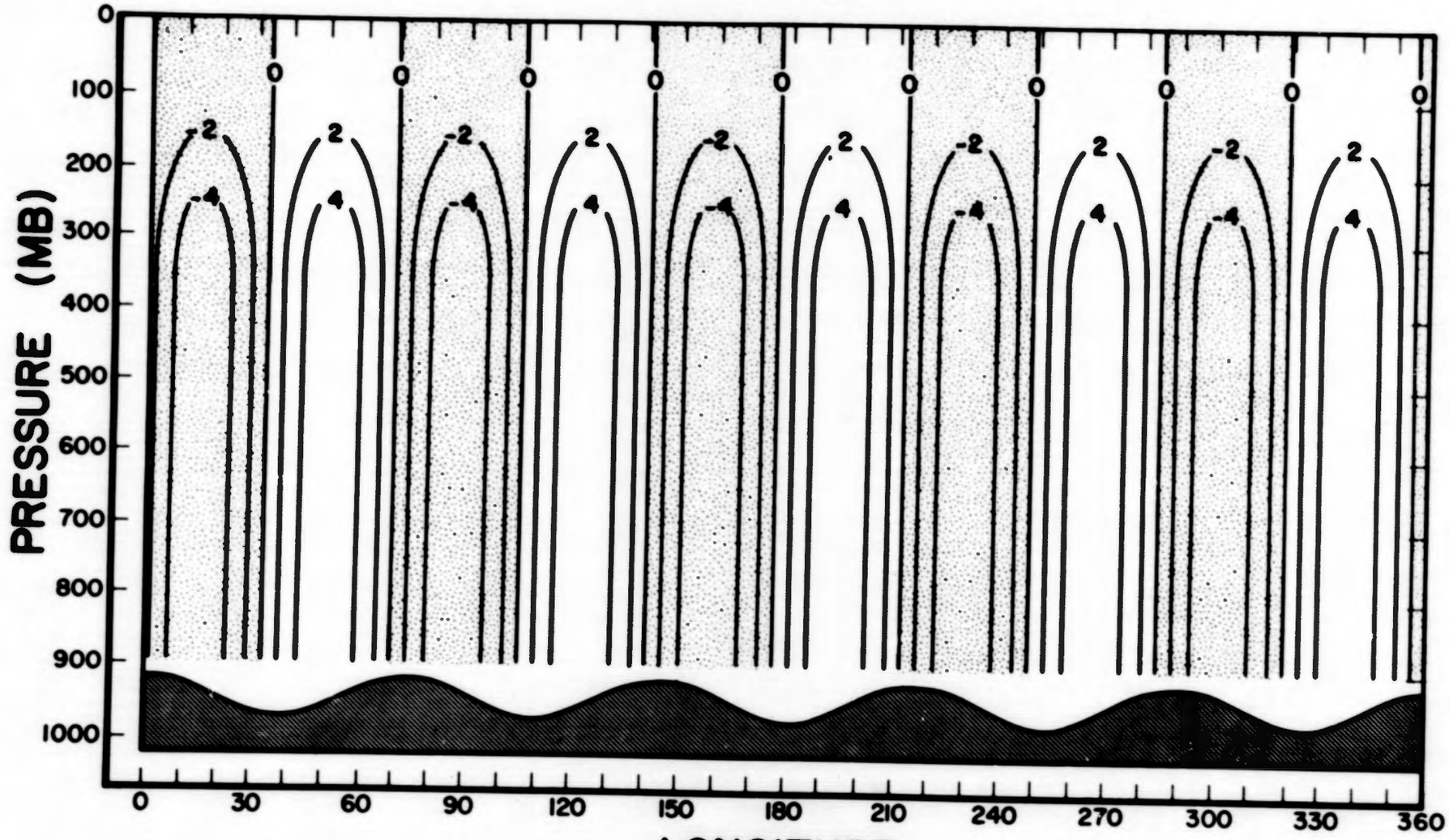

Fig. 13. Mean meridional wind response, v_1, to uniform airflow over topographic harmonic, $h^{(5,1)}$, along y=L/2 in units of 10^{-1}m sec^{-1}.

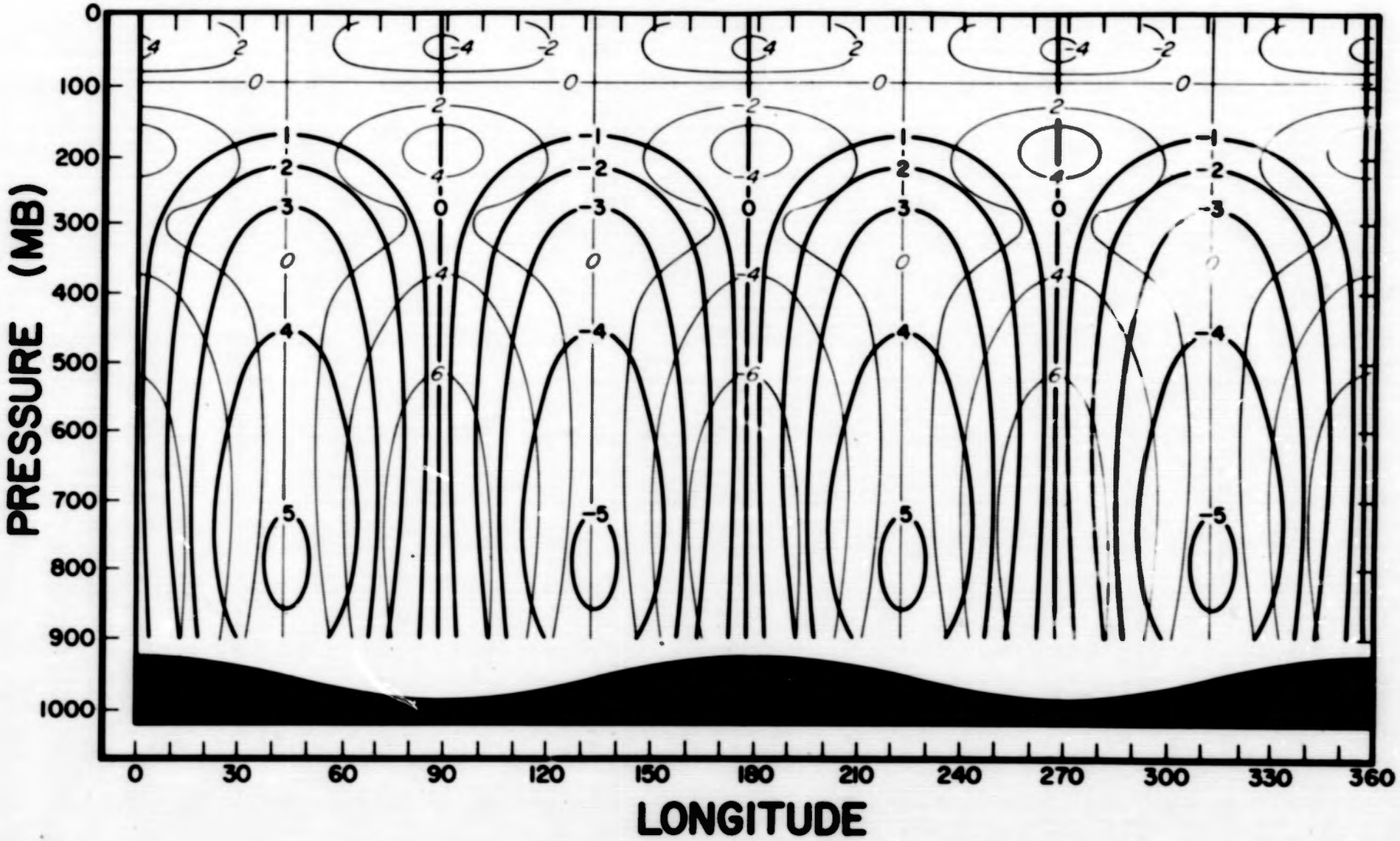

Fig. 14. Cross-section along y=L/2 of w_1 (thick line) in units of 10^{-2}gm cm^{-1} sec^{-3}, and T_1 (thin line) in units of 10^{-1} deg, corresponding to the solution for $h^{(2,0)}$ shown in Fig. 4.

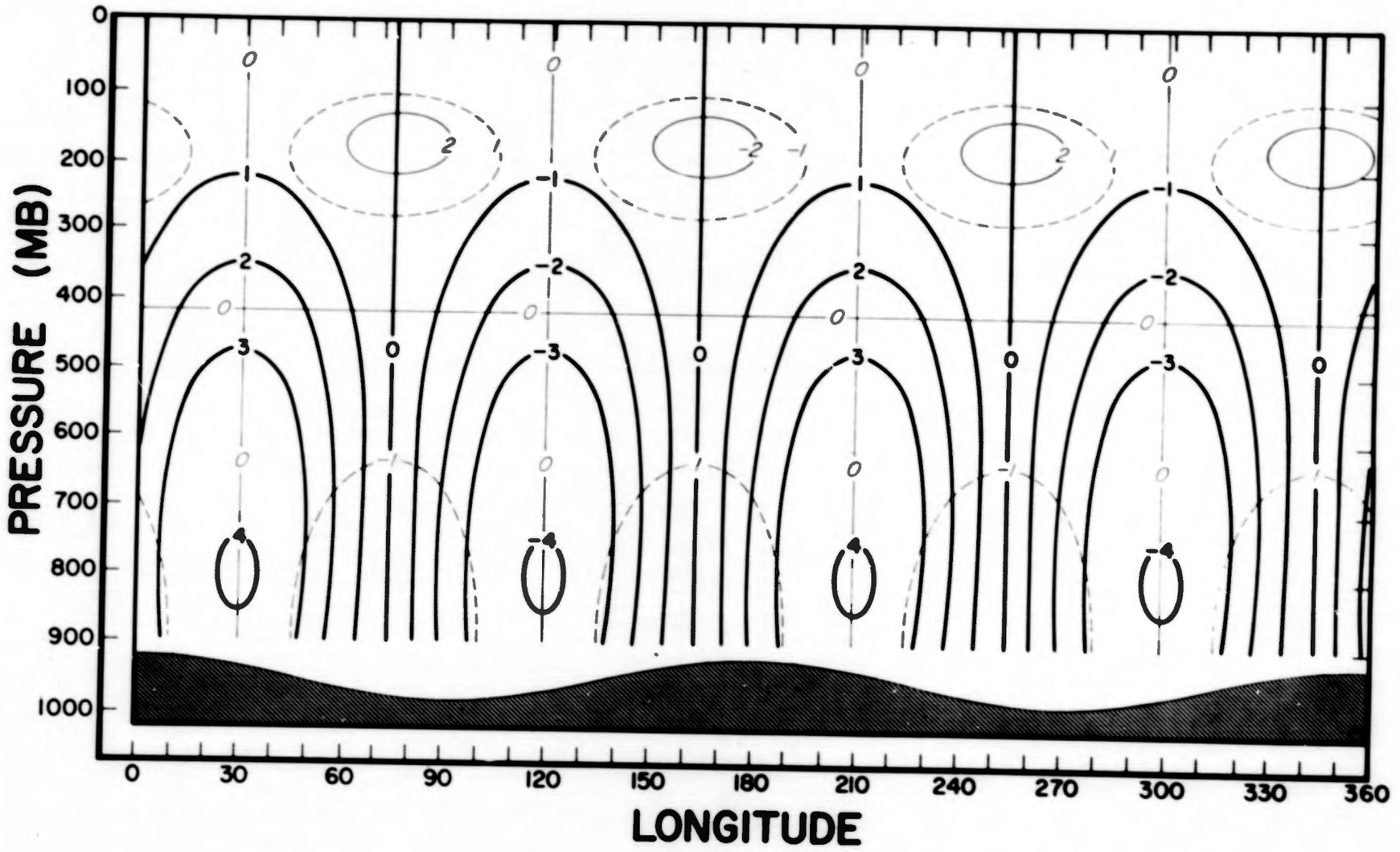

Fig. 15. Cross-section along y=L/2 of w_1 (thick line) in units of 10^{-2}gm cm^{-1} sec^{-3}, and T_1 (thin line) in units of 10^{-1} deg, corresponding to the solution $h^{(2,1)}$, corresponding to the solution shown in Fig. 10.

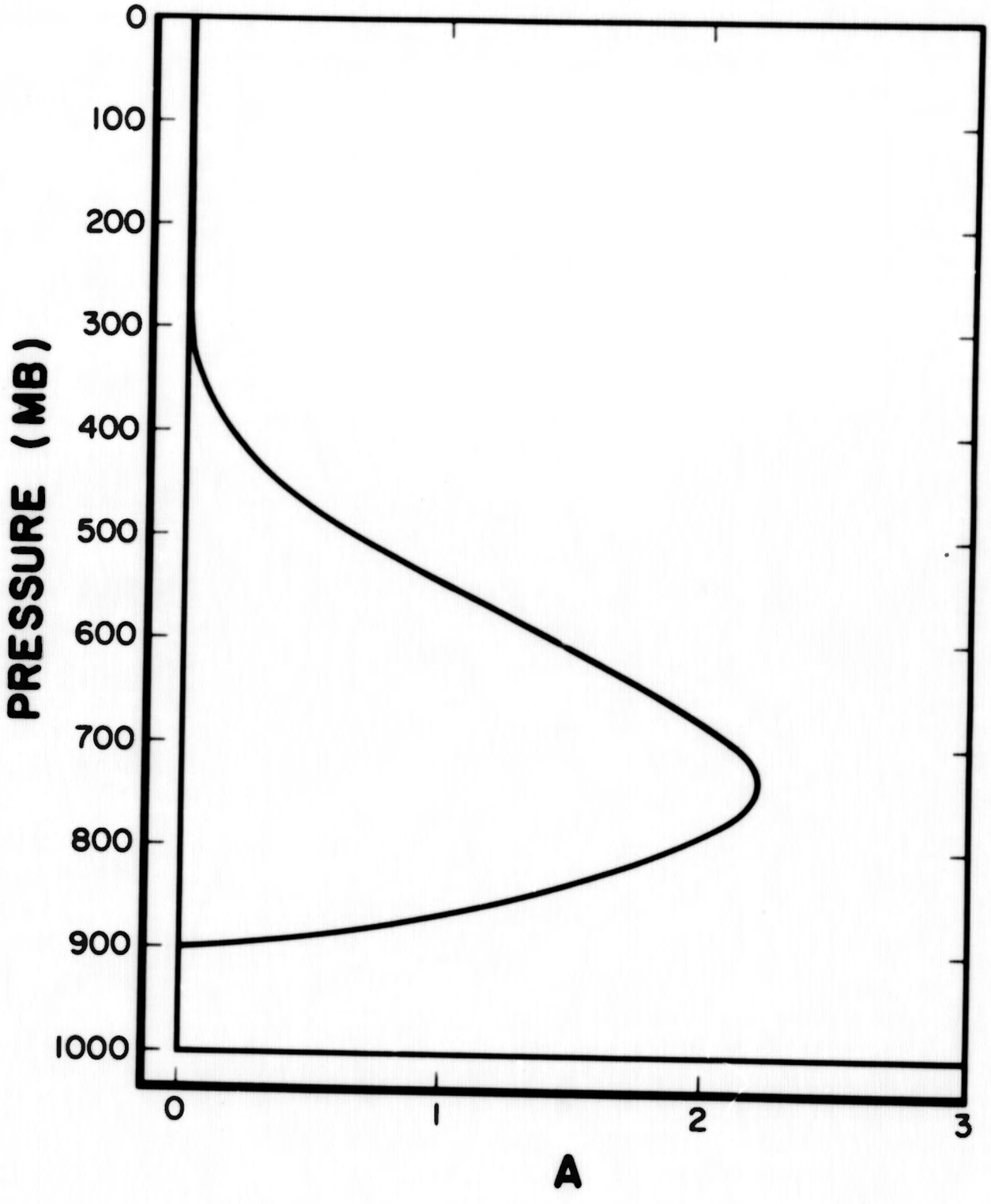

Fig. 16. Vertical amplitude function for internal heating, A(p).

d) Response to Sources and Sinks of Heat - The distribution of $Q_1(x,y,p)$ is very poorly known. For want of a better estimate, we shall adopt a distribution similar to that assumed previously by Smagorinsky (1953) and the writer (1963)—i.e.,

$$Q_1(x,y,p) = \sum_{m=-\infty}^{\infty} \sum_{n=-\infty}^{\infty} Q_{m,n}(p)\, e^{i(mkx+nly)} \qquad (20)$$

where

$$Q_{m,n}(p) = A(p)\, N_{m,n}$$

the vertical function $A(p)$ having the form shown in Figure 16. If we wish, we can expand (20) further in the manner of (19).

As in the mountain case, we shall examine the effect of the scale only by computing the response v_1 assuming the amplitudes and phases are the same for all forcing harmonics. The following uniform magnitudes of $N_{m,n}\,(= N^{(r)}_{m,n} - i\,N^{(i)}_{m,n})$ were adopted, all referred to a phase origin at $kx = \epsilon$,

$$N^{(r)}_{m,0} = -2\,N^{(r)}_{m,1} = -2\,N^{(r)}_{m,-1} = 10^{-5} \text{ deg sec}^{-1}$$

$$N^{(i)}_{m,0} = N^{(i)}_{m,1} = N^{(i)}_{m,-1} = 0$$

which implies that

$$Q_1(x,y,p) = \sum_{m=1}^{\infty} \left[Q_1^{(m,0)} + Q_1^{(m,1)} \right]$$

where

$$Q_1^{(m,0)} = 2\,N^{(r)}_{m,0}\, A(p) \cos m(kx - \epsilon_{m,0})$$

$$Q_1^{(m,1)} = -4\,N_{m,1}\, A(p) \cos m(kx - \epsilon_{m,1}) \cos ly \qquad (21)$$

For case $\epsilon_{m,0} = \epsilon_{m,1}$ we have

$$Q_1^{(m,1)} = Q_1^{(m,0)} \quad \text{at} \quad y = \frac{L}{2} \quad (45°N) \; .$$

From these expressions for $\mathcal{Q}_{m,n}$ it is easy to calculate the forcing functions $\mathcal{F}_{m,n}$ and hence to solve for v_1 from (13) given the values of $G_{m,n}$ shown in Table 3. The results, again for m = 1 through 6, excluding (6,1), are shown in Figures 17 through 27 for $\epsilon = 0$ (i.e., maximum heating at zero longitude). Figures 28 and 29 show the values of ω_1 and T_1 corresponding to the same two harmonics, $(m,n) = (2,0)$ and $(2,1)$, used to illustrate the mountain response (see Figure 14).

For the value of $N_{m,0}^{(2)} = 10^{-5}$ deg sec^{-1} used here, the maximum vertical-mean heating, given by

$$\{Q_1\} = \frac{1}{\phi_N - \phi_T} \int_{\phi_T}^{\phi_N} Q_1 \, d\phi$$

is 1.438 X 10^{-5} deg/sec, which is of the order of observational estimates (e.g., Staff members, Academia Sinica, 1958).

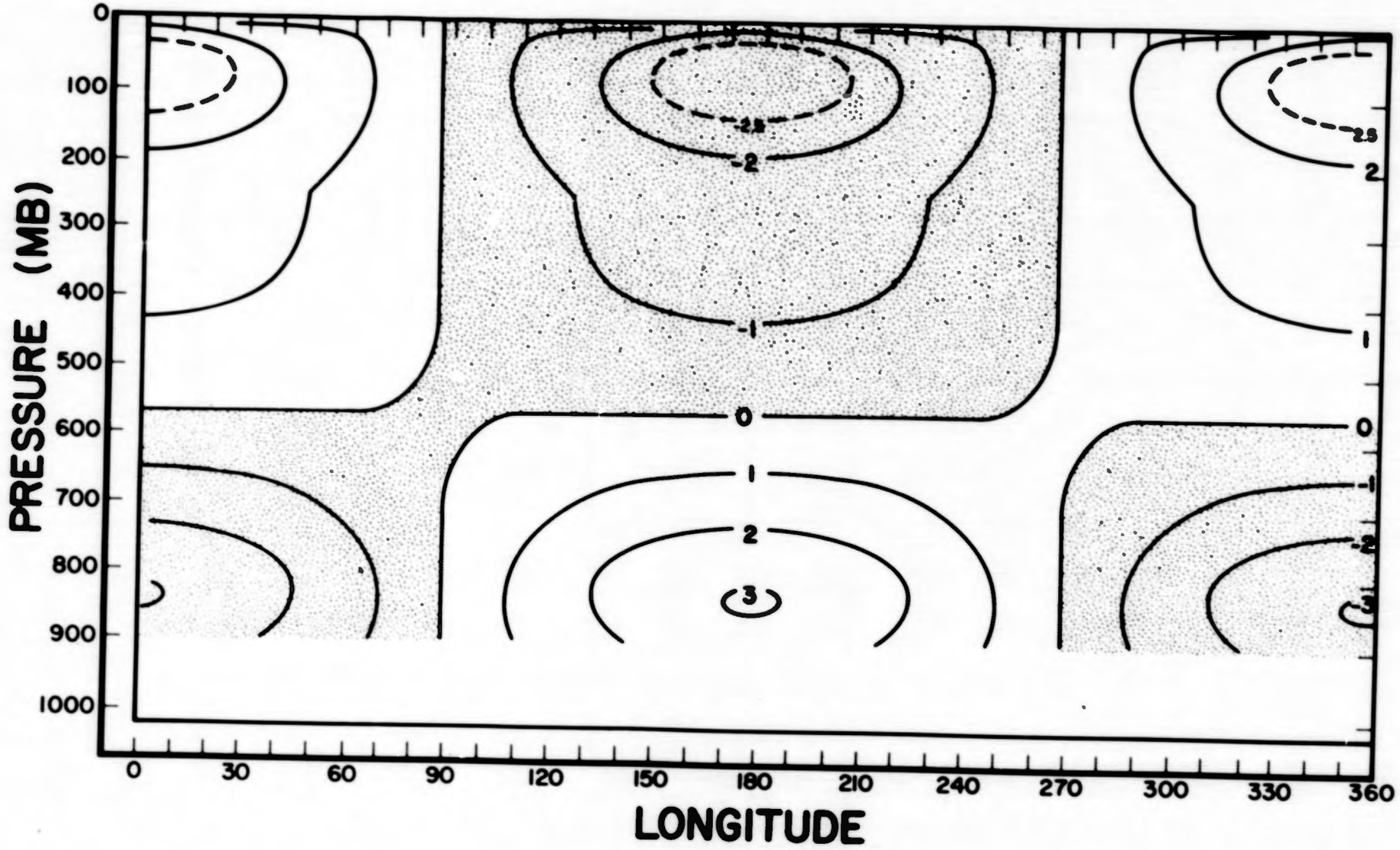

Fig. 17. Mean meridional wind response, v_1, to the internal heating function $Q_1^{(1,0)}$, along y=L/2, in units of m sec^{-1}.

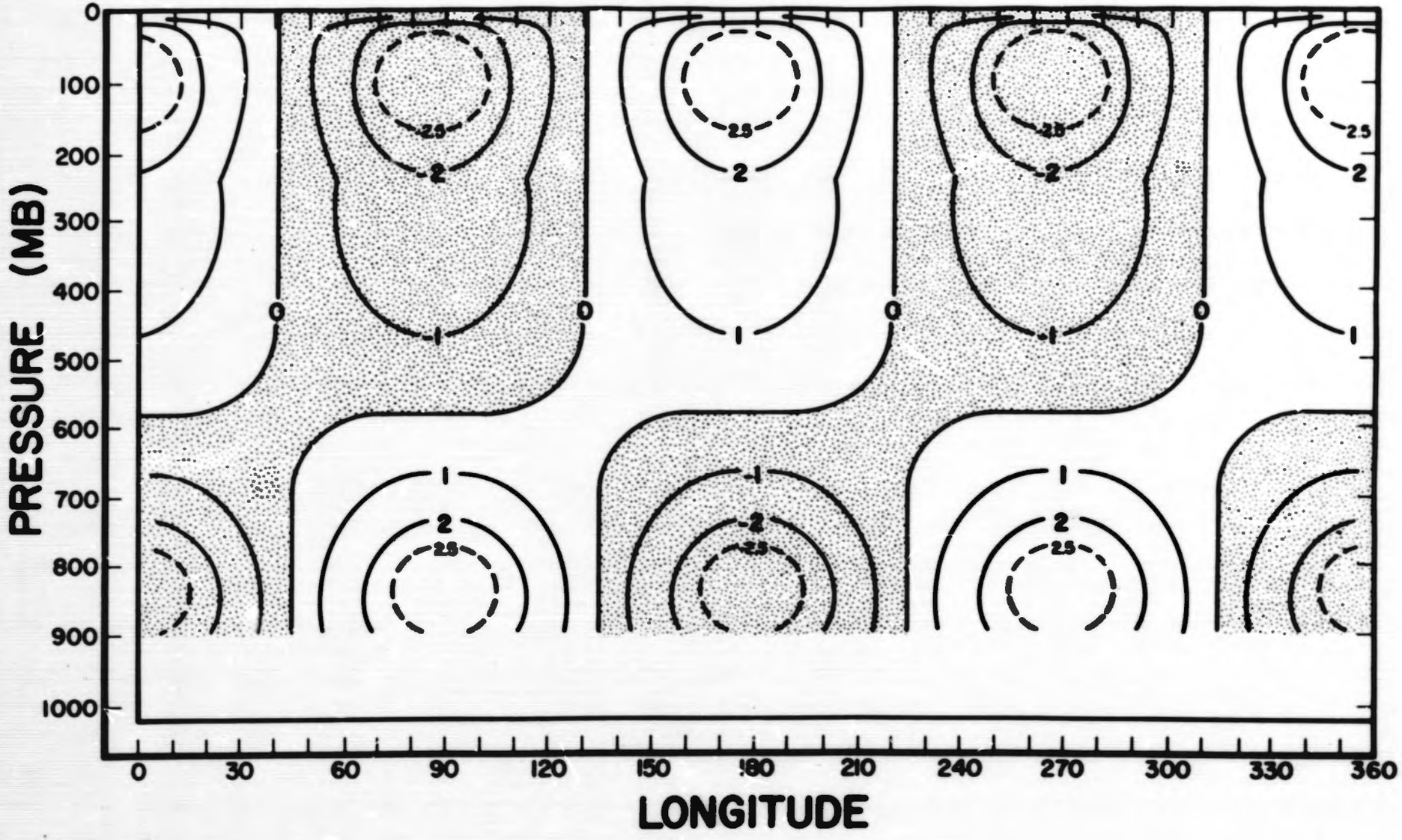

Fig. 18. Mean meridional wind response, v_1, to the internal heating function $Q_1^{(2,0)}$, along $y=L/2$, in units of m sec^{-1}.

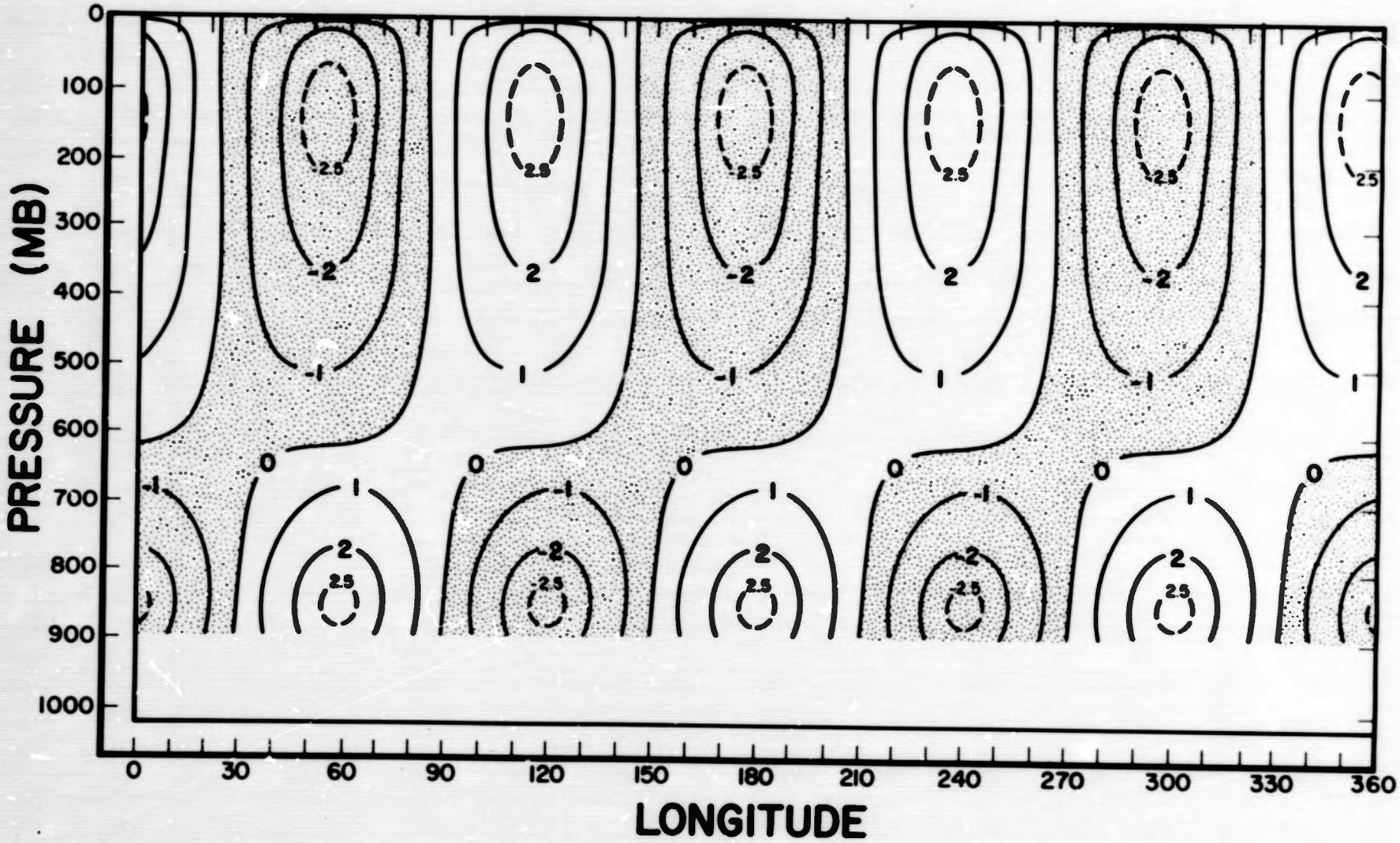

Fig. 19 Mean meridional wind response, v_1, to the internal heating function $Q_1^{(3,0)}$, along y=L/2, in units of m sec^{-1}.

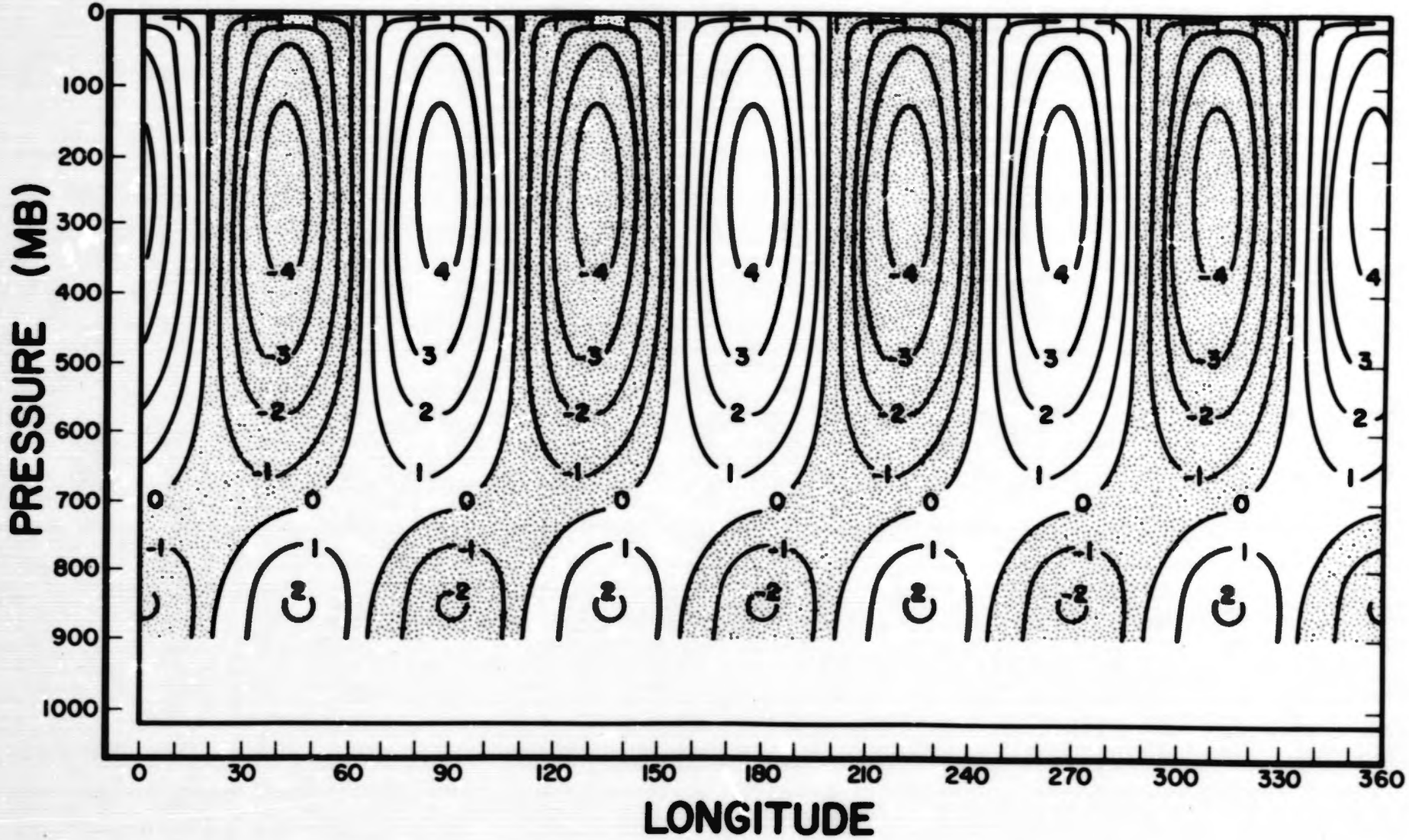

Fig. 20. Mean meridional wind response, v_1, to the internal heating function $Q_1^{(4,0)}$, along y=L/2, in units of m sec^{-1}.

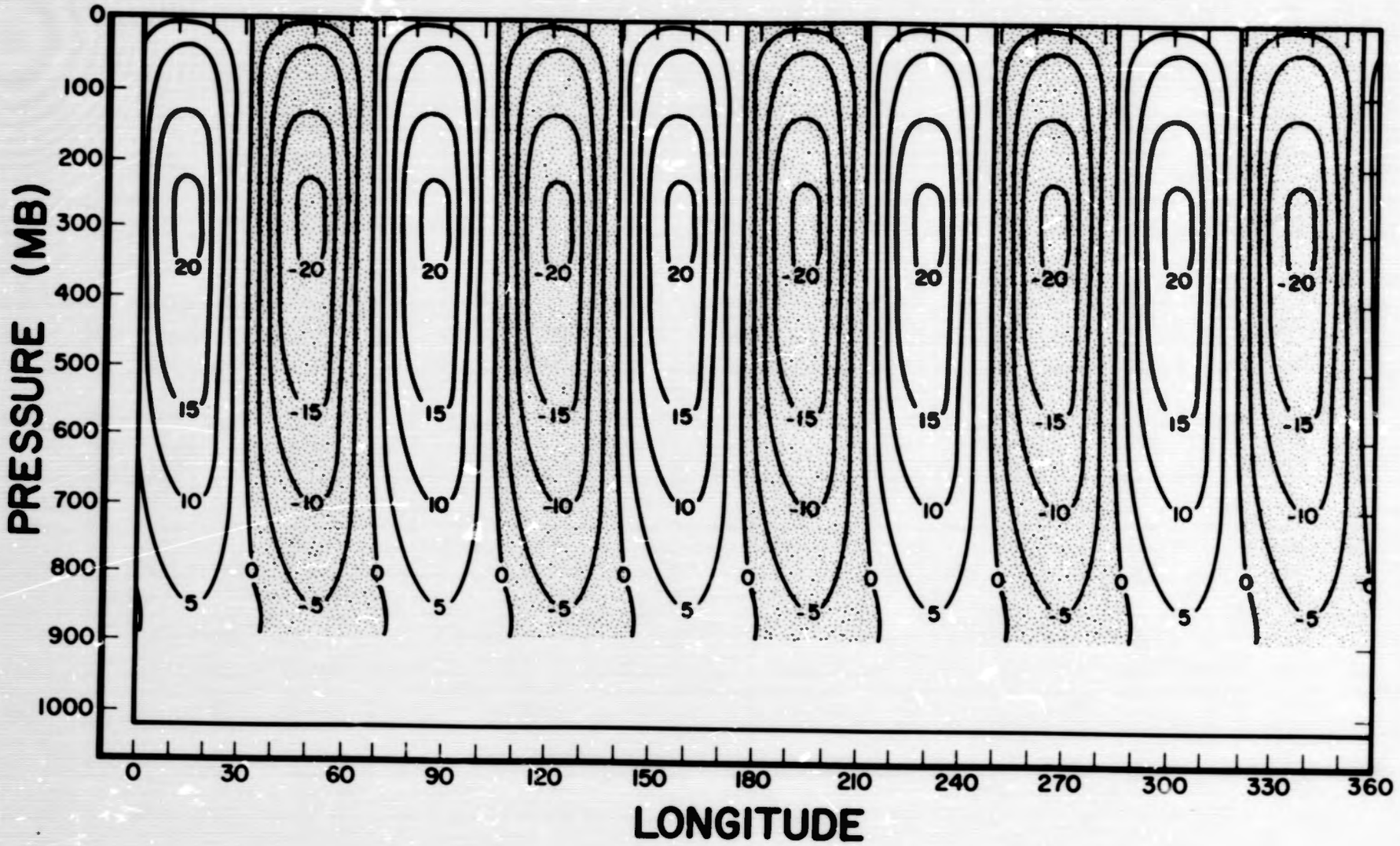

Fig. 21. Mean meridional wind response, v_1, to the internal heating function $Q_1^{(5,0)}$, along y=L/2, in units of m sec^{-1}.

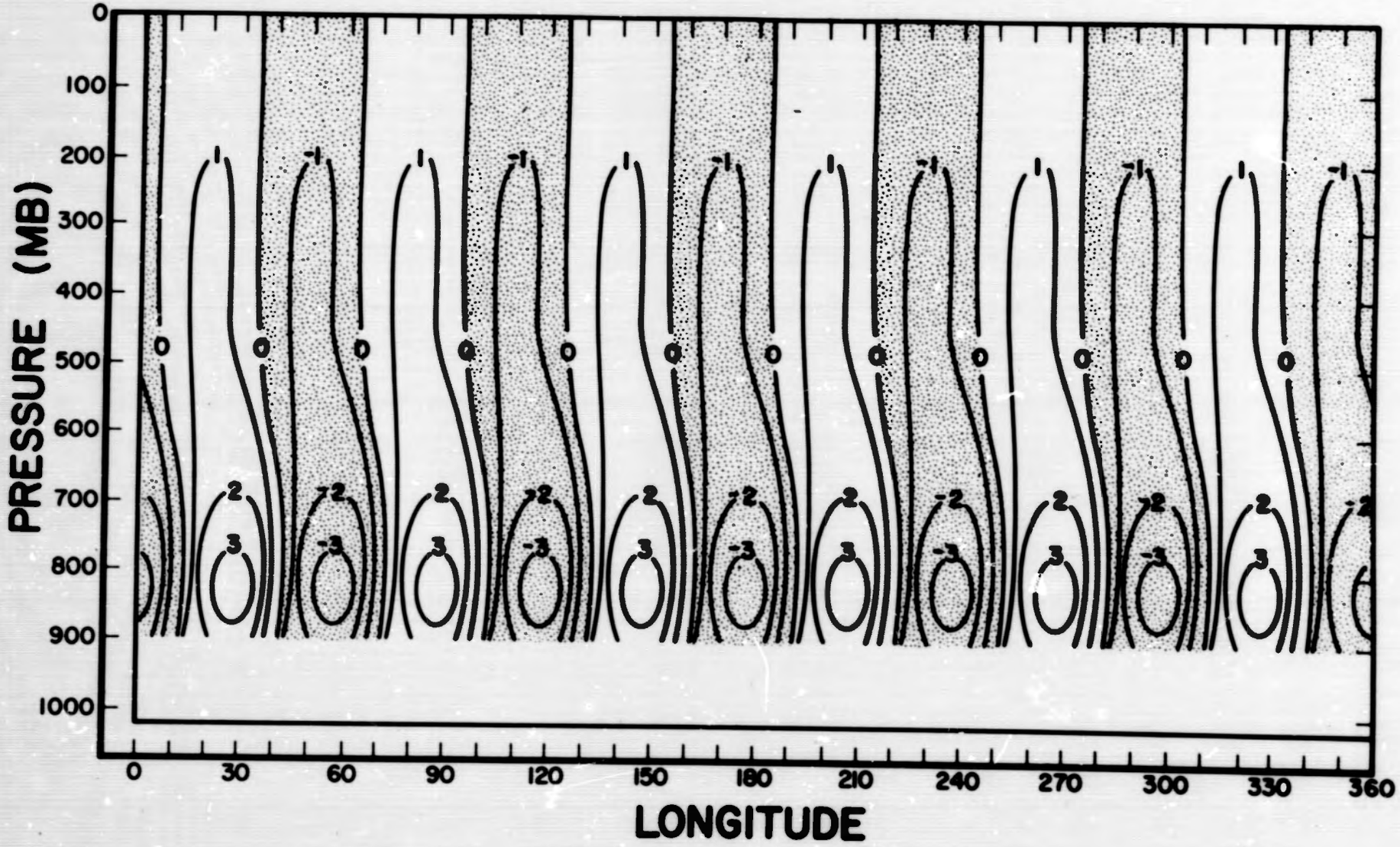

Fig. 22. Mean meridional wind response, v_1, to the internal heating function $Q_1^{(6,0)}$, along y=L/2, in units of m sec^{-1}.

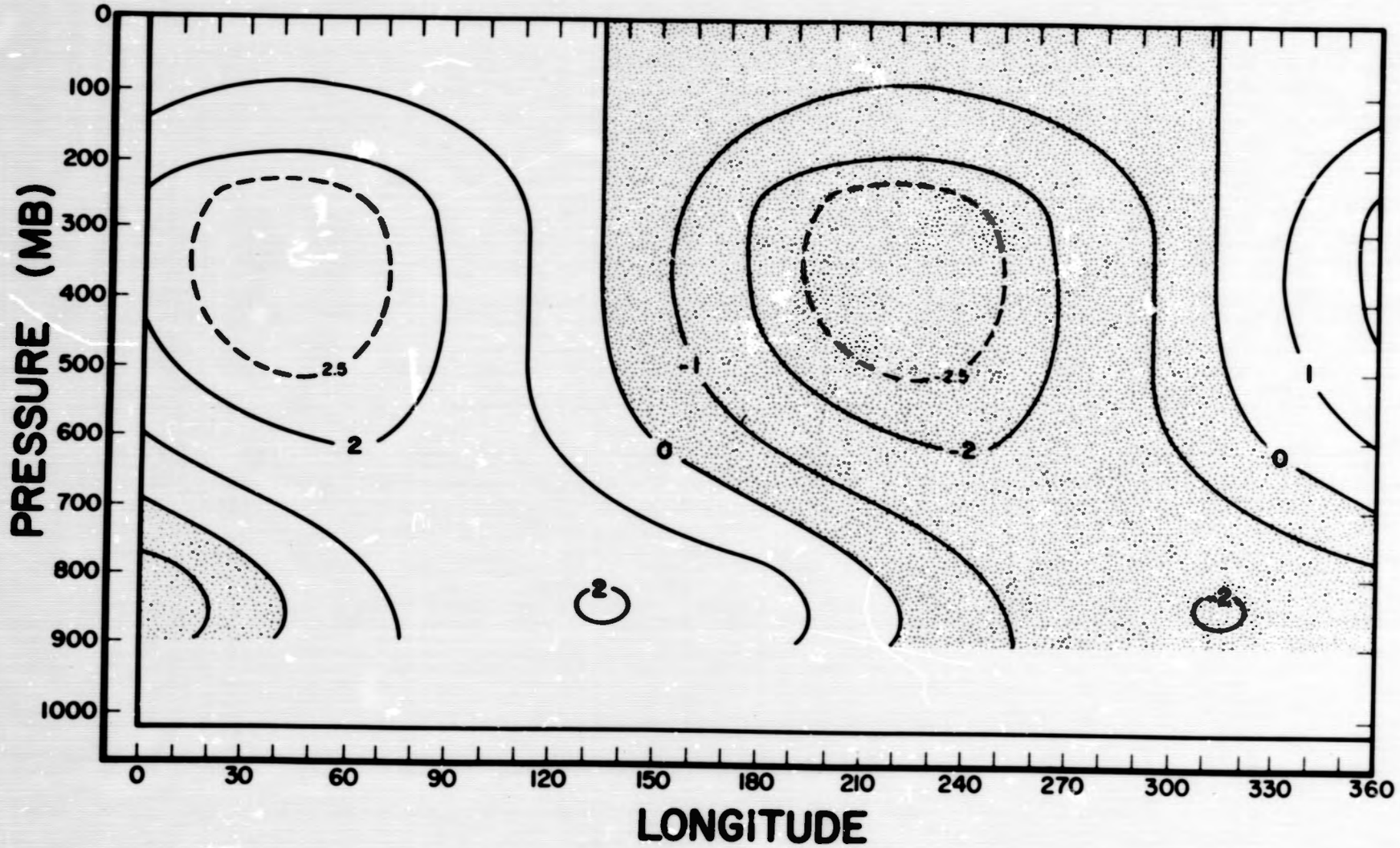

Fig. 23. Mean meridional wind response, v_1, to the internal heating function $Q_1^{(1,1)}$, along y=L/2, in units of m sec^{-1}.

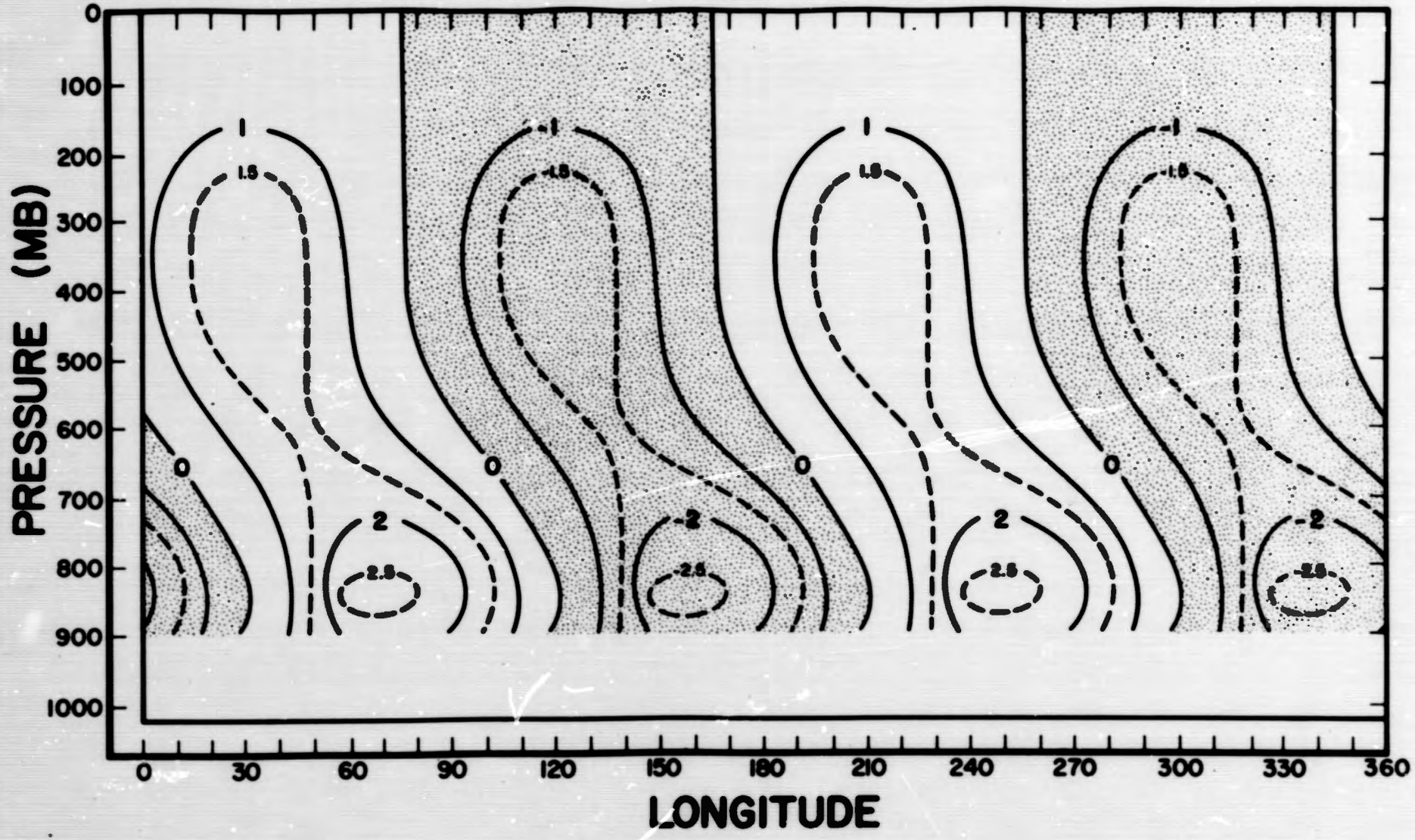

Fig. 24. Mean meridional wind response, v_1, to the internal heating function $Q_1^{(2,1)}$, along y=L/2, in units of m sec^{-1}.

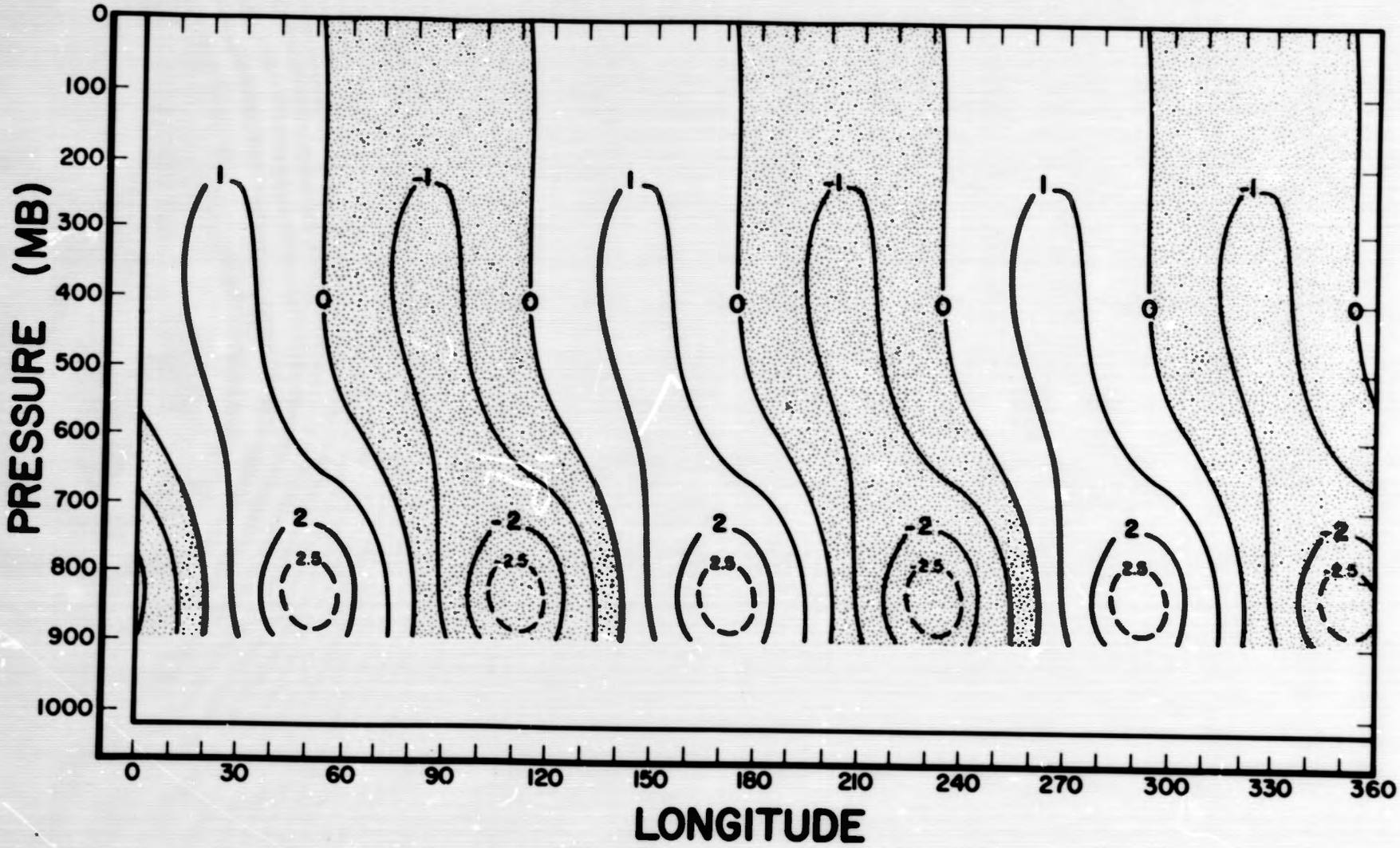

Fig. 25. Mean meridional wind response, v_1, to the internal heating function $Q_1^{(3,1)}$, along y=L/2, in units of m sec^{-1}.

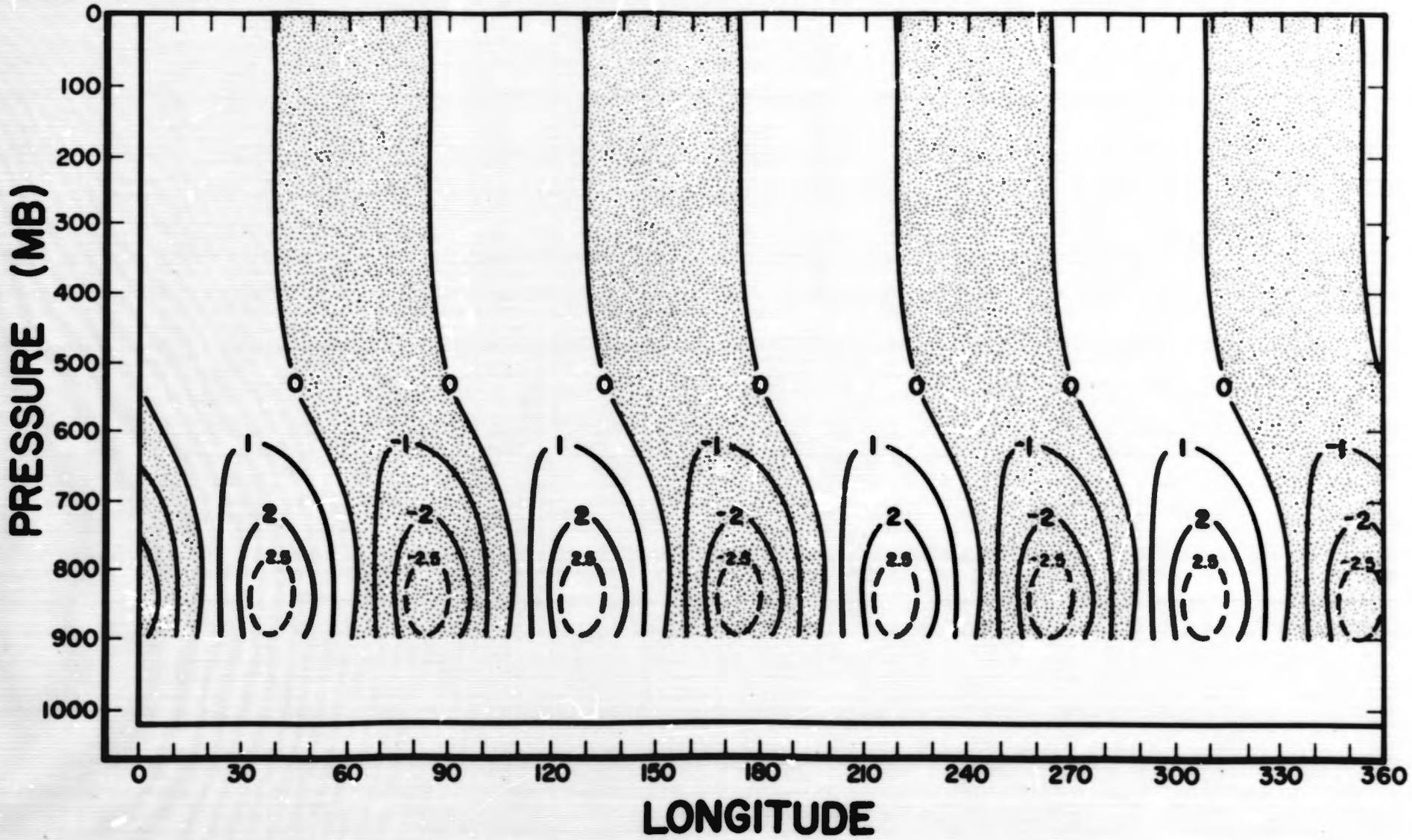

Fig. 26. Mean meridional wind response, v_1, to the internal heating function $Q_1^{(4,1)}$, along y=L/2, in units of m sec^{-1}.

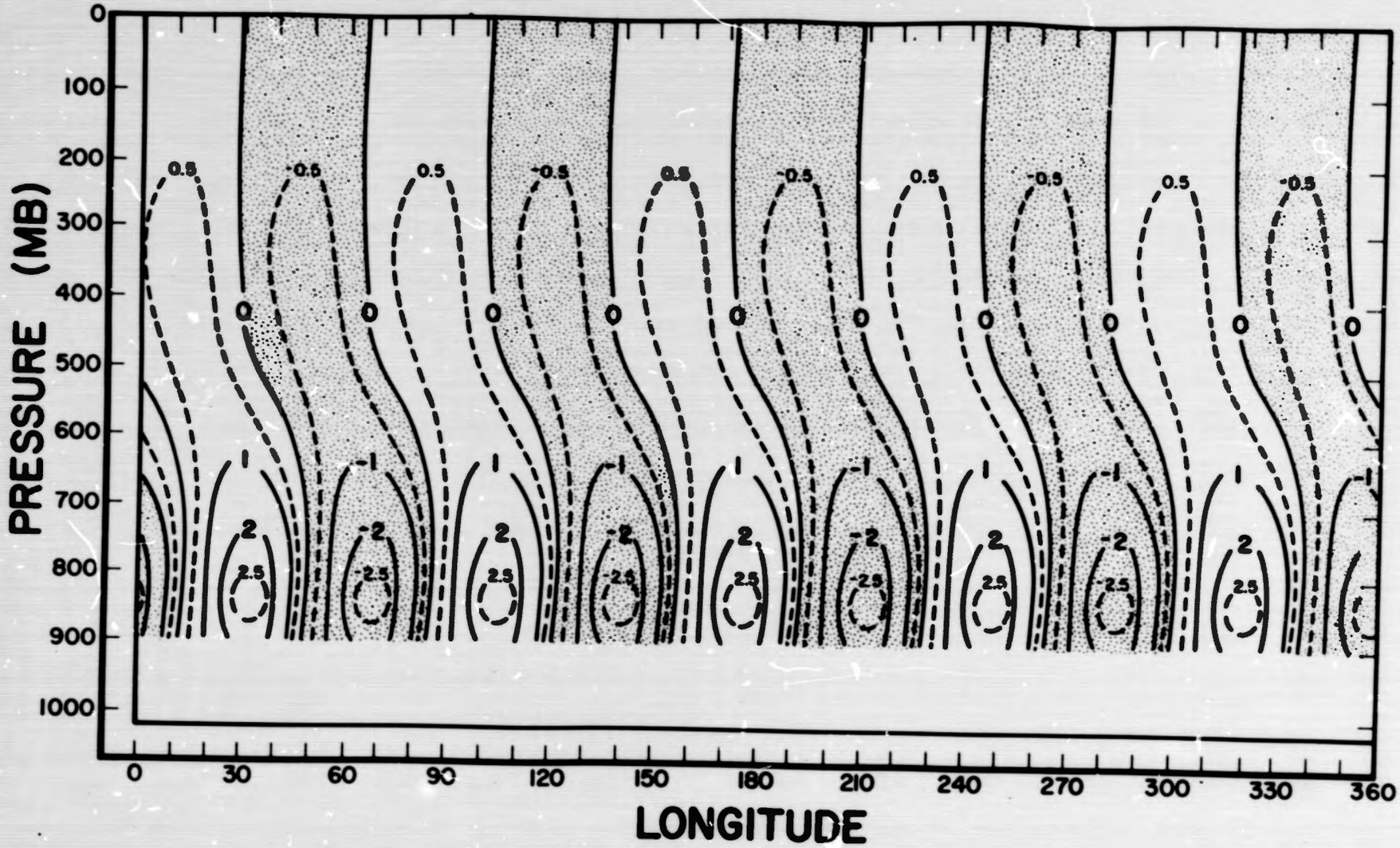

Fig. 27. Mean meridional wind response, v_1, to the internal heating function $Q_1^{(5,1)}$, along y=L/2, in units of m sec^{-1}.

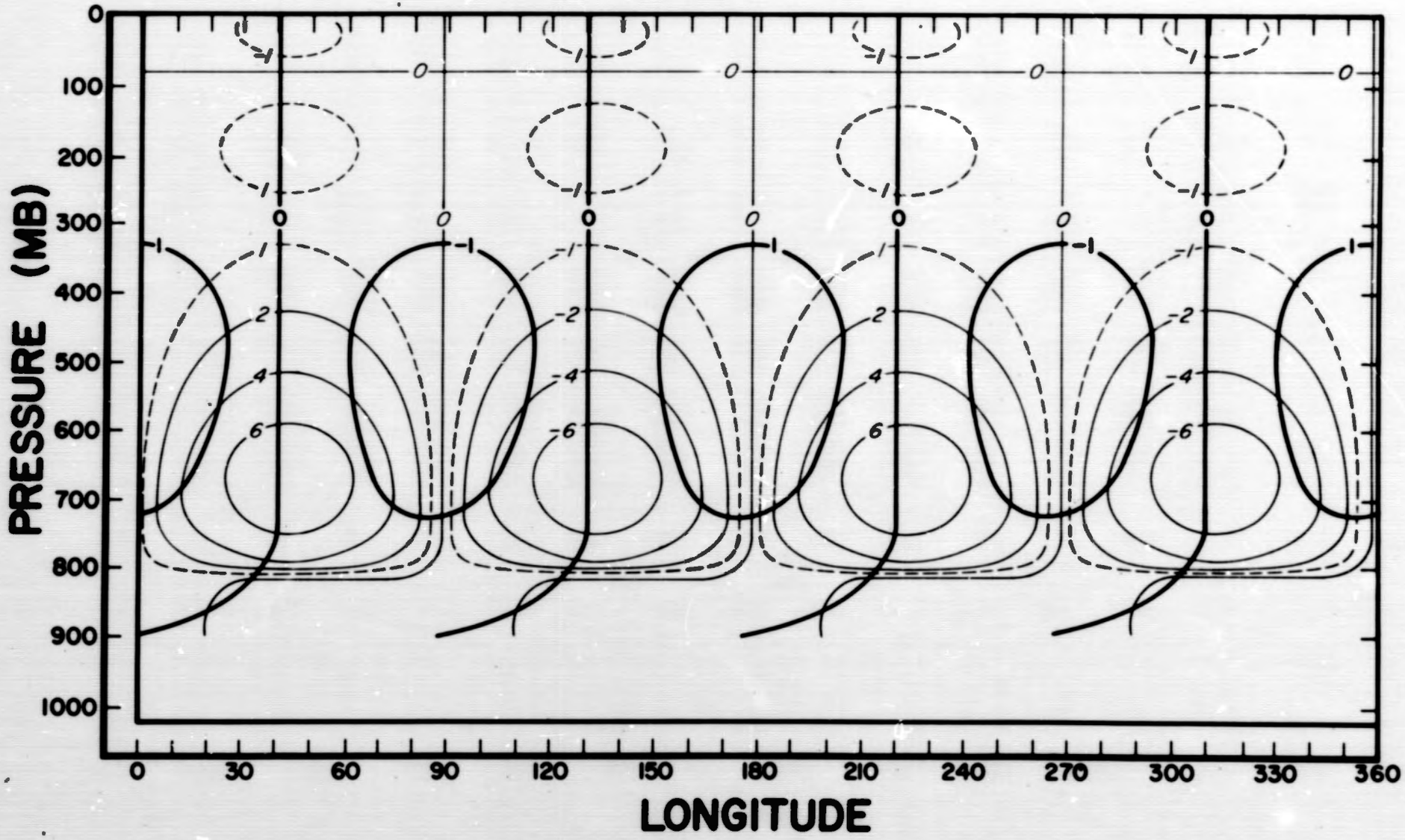

Fig. 28. Cross-section along y=L/2 of w_1 (thick line) in units of 10^{-1}gm sm^{-1} sec^{-3}, and T_1 (thin line) in units of deg, corresponding to the solution for $Q_1^{(2,0)}$ shown in Fig. 18.

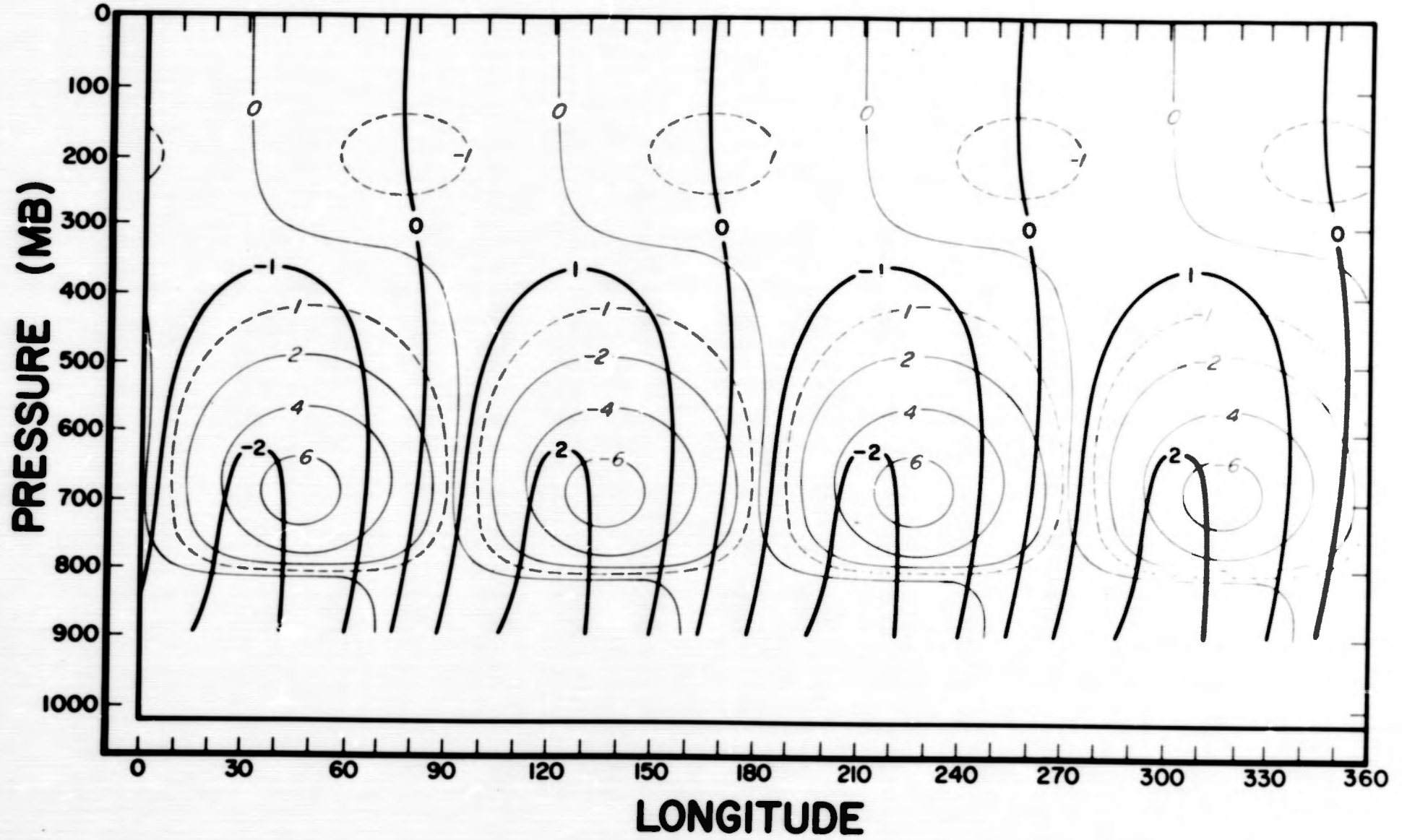

Fig. 29. Cross section along y=L/2 of w_1 (thick line) in units of 10^{-1}gm sm^{-1} sec^{-3}, and T_1 (thin line) in units of deg, corresponding to the solution for $Q_1^{(2,1)}$ shown in Fig. 18.

5. Energetics

From the basic perturbation equations and boundary conditions for our study, we can derive the following pair of equations for the energy balance of the mean perturbations:

$$\frac{d}{dt}\{A_1\} = \left\{\frac{R}{p\Gamma_0}\frac{\partial T_0}{\partial y}(v_1 T_1)_0\right\} + \left\{\frac{R}{p}(\omega_1 T_1)_0\right\} - \left\{\frac{R}{p\Gamma_0}(Q_1 T_1)_0\right\} = 0 \tag{22}$$

$$\frac{d}{dt}\{K_1\} = \left\{-(u_1\omega_1)\frac{\partial u_0}{\partial p}\right\} + \left\{-\frac{R}{p}(\omega_1 T_1)_0\right\} + \{u_1\hat{X}_1 + v_1\hat{Y}_1\} \tag{23}$$

$$- \frac{(\omega_1\phi_1)_{0S}}{p_S - p_T} + \frac{(\omega_1\phi_1)_{0T}}{p_S - p_T} = 0$$

where

$$\{()\} = \frac{1}{p_S - p_T}\int_{p_T}^{p_S}() dp$$

$A_1 = \left(-\frac{R}{p\Gamma_0}\frac{T_1^2}{2}\right)$ = Available potential energy of the mean perturbations, per unit mass

$K_1 = \left(\frac{u_1^2 + v_1^2}{2}\right)$ = Kinetic energy of the mean perturbations per unit mass

$$\phi = gz$$

$$\hat{X}_1 = X - \left(\frac{\partial\overline{u'^2}}{\partial x} + \frac{\partial\overline{u'v'}}{\partial y} + \frac{\partial\overline{u'\omega'}}{\partial p}\right)$$

$$\hat{Y}_1 = Y - \left(\frac{\partial\overline{u'v'}}{\partial x} + \frac{\partial\overline{v'^2}}{\partial y} + \frac{\partial\overline{v'\omega'}}{\partial p}\right)$$

These equations are a special case of the more general system of energy equations presented by Murakami (1960).

In our study, we have been concerned with modelling the mean state along a single parallel of latitude (45°N), and not with the properties of the solution far away from the given latitude. For this reason, we have not been concerned with assuring that the latitude band over which we made our Fourier expansion is energetically "closed." We are concerned, however, with the "contribution" which events near the given latitude circle can make to a closed system, on the assumption that conditions at this latitude circle are somewhat representative of average conditions over the whole atmosphere.

For the Fourier expansions used in the previous section, we have

$$u_1 = 0 \quad \text{at} \quad y = \frac{L}{2} \qquad (45^\circ N) \ ,$$

and we have taken

$$\hat{X}_1 = \hat{Y}_1 = 0$$

From the lower boundary condition, we have

$$\omega_{1S} = \omega_{1\phi} + \omega_{1h}$$

where

$$\omega_{1\phi} = -\rho_S g C \left(\frac{\partial v_1}{\partial x^*} - \frac{\partial u_1}{\partial y^*} \right)$$

$$\omega_{1h} \approx -\rho_S g u_{0S} \frac{\partial h}{\partial x^*}$$

From the upper boundary condition, we have

$$\phi_{1T} = 0.$$

With these relations, the kinetic energy equation (23 becomes

$$\frac{d}{dt}\{K_1\} = \left\{ -\frac{R}{p}(\omega_1 T_1)_0 \right\} + \frac{(\omega_{1\phi}\phi_{1S})_0}{p_T - p_S} + \frac{(\omega_{1h}\phi_{1S})_0}{p_T - p_S} = 0 \qquad (23')$$

The first term on the right of (23'), which has a counterpart with opposite sign in (22), represents the rate of conversion of available potential energy into kinetic energy of the mean perturbations. The second term represents the rate of frictional dissipation of kinetic energy, and the third represents the rate of generation of perturbation kinetic energy due to the presence of mountains at the lower boundary. In (22), the first term represents the rate of gain of mean perturbation potential energy from the mean zonal potential energy, and the third term represents the rate of generation of mean perturbation potential energy due to diabatic processes and heat transfers by transient eddies of all frequencies.

If we make a double Fourier expansion of ϕ_1 , T_1 , and ω_1 in the manner of (11), denoting the corresponding complex Fourier coefficients by

$$\Phi_{m,n} = \Phi^{(r)}_{m,n} - i\,\Phi^{(i)}_{m,n}$$

$$B_{m,n} = B^{(r)}_{m,n} - i\,B^{(i)}_{m,n}$$

$$\Omega_{m,n} = \Omega^{(r)}_{m,n} - i\,\Omega^{(i)}_{m,n}$$

respectively, we can write the following transforms of the energy equation for the individual harmonics (m,n),

$$\frac{d}{dt}\{A_1\}_{m,n} = \{A_0 \cdot A_1\}_{m,n} - \{A_1 \cdot K_1\}_{m,n} + \{Q_1 \cdot A_1\}_{m,n} = 0 \qquad (24)$$

where

$$\{A_0 \cdot A_1\} = \left\{\frac{2R}{p\Gamma_0}\frac{\partial T_0}{\partial y^*}\left[V^{(r)}B^{(r)} + V^{(i)}B^{(i)}\right]\right\}$$

$$\{A_1 \cdot K_1\} = \left\{\frac{2R}{p}\left[\Omega^{(r)}B^{(r)} + \Omega^{(i)}B^{(i)}\right]\right\}$$

$$\{Q_1 \cdot A_1\} = \left\{-\frac{2R}{p\Gamma_0}\left[\alpha^{(r)}B^{(r)} + \alpha^{(i)}B^{(i)}\right]\right\}$$

and $$\frac{d}{dt}\{K_1\}_{m,n} = \{A_1 \cdot K_1\}_{m,n} + \{D\}_{m,n} + \{h \cdot K_1\}_{m,n} = 0 \tag{25}$$

where

$$\{D\} = \frac{2}{p_T - p_S}\left[\Omega_f^{(n)}\Phi^{(n)} + \Omega_f^{(i)}\Phi^{(i)}\right]$$

$$\{h \cdot k_1\} = \frac{2}{p_T - p_S}\left[\Omega_h^{(n)}\Phi^{(n)} + \Omega_h^{(i)}\Phi^{(i)}\right]$$

From the geostrophic and hydrostatic relations, we have

$$V_{m,n} = \frac{2\pi m}{f K^*} i \Phi_{m,n} \tag{26}$$

$$U_{m,n} = -\frac{2\pi n}{f L^*} i \Phi_{m,n} \tag{27}$$

$$B_{m,n} = -\frac{p}{R}\frac{\partial \Phi_{m,n}}{\partial p} \tag{28}$$

and from the energy equation, we have

$$\Omega_{m,n} = \frac{f U_0 p}{\Gamma_0 R}\frac{\partial V_{m,n}}{\partial p} - \frac{1}{\Gamma_0}\frac{\partial T_0}{\partial y^*} V_{m,n} + \frac{\partial_{m,n}}{\Gamma_0} \tag{29}$$

With the use of (26) and (27), we can write the lower boundary work terms representing the effects of friction and mountains as follows

$$\{D\} = \frac{2fc\rho g}{p_T - p_S}\left(1 + \frac{n^2 k^{*2}}{m^2 L^{*2}}\right)\left[V^{(a)2} + V^{(i)2}\right] \tag{30}$$

$$\{h \cdot k_1\} = \frac{2f\rho g u_0 \delta}{p_T - p_S}\left[E^{(a)} V^{(a)} + E^{(i)} V^{(i)}\right] \tag{31}$$

It follows from (13), (15), (28), and (29) that for a single harmonic response, only to airflow over <u>mountains</u>, there can be no internal conversion of energy; i.e., $\{A_1 \cdot K_1\}$ must vanish. Hence there must be an exact balance between $\{D\}$ and $\{i \cdot k_1\}$. On the other hand, for a harmonic response, only to <u>internal heating</u> (Q_1), we must have an exact balance between frictional dissipation $\{D\}$ and the conversion of available potential energy into kinetic energy $\{A_1 \cdot K_1\}$. (By setting $\hat{X}_1 = \hat{Y}_1 = 0$ we have excluded transfer of kinetic energy between the transient perturbations and mean perturbations, the possible importance of which was discussed by the writer, 1959.)

As an example, in Table 4, we present the values of the energy conversion integrals at $y = L/2$ for $(m, n) = (2, 0)$ and $(2, 1)$ for the heating solutions only. It can be seen that the rates of dissipation and transformation of energy in the solution for (2,1) are about an order of magnitude larger than in the (2,0) solution. We also see that for the "ultra long wave" (2,0), the temperature perturbation leads the pressure perturbation with a resulting negative value of $\{A_0 \cdot A_1\}$. This is in agreement with the results of Wiin-Nielsen, (1961).

If we combine the solutions for heating and mountains for a given harmonic, or, for example, if we combine two harmonics having the same value of m but different values of n (such as is implicit in some observational studies, e.g., Saltzman and Fleisher, 1960), we introduce the possibility for a form of "resonance"

Table 4. Energy integrals, evaluated along $y = L/2$, corresponding to the solutions for $Q_1^{(2,0)}$ and $Q_1^{(2,1)}$, in units of 10^{-3} ergs gm^{-1} sec^{-1}.

Forcing Function	$\{A_0 A_1\}$	$\{A_1 K_1\}$	$\{Q_1 A_1\}$	$\{D\}$
$Q_1^{(2,0)}$	- 111	75	186	- 75
$Q_1^{(2,1)}$	1025	719	-306	-719

between the individual solutions which can lead to values of the quadratic energy integrals along $y = L/2$ which are much different from the simple sum of the integrals for the individual harmonic solutions. Thus it is possible that on one scale, the combination of fields of ω_1 and T_1 due to mountains and heating are such as to reinforce and give a large conversion of energy, and on another scale the effect may be the opposite.

6. Discussion and Conclusions

In trying to compare these theoretical results with real mean conditions in the atmosphere, we are confronted with serious difficulties due to factors falling into two main categories:

a) Lack of knowledge of the true forcing distribution - Despite recent observational studies (e.g., Clapp, 1961), we must admit that the vertical structure and amplitudes and phases of the internal forcing functions are very poorly known. In addition, the mean surface heating due to airflow over the topographic features has not yet been determined accurately, and the assumption used here of a uniform surface zonal wind may be significantly in error. It would be worthwhile to make a serious observational study of $S_1^{(4)}$ using anemometer level wind data for the global station network, as well as to make refinements of such estimates of Q_{16} as have already been given (e.g., Budyko, 1956).

b) Sensitivity of the solutions to the geometrical and basic-state parameters - The artificiality of the β -plane geometry, and the choice of the dimension L^* in particular, makes it difficult to associate the harmonic solutions with the harmonics along parallels of latitude of the real atmospheric variables. In the extreme case, it is possible to introduce quasi-resonant conditions at zonal wave numbers lower than $\omega = 5$ simply by increasing the dimension L^*. For this reason alone, we should be cautious about making comparisons with the real atmosphere.

In spite of these reservations, we should expect that the solutions obtained here do demonstrate at least the gross forms of the possible responses to forcing on different scales, the combination of which in the proper spherical geometry can account for the observations.

An an illustration of the possibilities, let us attempt to assign amplitudes and phases to the forcing functions studied here for $m = 2$ (the scale of the major continent and ocean system), based on empirical data given by Peixoto et al. (1964) and the Staff members, Academia Sinica (1958). The forms taken are,

$$h_1(x,y) = \Lambda_1 \cos 2(kx - \epsilon)\cdot(1 - \cos ly) \tag{32}$$

where

$$\Lambda_1 = \frac{C_{2,0}}{2} = C_{2,1} = 100 \text{ meters}$$

$$\epsilon = 85^\circ\text{E longitude}$$

and

$$Q_1(x,y,p) = \Lambda_2 A(p) \cos 2(kx - \theta)\cdot(1 - \cos ly) \tag{33}$$

where

$$\Lambda_2 = 2|N_{2,0}| = 4|N_{2,1}| = 1.5 \times 10^{-5} \text{ deg sec}^{-1}$$

$$\theta = 155^\circ\text{E longitude}$$

and $A(p)$ is given in Figure 16.

The solutions are given in Figures 30 and 31, respectively, in the form of cross sections of v_1 along $y = L/2(45^\circ\text{N})$. Comparison with the results of Teweles (1963) for 500 mb and 50 mb indicate that the heating solution in particular shows a good deal of agreement with the observations, with nearly correct positioning and amplitude of the stratospheric and mid-tropospheric mean waves.

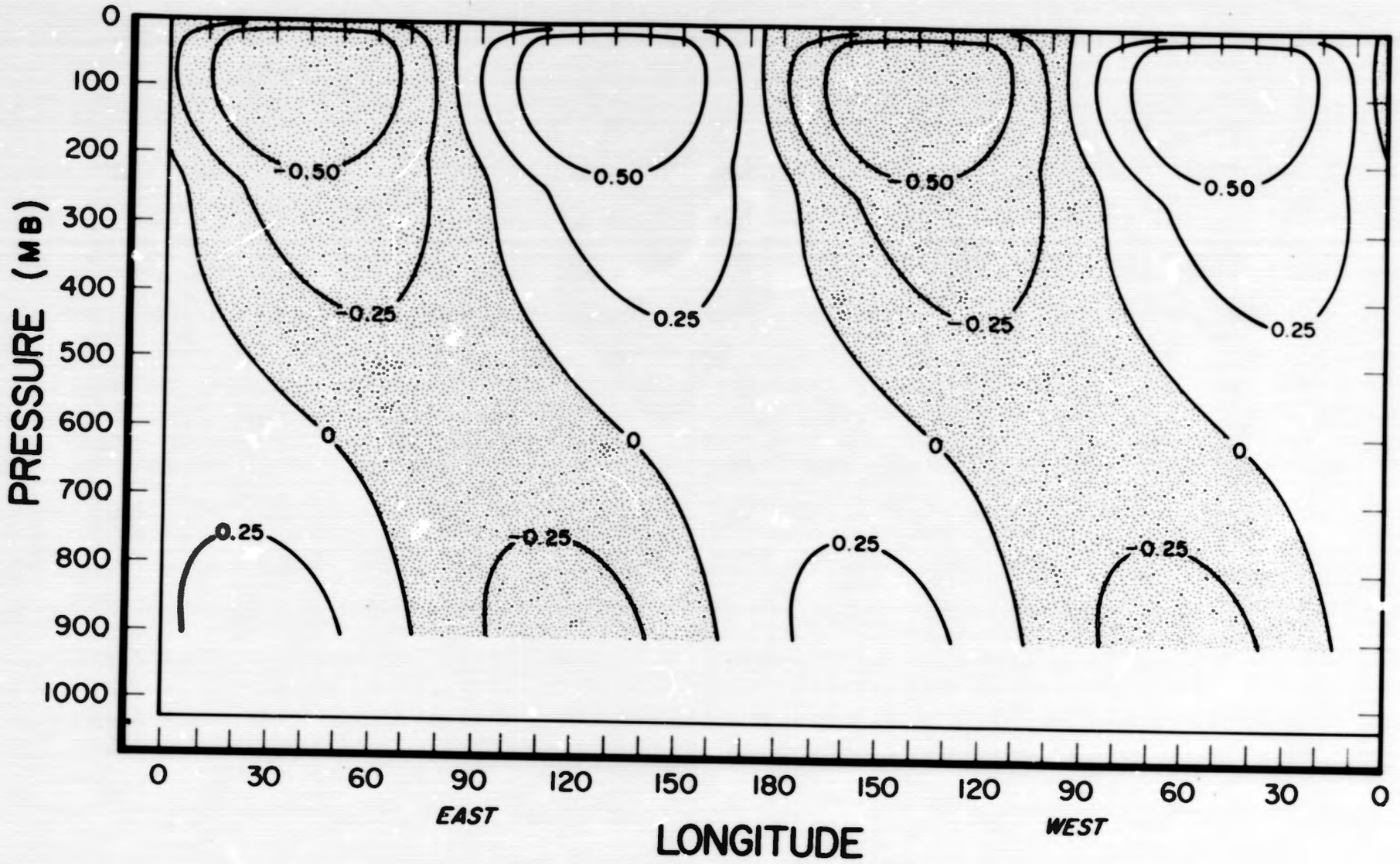

Fig. 30. Mean meridional wind response, v_1, along 45°N, to uniform airflow over the topographic representation (32), in units of m sec^{-1}.

Acknowledgements

I am grateful to Dr. M. Sankar Rao for the benefit of discussions on this problem, to Mr. John Sopka for programming assistance, to Mr. Charles Gadsden for computational assistance, and to Miss Peggy Atticks for typing the manuscript.

This work has been supported by the U.S. Weather Bureau under Contract Number Cwb-10763 and was written in part during my stay at the National Center for Atmospheric Research.

Teweles, S., 1963: A spectral study of the warming epoch of January-February 1958. Mon. Wea. Rev., 92, 505-519.

Wiin-Nielsen, A., 1961: On the distribution of temperature relative to height in stationary planetary waves. Tellus, 13, 127-139.

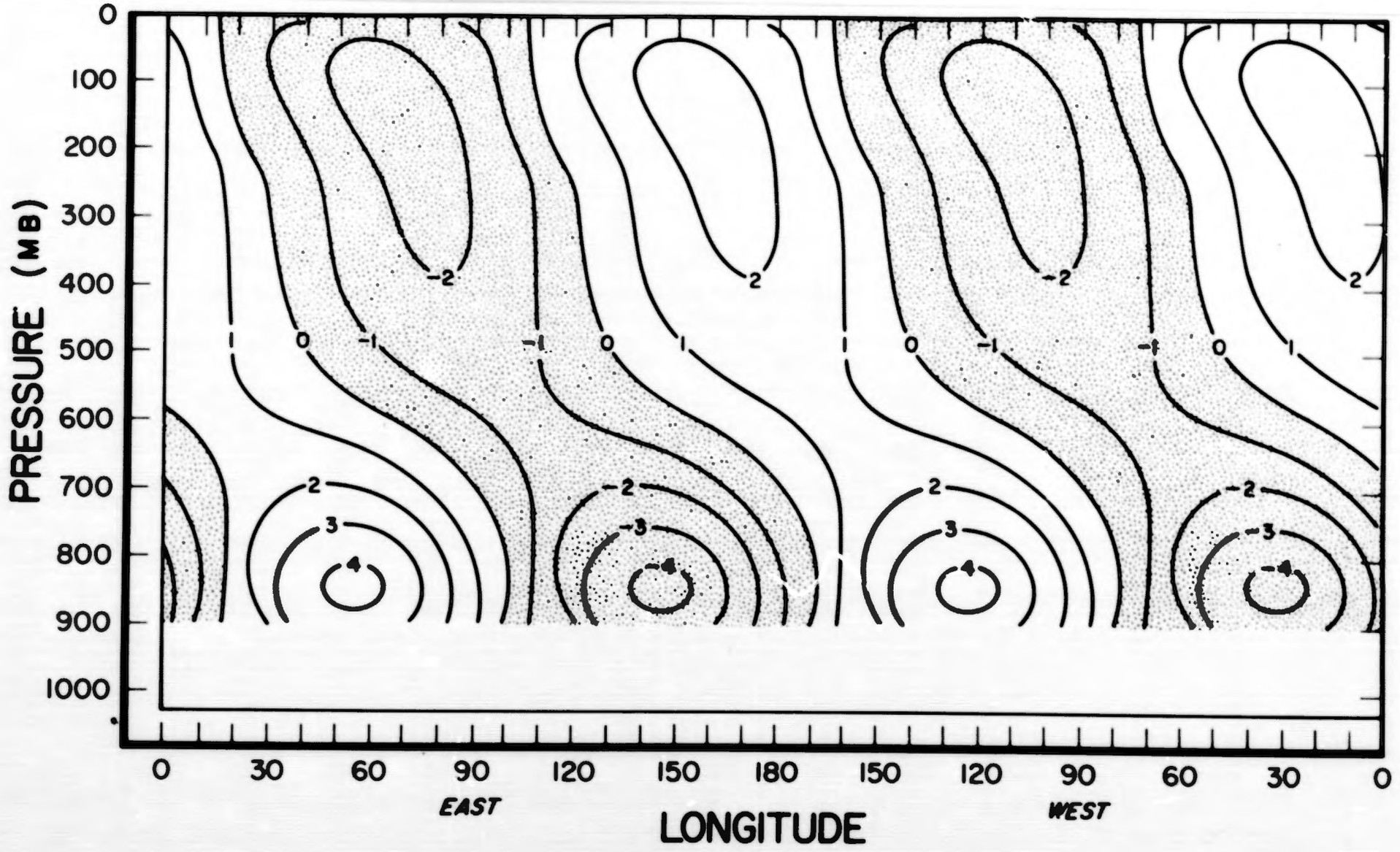

Fig. 31. Mean meridional wind response, v_1, along 45°N, to the internal heating function (33), in units of m sec^{-1}.

The possibility of achieving plausible solutions for the troposphere was demonstrated in the previous study by the writer (1963), as well as by the studies of Smagorinsky (1953) and Döös (1962), for example. We view the results here as demonstrating the possibility for accounting also for the stratospheric mean state as a response to forcing processes within the troposphere.

In conclusion, we refer the reader to the list of general suggestions for the improvement and extension of the problem of the mean waves which were given in the last section of the previous study (1963). Our main concern here has been with item 4 of this list which called for improvement of the representation of the basic zonal state. Much work remains to be done on this as well as the other items. The recent work of Rao (1964), which is based on numerical rather than analytical methods, seems especially promising.

Peixoto, J.P., Saltzman B., and Teweles, S., 1964: Harmonic analysis of the topography along parallels of the earth. J. Geophys. Res., 69, 1501-1505.

Phillips, N., 1963: Geostrophic motion. Rev. Geophys., 1, 123-176.

Rao, M. Sankar, 1964: Finite difference models for the stationary harmonics of atmospheric motion (to be published).

Saltzman, B., 1959: On the maintenance of the large-scale quasi-permanent disturbances in the atmosphere. Tellus, 11, 425-431.

Saltzman, B., 1961: Perturbation equations for the time-average state of the atmosphere including the effects of transient disturbances. Geofisica Pura e Applicata, 48, 143-150.

Saltzman, B., 1962: Empirical forcing functions for the large-scale mean disturbances in the atmosphere. Geofisica Pura e Applicata, 52, 173-183.

Saltzman, B., 1963: A generalized solution for the large-scale, time-average, perturbations in the atmosphere. J. Atmos. Sci., 20, 226-235 (Corrigenda, ibid., 20, 465).

Saltzman, B., and A. Fleisher, 1960: The exchange of kinetic energy between larger scales of atmospheric motion. Tellus, 12, 374-377.

Saltzman, B., and J.P. Peixoto, 1957: Harmonic analysis of the mean Northern Hemisphere wind field for the year 1950, Quart. J. R. Met. Soc., 83, 360-364.

Saltzman, B., and M.S. Rao, 1963: A diagnostic study of the mean state of the atmosphere. J. Atmos. Sci., 20, 438-447.

Smagorinsky, J., 1953: The dynamical influence of large-scale heat sources and sinks on the quasi-stationary mean motions of the atmosphere. Quart. J. R. Met. Soc., 79, 342-366.

Staff Members, Academia Sinica, 1958: On the general circulation over eastern Asia (II), Tellus, 10, 299-312.

Stern, M.E., and Malkus, J.S., 1953: The flow of a stable atmosphere over a heated island, Part II., J. Meteor., 10, 105-120.

References

Arctic Meteorology Research Group, 1963: An atlas of stratospheric circulation. Publ. No. 56, Dept. of Meteor., McGill University, Montreal.

Barrett, E.W., 1961: Some applications of harmonic analysis to the III. A theory of three-dimensional atmospheric waves, with special reference to topographically induced perturbations. Beitr. Phys. Atmos., 34, 167-197.

Budyko, M.I., 1954: The Heat Balance of the Earth's Surface, Hydrometeorological Publishing House, Leningrad, 254 pp. (Translated by N.A. Stepanova, U.S. Weather Bureau, 1958).

Burger, A.P., 1958: Scale consideration of planetary motions of the atmosphere. Tellus, 10, 195-205.

Charney, J.G. and A. Eliassen, 1949: A numerical method for predicting the perturbations of the middle latitude westerlies. Tellus, 1, 38-54.

Clapp, P.F., 1961: Normal heat sources and sinks in the lower troposphere in winter. Mon. Wea. Rev., 89, 147-162.

Crutcher, H.L., 1959: Upper wind statistics charts of the Northern Hemisphere. Office of the Chief of Naval Operations, NAVAER 50-1C-535, 2 Vols.

Dóös, B.R., 1962: The influence of exchange of sensible heat with the earth's surface on the planetary flow. Tellus, 14, 133-147.

Gates, W.L. 1961: Static stability measures in the atmosphere. J. Meteor., 18, 526-533.

Gilchrist, B., 1953: The seasonal phase changes of thermally produced perturbations in the westerlies. Proceedings of the Toronto Meteorological Conf., 129-131.

Murakami, T., 1960: On the maintenance of kinetic energy of the large-scale stationary disturbances in the atmosphere. Sci. Rpt. No. 2, M.I.T. Planetary Circulations Project, Contract No. AF 19(604)-6108, 42pp.

BLANK PAGE

PAPER B

FINITE DIFFERENCE MODELS FOR THE STATIONARY HARMONICS OF ATMOSPHERIC MOTION

M. Sankar Rao

ABSTRACT

A finite difference procedure is utilized for the solution of a coupled system of two ordinary differential equations governing the time averaged quasi-geostrophic perturbations in the atmosphere. Some interesting effects of the seasonal changes in the zonal mean state are discussed.

1. Introduction

The long standing debate on the relative importance of the thermal and orographic influences in maintaining the stationary zonally-asymmetric perturbations of the atmosphere can not yet be considered resolved despite much theoretical effort on this subject. As is well known, the solutions of the linearised approximate potential vorticity equation for the stationary zonally-asymmetric state, which is the basis of the most of the theoretical discussions, are controlled not only by the assumed distribution of the forcing due to the thermal, orographic and transient eddy effects, but also by the assumed form of the basic zonal mean state, rotation, and friction. Even when the forcing functions are assumed to be explicitly known, this equation in its general form is not separable except under certain restrictive assumptions regarding the zonal mean state, the coriolis parameter f and its variation with latitude β. The theoretical studies up to the recent past naturally fall into four broad groups, depending on the combination of, and assumptions about the influencing factors considered in each case.

A. Researches in which the effect of forcing due to heating only is investigated

In these works, some or all the variables of the basic zonal mean state are generally considered either constant or pressure dependent only. f and β are taken as constants. Friction is generally considered. Sometimes when an equivalent barotropic or two-level baroclinic model is used, implicit assumptions are made regarding the variation of even the zonally asymmetric perturbations with pressure. Examples of studies in this group are Smagorinsky (1953),

Gilchrist (1953), Delisle and Harper (1961), and Döös (1961)[1].

B. Studies in which the effect of forcing due to orography only is investigated

In these researches, the treatment of the basic zonal mean state, f, β and friction is similar to that of the thermal case, and here also, implicit assumptions are usually made regarding the variation of the zonally-asymmetric perturbations with pressure. Examples are Queney (1948), Charney and Eliassen (1949), Bolin (1940), Gambo (1956, 1957), Magata (1957), and Kawata (1957).

C. Investigations in which attempts are made to study the results of forcing due to a combination of heating, orography, and transient eddy effects, of different spatial scales

In these studies, also, the treatment of the basic zonal mean state, f, β and friction is similar to the above cases. No assumptions are made regarding the variation of the zonally-asymmetric perturbations with pressure (e.g., Saltzman, 1963, 1964).

D. Researches in which attention is focussed not only on the forcing functions, but also on the latitudinal variation of f and u_0, the zonal mean east-west component of the wind

Friction is not considered in these works. In some cases, mainly as a mathematical expedient, barotropy, or in effect equivalent barotropy, is forced on the zonal mean state or on both the zonal mean state and the perturbations. Examples of studies of this kind are Kuo (1958)[2], Staff Members Academia Sinica (1957), and Barrett (1961).

---

1 Döös parameterised one part of the heating by a heating function similar to that used by Mintz (1958). Future advances seem to lie in parameterisations of this kind.

2 Though Kuo treated a homogeneous problem, his work is of great importance for the question of forced perturbations.

In addition to these theoretical works, a great number of published diagnostic observational results are of pertinence to this problem. Examples are Sutcliffe (1951), Haurwitz and Craig (1952), Saltzman and Peixoto (1957), Van Mieghem, Defrise, and Van Isacker (1960), Clapp (1960), Saltzman and Fleisher (1962), and Saltzman and Rao (1963).

Even when the components of the basic zonal mean state are taken as functions of pressure alone, the analytical solution of the resulting coupled system of ordinary differential equations, is very laborious and time consuming. Introduction of realistic zonal mean vertical profiles is extremely difficult, if not impossible in the usual analytical methods. It is the main purpose of this paper to demonstrate a powerful finite difference method which not only reduces the labor to an insignificant amount of computer time, but also opens new possibilities for many kinds of numerical experimentation. As examples, some interesting results will also be discussed.

2. Approximate Equation Governing the Time Averaged Axially Asymmetric Perturbations of the Atmosphere

We adopt the same notation of Saltzman (1964-) except for the following changes. x^*, y^*, x, y, Q, H, and the subscript δ of Saltzman, are replaced here by X, Y, A_x, A_y, H, Q and the subscript $\vdash$, respectively. Also, we further define

$$D_* = \bar{D} - D_0$$

$$k = \Pi^{-1}$$

$$X = L x$$

$$Y = L y$$

$$\xi = P_s P$$

where

D = Any dependent variable

L = Any scaling length $\neq 0$

P_s = Any scaling pressure $\neq 0$.

With the use of the above notation, the approximate nondimensionalised equations governing the time averaged axially asymmetric perturbations of the atmosphere, along with the top and bottom boundary conditions, in X , Y and ξ system, assume the form (Saltzman 1964).

$$\frac{\partial^2 v_*}{\partial x^2} + \frac{\partial^2 v_*}{\partial y^2} + \gamma \frac{\partial^2 v_*}{\partial \xi^2} + \delta \frac{\partial v_*}{\partial \xi} + \epsilon v_* = (L^2 F_*) / u_0 \qquad (1)$$

$$\frac{\partial v_*}{\partial \xi} + b v_* = d H_* \qquad \text{at } \xi = \xi_T \qquad (1a)$$

$$\frac{\partial v_*}{\partial \xi} + B v_* + C \left(\frac{\partial v_*}{\partial x} - \frac{\partial u_*}{\partial y} \right) = E \frac{\partial h_*}{\partial x} + N H_* \qquad \text{at } \xi = \xi_b \qquad (1b)$$

where

$$\gamma = \gamma_{(y,\xi)} = (-L^2 f^2 \rho K_0) / P_s^2 R$$

$$\delta = \delta_{(y,\xi)} = \left(-L^2 f^2 \frac{\partial}{\partial \xi} [\rho K_0] \right) / P_s R$$

$$\epsilon = \epsilon_{(y,\xi)} = \frac{L}{u_0} \left[\frac{\partial \eta_0}{\partial y} + \frac{f}{P_s} \frac{\partial}{\partial \xi} \left(K_0 \cdot \frac{\partial T_0}{\partial y} \right) \right]$$

$$\eta_0 = \left[f - \frac{1}{L} \frac{\partial u_0}{\partial y} \right]$$

$$b = b_{(y)} = -\frac{P_s R}{u_o P_f}\,\frac{1}{L}\,\frac{\partial T_o}{\partial y} \qquad \text{at } \xi = \xi_T$$

$$d = d_{(y)} = (-P_s R)/u_o P_f \qquad \text{at } \xi = \xi_T$$

$$B = B_{(y)} = -\frac{P_s R}{u_o P_f}\,\frac{1}{L}\,\frac{\partial T_o}{\partial y} \qquad \text{at } \xi = \xi_b$$

$$\tau = \tau_{(y)} = \frac{g \rho_b C}{K_o L} \cdot \frac{P_s R}{u_o P_f} \qquad \text{at } \xi = \xi_b$$

$$E = E_{(y)} = -\frac{g \rho_b}{K_o L}\,\frac{P_s R}{P_f} \qquad \text{at } \xi = \xi_b$$

$$N = N_{(y)} = (-P_s R)/u_o P_f \qquad \text{at } \xi = \xi_b$$

In the X and Y direction, we assume periodicity. Also here F_*, H_*, and h_*, which denote the axially asymmetric manifestation of internal and external forcing functions, and γ, δ, ϵ, b, d, B, τ, E, and N, which denote the axially symmetric state, are considered given.

3. Mathematical Problem

Given the coefficients and forcing functions in (1), (1a), and (1b), the problem is to solve (1) with periodicity conditions in the X and Y directions, while at ξ_T and ξ_b, (1a) and (1b) have to be satisfied respectively. Before considering the relaxation technique which naturally suggests itself for such a problem, we should note that the lower boundary condition (1b) contains a second dependent variable u_* which can be written in

terms of $\mathcal{V}_*$ through the geostrophic assumption. Then (1), (1a), and (1b) will be in one dependent variable v_* only, but (1b) will be an integro-differential equation. The order change by the introduction of geopotential will not solve the difficulties completely. This is because the zero order term in (1) is usually positive for most of the earth's atmosphere. It is found that under these circumstances the relaxation method can not be applied to solve (1) with its above mentioned boundary conditions (Rao 1963). Thus mostly for mathematical expediency, we assume that

(Assumption 1) $D_0 = D_0(\xi)$ AND

(Assumption 2) $\frac{1}{L}\frac{\partial f}{\partial y} = \beta = \text{CONSTANT}$

so that $\gamma = \gamma(\xi)$, $\delta = \delta(\xi)$, $\epsilon = \epsilon(\xi)$ while σ, d, B, τ, E, N become constants. Now let us introduce σ_k, d_k, B_k, τ_k, E_k, and N_k to denote the new constants σ, d, B, τ, E, and N respectively. Also let $\overbrace{H}$, Θ, and $\wedge$ represent $\gamma(\xi)$, $\delta(\xi)$, and $\epsilon(\xi)$ respectively. With this notation, (1), (1a), and (1b) take the form

$$\frac{\partial^2 v_*}{\partial x^2} + \frac{\partial^2 v_*}{\partial y^2} + \overbrace{H}\frac{\partial^2 v_*}{\partial \xi^2} + \Theta\frac{\partial v_*}{\partial \xi} + \wedge v_* = G_* \qquad (2)$$

$$\frac{\partial v_*}{\partial \xi} + \sigma_k v_* = d_k H_* \quad \text{at} \quad \xi = \xi_T \qquad (2a)$$

$$\frac{\partial v_*}{\partial \xi} + B_k v_* + \tau_k\left(\frac{\partial v_*}{\partial x} - \frac{\partial u_*}{\partial y}\right) = E_k\frac{\partial h_*}{\partial x} + N_k H_* \quad \text{at } \xi = \xi_b \qquad (2b)$$

where

$$G_* = (L^2 F_*)/u_0$$

The simplified problem is now to solve (2) with its prescribed boundary conditions. To this effect, we can now use the double Fourier expansion method which is equivalent to the method of separation of variables.

4. Fourier Expansion and the Resulting System of Ordinary Differential Equations

Assuming that all the time averaged axially asymmetric dependent variables satisfy the Dirichlet conditions, we can expand any such dependent variable D_* as

$$D_*(X,Y,\xi) = \sum_{m=1}^{\infty} \sum_{n=0}^{\infty} \left[D^{\xi}_{1,m,n} \cos \frac{2\pi m X}{\ell} + D^{\xi}_{2,m,n} \sin \frac{2\pi m X}{\ell} \right] \cos \frac{2\pi n Y}{k} +$$

$$+ \left[D^{\xi}_{3,m,n} \cos \frac{2\pi m X}{\ell} + D^{\xi}_{4,m,n} \sin \frac{2\pi m X}{\ell} \right] \sin \frac{2\pi n Y}{k} .$$

Here ℓ and k are the lengths of the fundamental region in X and Y directions respectively. m and n are wave numbers. The subscripts m, n and ξ indicate that the Fourier coefficients are functions of m, n and ξ.

Now dropping subscripts m, n and ξ for convenience in writing and substituting expansions of the above type in (2), (2a), and (2b) we get two coupled systems of ordinary differential equations with ξ as the independent variable (after writing u_* in terms of v_* in (2b) through the grostrophic

approximation) as follows:

First System -

$$\frac{d^2 v_1}{d\xi^2} + \Theta \frac{dv_1}{d\xi} + (\Lambda - \nu^2) v_1 = G_1 \qquad (3)$$

$$\frac{dv_1}{d\xi} + b_k v_1 = d_k H_1 \quad \text{at } \xi = \xi_T \qquad (3a)$$

$$\frac{dv_1}{d\xi} + B_k v_1 + c_k \cdot \frac{l\nu^2}{2m\pi} v_2 = E_k \cdot \frac{2m\pi}{l} h_2 + N_k H_1 \quad \text{at } \xi = \xi_b \qquad (3b)$$

$$\frac{d^2 v_2}{d\xi^2} + \Theta \frac{dv_2}{d\xi} + (\Lambda - \nu^2) v_2 = G_2 \qquad (4)$$

$$\frac{dv_2}{d\xi} + b_k v_2 = d_k H_2 \quad \text{at } \xi = \xi_T \qquad (4a)$$

$$\frac{dv_2}{d\xi} + B_k v_2 - c_k \cdot \frac{l\nu^2}{2m\pi} v_1 = -E_k \cdot \frac{2m\pi}{l} h_1 + N_k H_2 \quad \text{at } \xi = \xi_b \qquad (4b)$$

Here

$$\nu^2 = 4\pi^2 \left[\frac{m^2}{l^2} + \frac{n^2}{k^2} \right]$$

Symbols with lower subscripts 1 and 2 refer to the Fourier coefficients, which are functions of m, n, and ξ, for the respective dependent variables. We note that the coupling in the first system comes through the friction term.

Second System -

The second system is exactly similar to the first; the lower subscripts 3 and 4 replacing 1 and 2 respectively in the first system.

5. Some Remarks

We shall concern ourselves with the first system only because the second system is exactly similar. The first system is generally solved (Smagorinsky, 1953 ; Saltzman, 1963) by making further analytical assumptions regarding the coefficients, Ξ , Θ , and $\wedge$ so that the resulting second order ordinary differential equations contain coefficients which are linear functions of the independent variable and therefore can always be transformed to standard confluent hypergeometric type of equations (c.f., Bateman, 1953, p. 249). At this point, we shall depart from the analytical approach and follow a finite difference method. For this we have to assume that

(Assumption 3) No point of the finite difference lattice for the region considered coincides with a singular point.

6. Finite Difference Method of Solution

The fundamental difficulty in applying the finite difference technique to solve the system (1) is the coupling which cannot be broken up by simple addition or subtraction. The first method, naturally suggesting itself, is to take an arbitrary v_2 and solve for v_1 from (3), (3a), and (3b) and take that v_1 and solve for a new v_2 from (4), (4a), and (4b) and to repeat this process until we arrive at stationary values of v_1 and v_2 . There is no guarantee that such a process will lead to convergence unless we are able to

prove it by numerical analysis. A superior method which takes advantage of the fact that the upper boundary conditions are not coupled, will be described now. In this context we shall introduce multiple letter symbols which are like FORTRAN floating point variables.

A. The finite difference interior equation

The centered difference equation corresponding to (3) can be written at any grid point j as (Fig. 1)

$$A2N(j)\,U_1(j+1)+BIN(j)\cdot U_1(j-1)+CON(j)\cdot U_1(j)=DFN(j) \qquad (5)$$

where

$$A2N(j)=2\cdot\overline{H}(j)-\Theta(j)\cdot\delta\xi$$

$$BIN(j)=2\cdot\delta\xi^2\cdot\Lambda(j)-4\cdot\overline{H}(j)$$

$$CON(j)=2\cdot\overline{H}(j)+\Theta(j)\cdot\delta\xi$$

$$DFN(j)=2\cdot\delta\xi^2\cdot G_1(j)$$

$\delta\xi$ = grid spacing

j = an index referring to grid points from 1 to J.

$$(J-1)\delta\xi=\left[\xi_r-\xi_b\right]$$

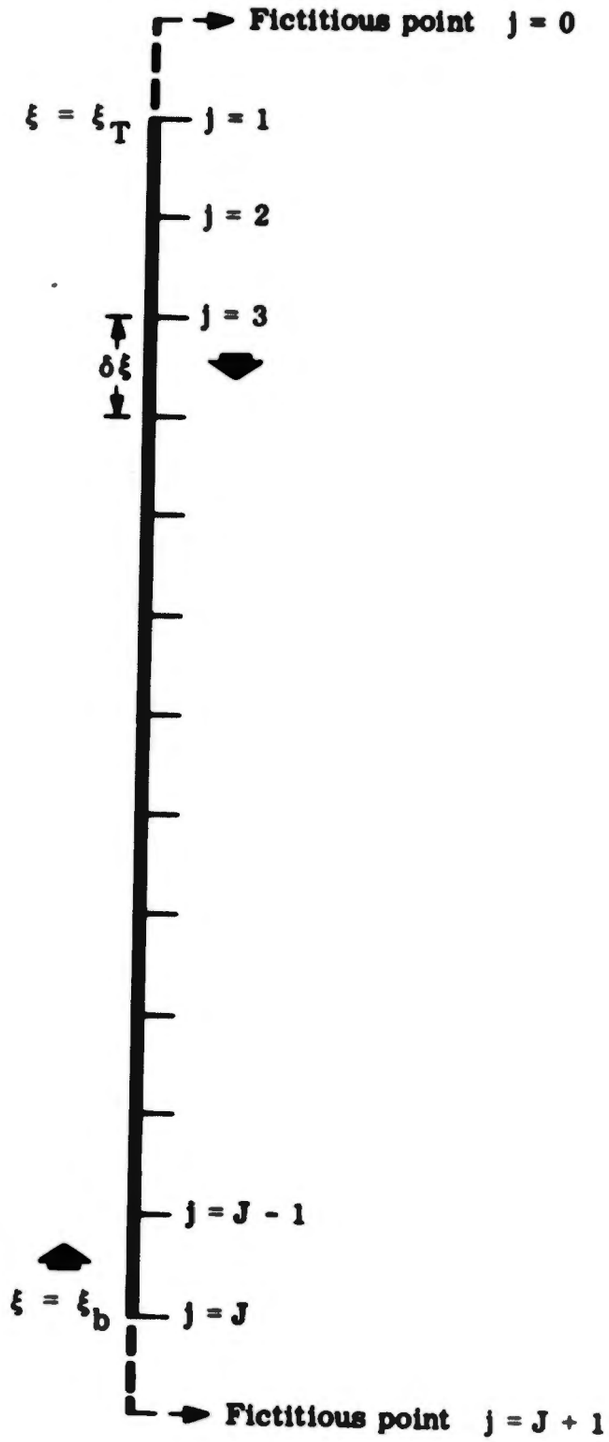

Fig. 1. Finite difference scheme.

of increasing j ($j = 1, 2, 3 \cdots J-1$) . Now we use the lower boundary condition to get $v_1(J)$ and $v_2(J)$.

C. Application of the lower boundary condition

As in the case of upper boundary condition, we invoke the Assumption 4, introduce a fictitious point at $J+1$, and write the boundary condition at J in the finite difference form. Thus we get

$$[A2N(J) + CON(J)]\, v_1(J-1) + [BIN(J) + A2N(J) \cdot gLIN] \cdot v_1(J) -$$
$$- [DFN(J) + A2N(J) \cdot hLIN] + A2N(J) \cdot FRN(J) \cdot v_2(J) = 0 \qquad (5b)$$

$$[A2N(J) + CON(J)]\, v_2(J-1) + [BIN(J) + A2N(J) \cdot gL2N] \cdot v_2(J) - \qquad (6b)$$
$$- [EFN(J) + A2N(J) \cdot hL2N] - A2N(J) \cdot FRN(J) \cdot v_1(J) = 0$$

where,

$$gLIN = 2 \cdot \delta\xi \cdot \tau_k \frac{l\nu^2}{2m\pi} = gL2N \qquad \text{at } j = J$$

$$FRN = 2 \cdot \delta\xi \cdot \tau_k \cdot \frac{l\nu^2}{2m\pi} \qquad \text{at } j = J$$

$$hLIN = 2 \cdot \delta\xi \cdot \left[E_k \cdot \frac{2m\pi}{l} h_2 + N_k H_1 \right] \qquad \text{at } j = J$$

$$hL2N = 2 \cdot \delta\xi \cdot \left[-E_k \cdot \frac{2m\pi}{l} \cdot h_1 + N_k H_2 \right] \qquad \text{at } j = J$$

we can write for $v_1(J-1)$ and $v_2(J-1)$ in (5b) and (6b), as

$$v_1(J-1) = E1N(J-1) \cdot v_1(J) + F1N(J-1) \qquad (5b.1)$$

$$v_2(J-1) = E2N(J-1) \cdot v_2(J) + F2N(J-1) \qquad (6b.1)$$

$$FIN(1) = \frac{[DFN(1) - CON(1) \cdot HIN]}{[BIN(1) - CON(1) \cdot GIN]} \qquad (5a.2)$$

$$E2N(1) = -\frac{[A2N(1) + CON(1)]}{[BIN(1) - CON(1) \cdot G2N]} \qquad (6a.1)$$

$$F2N(1) = \frac{[EFN(1) - CON(1) \cdot h2N]}{[BIN(1) - CON(1) \cdot G2N]} \qquad (6a.2)$$

$$GIN = 2 \cdot \delta\xi \cdot b_k \quad \text{at } j = 1$$

$$G2N = 2 \cdot \delta\xi \cdot b_k \quad \text{at } j = 1$$

$$HIN = 2 \cdot \delta\xi \cdot d_k \cdot H_1 \quad \text{at } j = 1$$

$$H2N = 2 \cdot \delta\xi \cdot d_k \cdot H_2 \quad \text{at } j = 1$$

From (5.1), (5.2), (6.1), (6.2) together with (5a.1), (5a.2), (6a.1), (6a.2) we can inductively calculate $EIN(j)$, $E2N(j)$, $FIN(j)$, and $F2N(j)$ in order

$$F2N(j) = \frac{[EFN(j) - CON(j) \cdot F2N(j-1)]}{[BIN(j) + CON(j) \cdot E2N(j-1)]} \qquad (6.2)$$

In order to get $EIN(1)$, $FIN(1)$, $E2N(1)$, and $F2N(1)$ which are necessary to calculate $EIN(j)$, $FIN(j)$, $E2N(j)$, and $F2N(j)$ from (5.1), (5.2), (6.1), and (6.2), we introduce the boundary condition at ξ_T.

B. Application of the upper boundary condition

To introduce the boundary conditions in finite difference form, we will assume that,

(Assumption 4) The dependent variables v_1 and v_2 are continuous across the boundaries at ξ_T and ξ_0 so that the interior equation as well as the boundary conditions are to be fulfilled at $j = 1$ and at $j = J$.

With this assumption, we can now introduce fictitious points at $j = 0$ and $j = J+1$ (see Fig. 1). Now if we write the upper boundary condition at $j = 1$ in the centered difference form and require that the iterative type of equations (5) and (6) must hold for any member of the family, we get

$$v_1(1) = EIN(1) \cdot v_1(2) + FIN(1) \qquad (5a)$$

$$v_2(1) = E2N(1) \cdot v_2(2) + F2N(1) \qquad (6a)$$

where

$$EIN(1) = - \frac{[A2N(1) + CON(1)]}{[BIN(1) - CON(1) \cdot GIN]} \qquad (5a.1)$$

and $D(j)$ = value of any dependent variable D at j . Here, without any loss of generality, we assumed that ξ is decreasing from 1 to J .

The centered difference equation for (4) is written similarly as

$$A2N(j)\, v_2(j+1) + BIN(j) \cdot v_2(j-1) + CON(j) \cdot v_2(j) = EFN(j) \qquad (6)$$

Now we consider a one parameter family of solutions for v_1 and v_2 which are of the iterative type (Ritchmyer, 1957, p. 103),

$$v_1(j) = EIN(j) \cdot v_1(j+1) + FIN(j)$$
$$v_2(j) = E2N(j) \cdot v_2(j+1) + F2N(j)$$

where

$$EIN(j) = \frac{-A2N(j)}{[BIN(j) + CON(j) \cdot EIN(j-1)]} \qquad (5.1)$$

$$FIN(j) = \frac{[DFN(j) - CON(j) \cdot FIN(j-1)]}{[BIN(j) + CON(j) \cdot EIN(j-1)]} \qquad (5.2)$$

$$E2N(j) = \frac{-A2N(j)}{[BIN(j) + CON(j) \cdot E2N(j-1)]} \qquad (6.1)$$

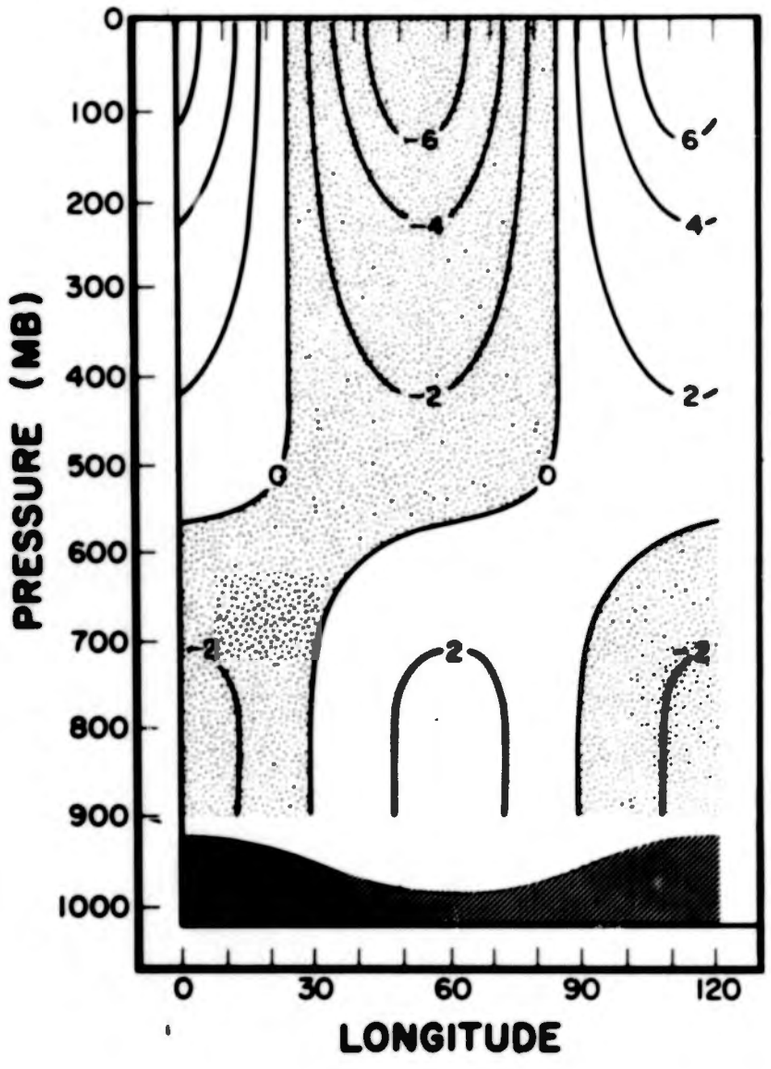

Fig. 2. v_* solution in m sec^{-1} for Saltzman's (1963) model. Heating with friction case. (m,n) = (3,0). $w_* = 0$ at the top.

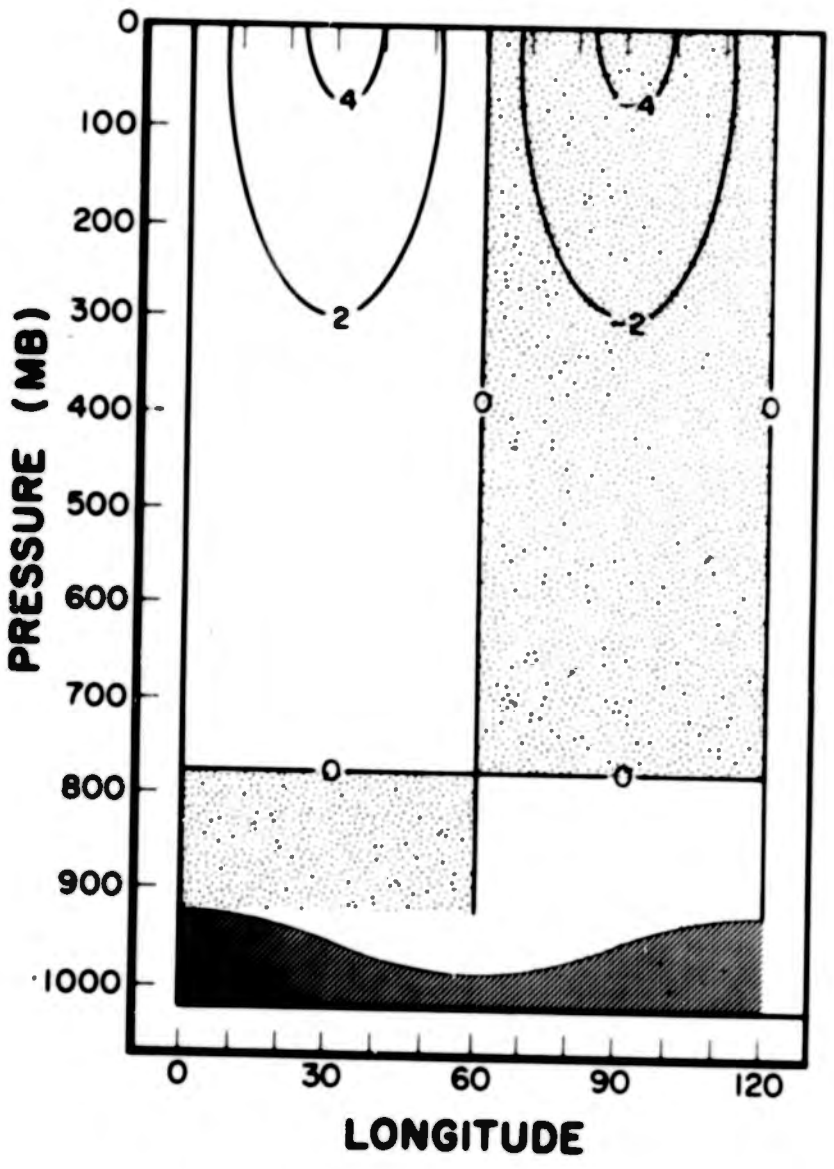

Fig. 3. v_* solution in m sec^{-1} for Saltzman's (1963) model. Mountain with friction case. (m,n) = (3,0). $w_* = 0$ at the top.

to calculate $v_1(j)$ and $v_2(j)$ inductively in the decreasing order of j $(j=J-1, J-2, \cdots 4,3,2,1)$. Thus we arrive at the complete solution.

7. Some Comparative Results

For comparison purposes, we take the Saltzman's (1963) model, for which some results were published. Finite difference solutions for wave number $(m,n)=(3,0)$ are obtained. Figure 2 shows the solution for heating with friction while Fig. 3 gives the solution for mountain with friction. Here the grid spacing is arbitrarily taken as 5 mb. Experimentation with different grid spacings is contemplated. The time taken by the IBM-7090 is less than a minute for one solution for v_* along with all the related fields like T_*, ω_*, and k_*. The agreement, at least for this type of atmospheric problem, can be considered very satisfactory. The results with the second model of Saltzman (1964) were equally successful and are not published here.

8. Some Experimental Results

Only the results of a few experiments will be discussed here. No attempt will be made, at present, to construct a general theory.

A. Top boundary condition

From Fig. 2, we can see that with $\omega_{*_T}=0$ as the top boundary condition, we get very large perturbations at the upper boundary for certain harmonics. If the top boundary condition is changed to $v_{*_T}=0$, which can be easily done in this numerical scheme, Fig. 4 is the result. Everything else is held the same as in Fig. 2. It is found that though this change in the upper boundary condition had an insignificant effect on the lower tropospheric perturbations,

Now substituting (5b.1) and (5b.2) in (5b) and (6b) we get

$$S1N \cdot v_1(J) + S2N + S3N \cdot v_2(J) = 0 \qquad (5b.2)$$

$$S4N \cdot v_2(J) + S5N + S6N \cdot v_1(J) = 0 \qquad (6b.2)$$

where

$$S1N = [A2N(J) \cdot E1N(J-1) + C0N(J) \cdot E1N(J-1) + B1N(J) + A2N(J) \cdot gL1N]$$

$$S2N = [A2N(J) \cdot F1N(J-1) + C0N(J) \cdot F1N(J-1) - DFN(J) - A2N(J) \cdot LL1N]$$

$$S3N = +[A2N(J) \cdot FRN]$$

$$S4N = [A2N(J) \cdot E2N(J-1) + C0N(J) \cdot E2N(J-1) + B1N(J) + A2N(J) \cdot gL2N]$$

$$S5N = [A2N(J) \cdot F2N(J-1) + C0N(J) \cdot F2N(J-1) - EFN(J) - A2N(J) \cdot LL2N]$$

$$S6N = -[A2N(J) \cdot FRN]$$

D. Final phase of the finite difference solution

From (5b.2) and (6b.2) we can very easily obtain $v_1(J)$ and $v_2(J)$ by direct elimination. After obtaining $v_1(J)$ and $v_2(J)$ we use (5) and (6)

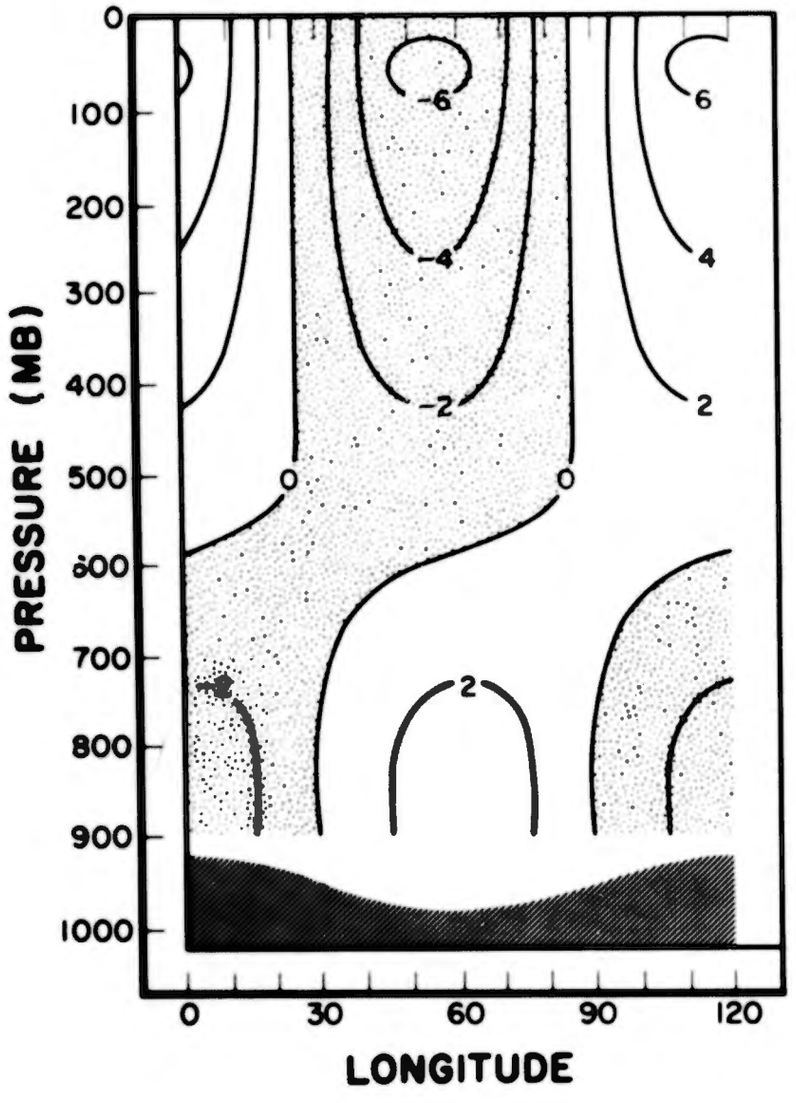

Fig. 4. v_* solution in m sec^{-1} for Saltzman's (1963) model. Heating with friction case. (m,n) = (3,0). $v_* = 0$ at the top.

the values obtained for levels above 50 mb appear to be more reasonable. So for all the remaining experiments, the top boundary condition is taken as $\sigma_{*T}=0$.

B. Influence of the seasonal change in the zonal mean state on the topographically forced perturbations

To study the effect of zonal mean state change on the perturbations, produced by the mountains, we take the following data:

$L = 8.3333 \times 10^{7}$ CM
$l = 36$
$k = 9$
$g = 980$ CM SEC^{-2}
$R = 2.87 \times 10^{6}$ CM^{-2} SEC^{-2} DEG^{-1}
$C_p = 1.00 \times 10^{7}$ CM^{2} SEC^{-2} DEG^{-1}
$C = 1.6 \times 10^{4}$ CM
$P_S = 1000$ MB
$P_b = 900$ MB
$P_T = 5$ MB
$h_* = h_1 \cos \frac{2\pi m x}{l} \cos \frac{2\pi n y}{k}$
$h_1 = 2 \times 10^{4}$ CM
$H_* = 0$
$\rho_b = 1.2 \times 10^{-3}$ gm CM^{-3}

Also the values of K_0 , $\frac{\partial T_0}{\partial y}$, and u_0 utilized here are given in Table I. At 30°N and 60°N the u_0 values at the lower boundary are arbitrarily taken as 1 m sec^{-1} both in winter and summer (because it is not still clear how far we can trust the observational 900-mb values at these latitudes). At 45°N, the u_0 values at the lower boundary are taken as 2.5 m sec^{-1} and 4.5 m sec^{-1} , for summer and winter respectively, which appear to agree with the observations. f and β values are taken to correspond to the latitude under consideration. In all these figures corresponding to mountain with friction cases, the atmospheric troughs and ridges show a slight shift from the topographic troughs and ridges.

Figures 5 to 10 give the solutions for $(m,n)=(3,0)$ at different latitudes. The changes in the intensity of circulation and the position of the nodes are of interest in this type of study. It is to be noted that at 30°N and 60°N the node appears at a lower pressure in winter than in summer. At 60°N, this results in a reversal of phase even at 500 mb from one season to the other. However, the zonal circulation at 30°N and 60°N is stronger in winter than in summer. This result is opposite from the analytical studies of Barrett, 1961. This is because the analytical studies generally have restrictions on K_0 and $\frac{\partial T_0}{\partial y}$ though they may be different for troposphere and stratosphere. To show this more clearly, a hypothetical K_0 (Table 1, col. 1), which has constant values in the troposphere and stratosphere with a linear variation between 300 and 100 mb, is taken. This K_0 is used at all the altitudes forboth the seasons keeping everything else the same. Figures 11-16 show the results which are self-explanatory. From these, we can conclude that for a quantitative theory of the stationary zonally asymmetric perturbations, the vertical structure of the zonal mean stability has to be

Latitude		30°N						45°N						60°N					
P	K_0HYP	K_0W	K_0S	$\frac{\partial T_0}{\partial y}$W	$\frac{\partial T_0}{\partial y}$S	U_0W	U_0S	K_0W	K_0S	$\frac{\partial T_0}{\partial y}$W	$\frac{\partial T_0}{\partial y}$S	U_0W	U_0S	K_0W	K_0S	$\frac{\partial T_0}{\partial y}$W	$\frac{\partial T_0}{\partial y}$S	U_0W	U_0S
900	-2.00	-2.60	-2.13	-6.13	-3.53	1.00	1.00	-1.81	-2.03	-8.50	-5.90	4.68	2.50	-1.23	-1.81	-6.39	-5.20	1.00	1.00
800	-2.00	-2.15	-2.27	-5.50	-3.00	3.64	2.50	-1.93	-2.07	-7.57	-5.57	7.34	4.45	-1.64	-1.98	-4.87	-4.56	2.43	2.27
700	-2.00	-2.08	-2.30	-5.30	-2.60	6.48	3.97	-2.12	-2.15	-7.30	-5.10	10.18	6.49	-2.07	-2.15	-4.48	-4.44	3.85	3.63
600	-2.00	-2.10	-2.17	-5.40	-2.50	9.73	5.51	-2.21	-2.17	-6.90	-5.05	13.32	8.74	-2.08	-2.15	-4.24	-4.17	4.37	5.14
500	-2.00	-2.13	-2.10	-5.50	-2.40	13.64	7.27	-2.19	-2.15	-6.50	-5.00	16.83	11.37	-2.08	-2.16	-3.99	-3.90	7.08	6.81
400	-2.00	-1.57	-1.75	-5.10	-2.45	18.29	9.40	-1.65	-1.70	-5.80	-4.80	20.76	14.50	-1.40	-1.48	-3.54	-3.09	8.98	8.58
300	-2.00	-1.00	-1.31	-4.70	-2.50	23.82	12.20	-0.95	-1.07	-5.10	-4.60	25.24	18.38	-0.72	-0.80	-3.09	-2.29	11.14	10.32
275	-1.63	-0.90	-1.13	-4.15	-1.80	25.34	12.94	-0.80	-0.91	-3.28	-2.80	26.28	19.30	-0.62	-0.68	-2.05	-1.20	11.65	10.67
250	-1.16	-0.80	-0.95	-3.60	-1.10	26.79	13.48	-0.65	-0.75	-1.45	-1.00	26.93	19.82	-0.52	-0.56	-1.01	-0.11	11.98	10.81
225	-0.70	-0.71	-0.77	-3.05	-0.40	28.17	13.79	-0.53	-0.60	0.38	0.80	27.08	19.84	-0.41	-0.44	0.03	0.98	12.10	10.70
200	-0.33	-0.62	-0.60	-2.50	0.30	29.45	13.81	-0.40	-0.45	2.20	2.60	26.64	19.26	-0.31	-0.32	1.08	2.06	11.94	10.29
175	-0.33	-0.51	-0.47	-0.28	1.55	30.17	13.32	-0.33	-0.39	3.40	3.60	25.57	18.07	-0.27	-0.28	1.03	2.68	11.63	9.57
150	-0.33	-0.40	-0.35	1.95	2.80	29.64	11.99	-0.26	-0.33	4.60	4.60	23.79	16.25	-0.23	-0.24	0.99	3.30	11.27	8.52
125	-0.33	-0.33	-0.30	4.18	4.05	27.42	9.52	-0.20	-0.23	5.80	5.60	21.06	13.57	-0.19	-0.20	0.94	3.91	10.87	7.02
100	-0.33	-0.25	-0.25	6.40	5.30	22.74	5.39	-0.15	-0.12	7.00	6.60	16.95	9.66	-0.16	-0.16	0.90	4.53	10.41	4.88
75	-0.33	-0.18	-0.17	4.80	3.98	16.46	0.18	-0.11	-0.09	5.25	4.95	11.93	4.92	-0.12	-0.12	0.67	3.40	9.90	2.31
50	-0.33	-0.10	-0.08	3.20	2.65	10.16	-5.04	-0.07	-0.05	3.50	3.30	6.90	0.19	-0.08	-0.08	0.45	2.26	9.39	-0.27
25	-0.33	-0.05	-0.04	1.60	1.33	3.86	-10.25	-0.04	-0.03	1.75	1.65	1.88	-4.54	-0.04	-0.04	0.22	1.13	8.88	-2.64
5	-0.33	-0.01	-0.01	0.32	0.27	-1.18	-14.43	-0.01	-0.05	0.35	0.33	-2.14	-8.33	-0.01	-0.01	0.05	0.23	8.47	-4.90

TABLE 1: Values of K_0, $\partial T_0/\partial y$, and U_0 utilized. Here, K_0 is in 10^4 CGS, $\partial T_0/\partial y$ is in 10^{-8} CGS, U_0 is in 10^2 CGS. W stands for winter, S stands for summer, HYP stands for hypothetical values, P stands for pressure in mb. Up to 100-mb level, K_0 and $\partial T_0/\partial y$ values for summer and winter were computed from Peixoto's standard-level (1961) data, assuming linear variation between the neighboring points for which the data are available for the use of centered differencing. Above 100-mb level, these values are hypothetical.

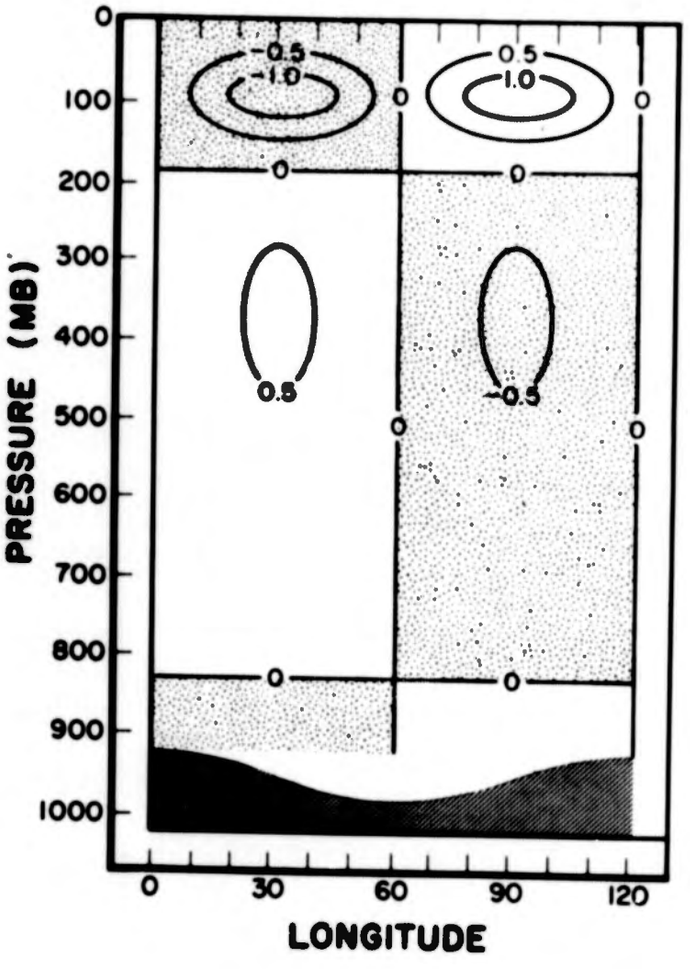

Fig. 5. v_* solution in m sec^{-1} at 30°N for summer. Zonal mean profiles taken from Table I. (m,n) = (3,0). Mountain with friction case.

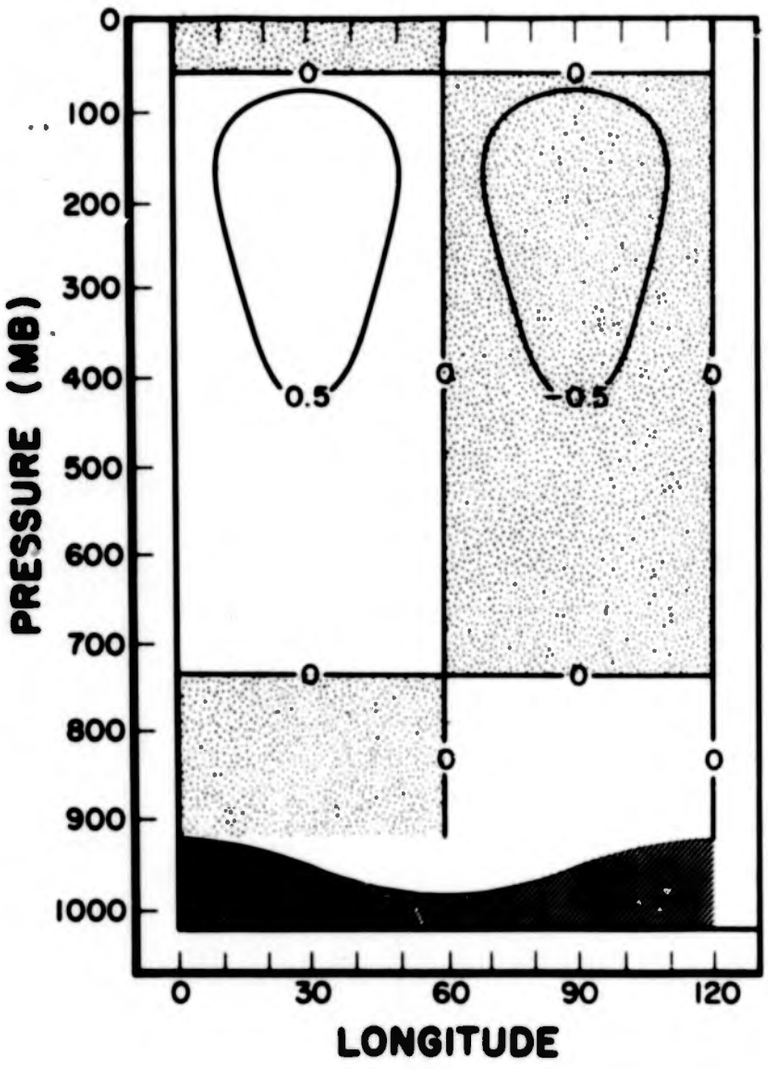

Fig. 7. v_* solution in m sec^{-1} at 45°N for summer. Zonal mean profiles taken from Table I. (m,n) = (3,0). Mountain with friction case.

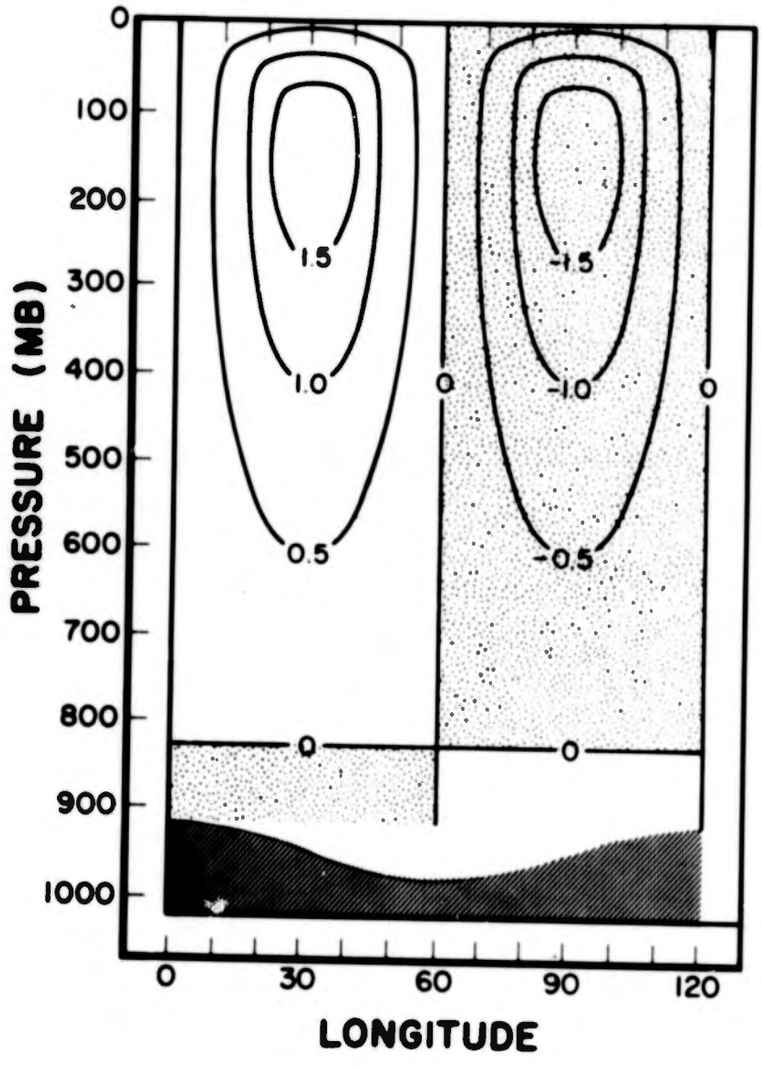

Fig. 8. v_* solution in m sec^{-1} at 45°N for winter. Zonal mean profiles taken from Table I. (m,n) = (3,0). Mountain with friction case.

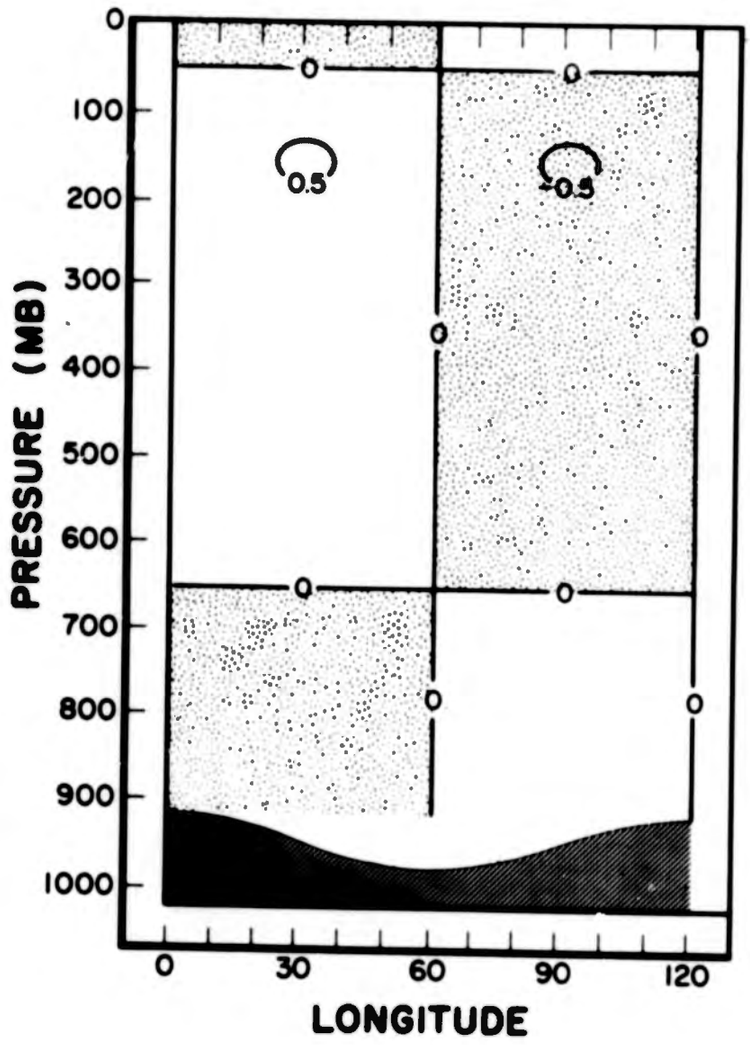

Fig. 6. v_* solution in m sec^{-1} at 30°N for winter. Zonal mean profiles taken from Table I. (m,n) = (3,0). Mountain with friction case.

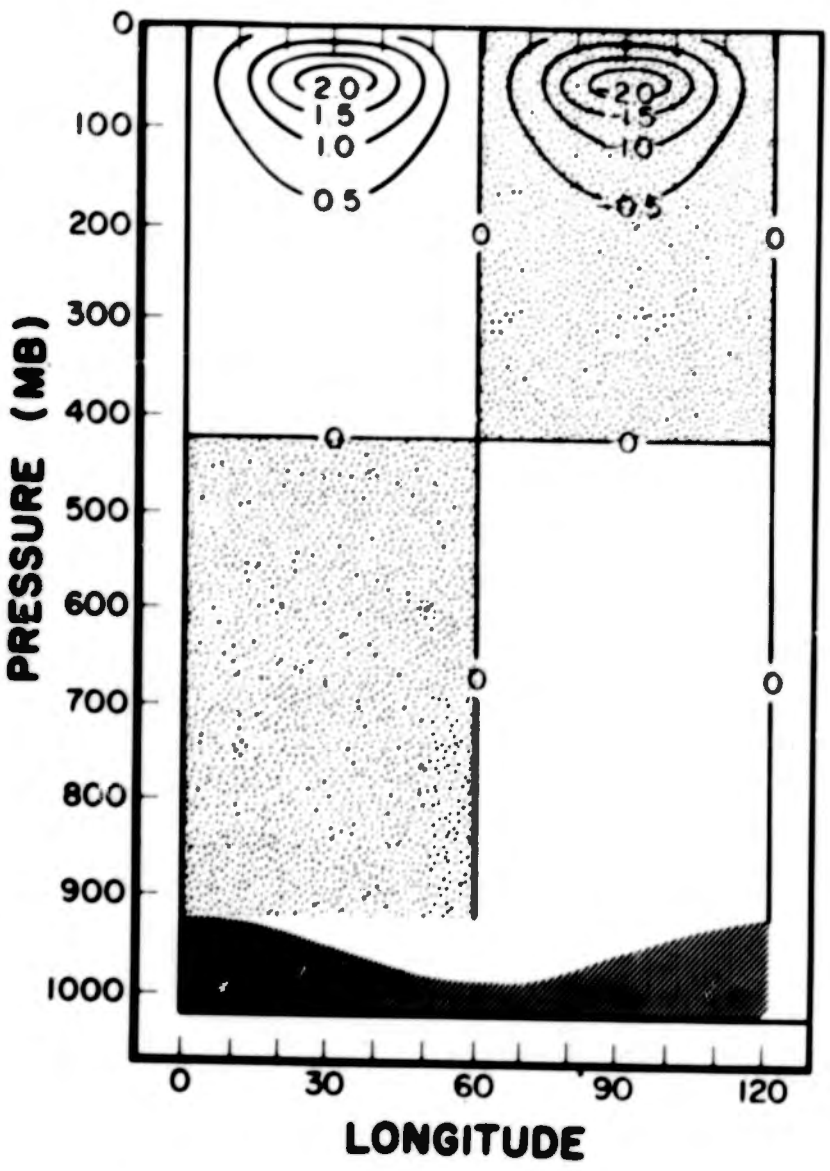

Fig. 10. v_* solution in m sec^{-1} at 60°N for winter. Zonal mean profiles taken from Table I. (m,n) = (3,0). Mountain with friction case.

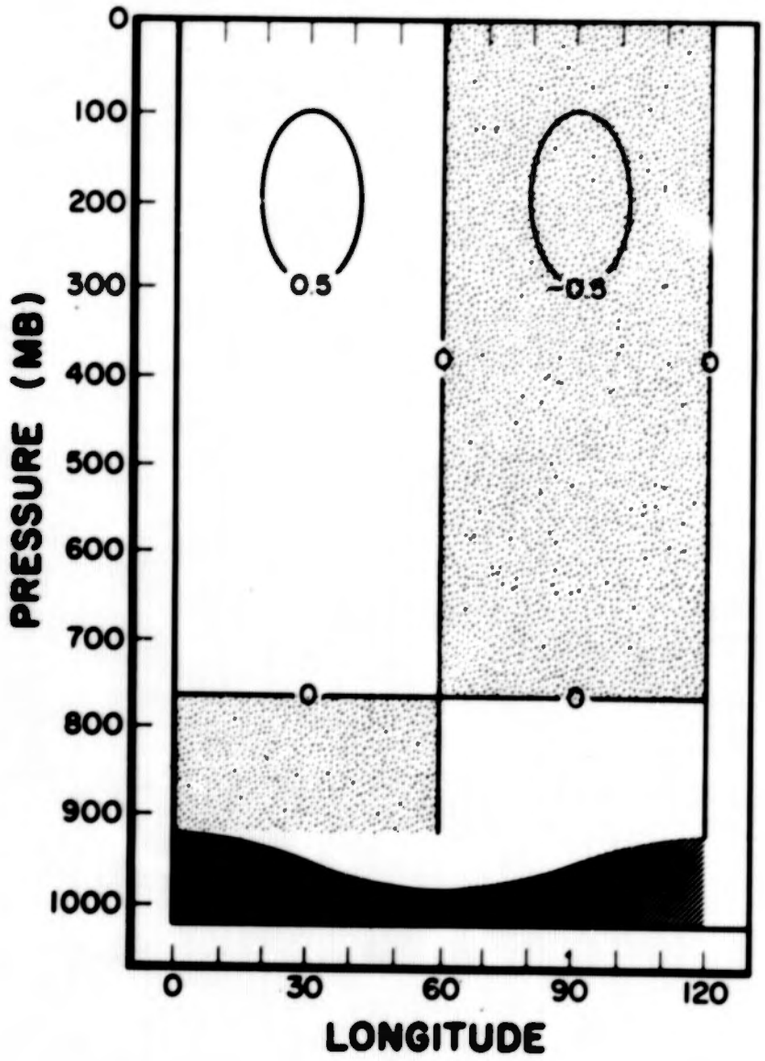

Fig. 9. v_ϕ solution in m sec^{-1} at 60°N for summer. Zonal mean profiles taken from Table I. (m,n) = (3,0). Mountain with friction case.

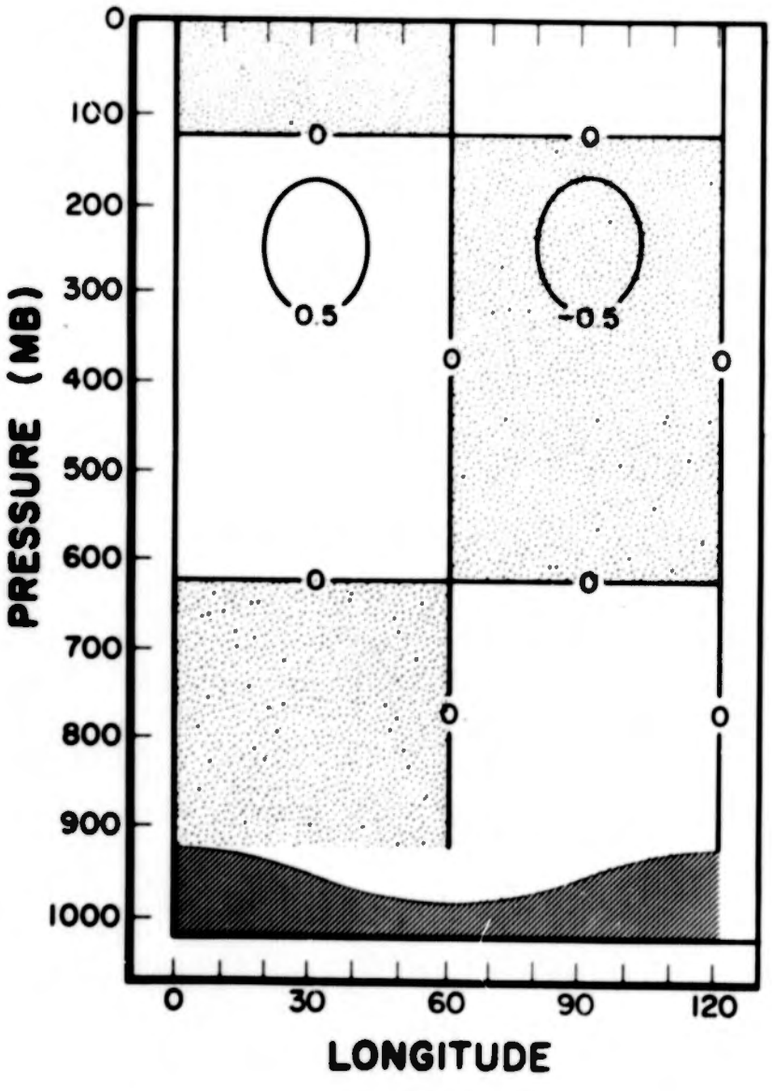

Fig. 11. v_* solution in m sec^{-1} at 30°N for summer. Hypothetical K_0 and other zonal mean profiles taken from Table I. (m,n) = (3,0). Mountain with friction case.

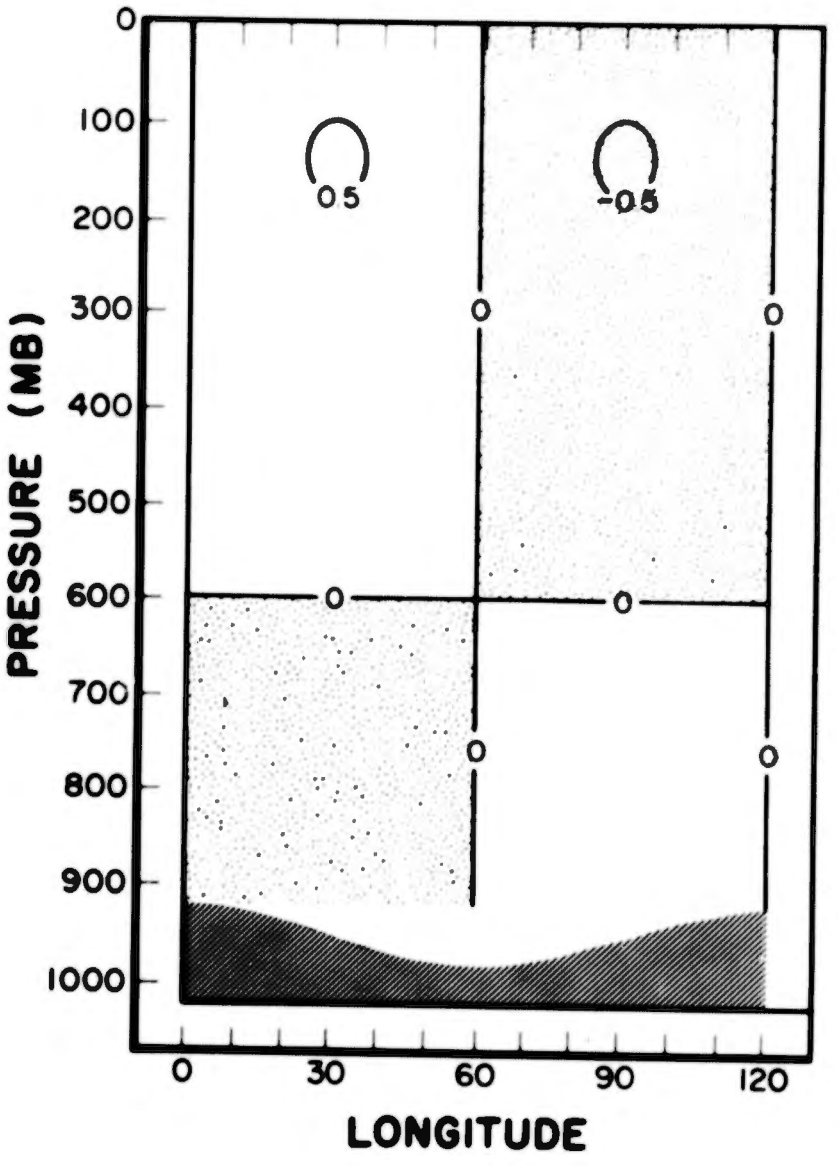

Fig. 12. v_* solution in m sec^{-1} at 30°N for winter. Hypothetical K_0 and other zonal mean profiles taken from Table I. (m,n) = (3,0). Mountain with friction case.

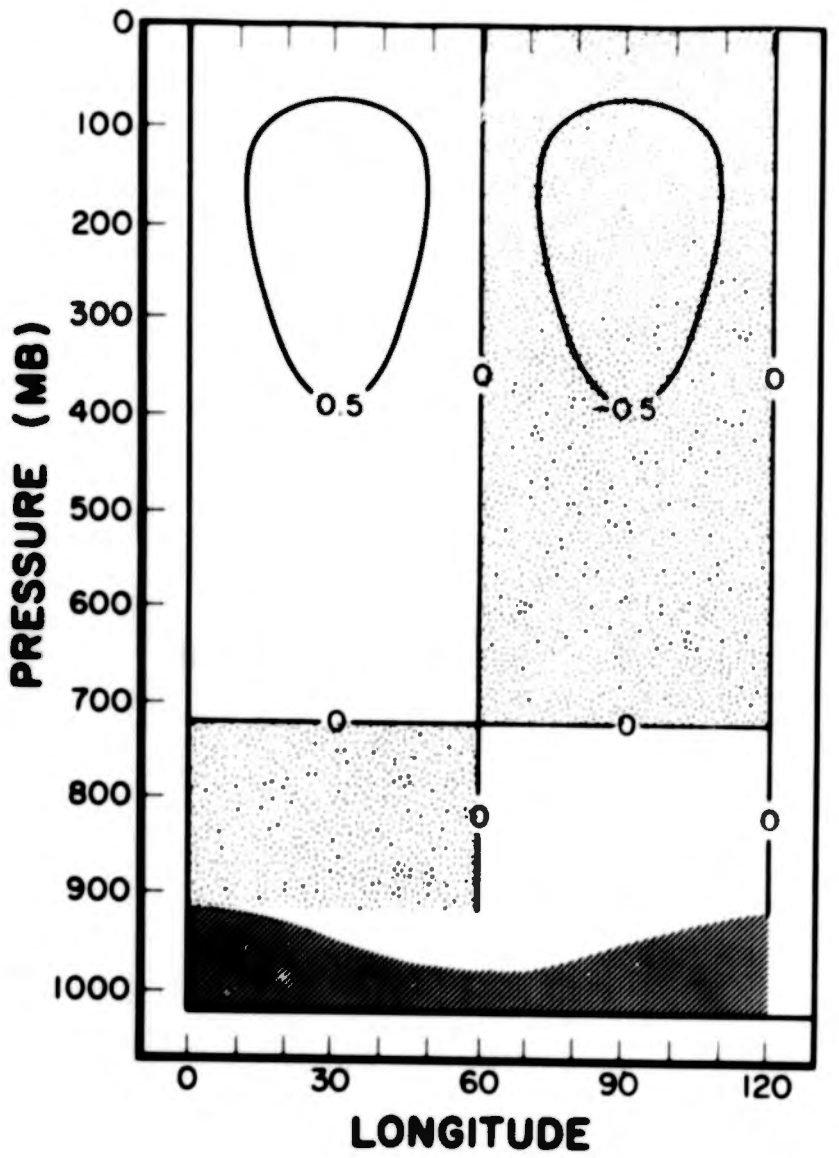

Fig. 13. v_* solution in m sec^{-1} at 45°N for summer. Hypothetical K_0 and other zonal mean profiles taken from Table I. (m,n) = (3,0). Mountain with friction case.

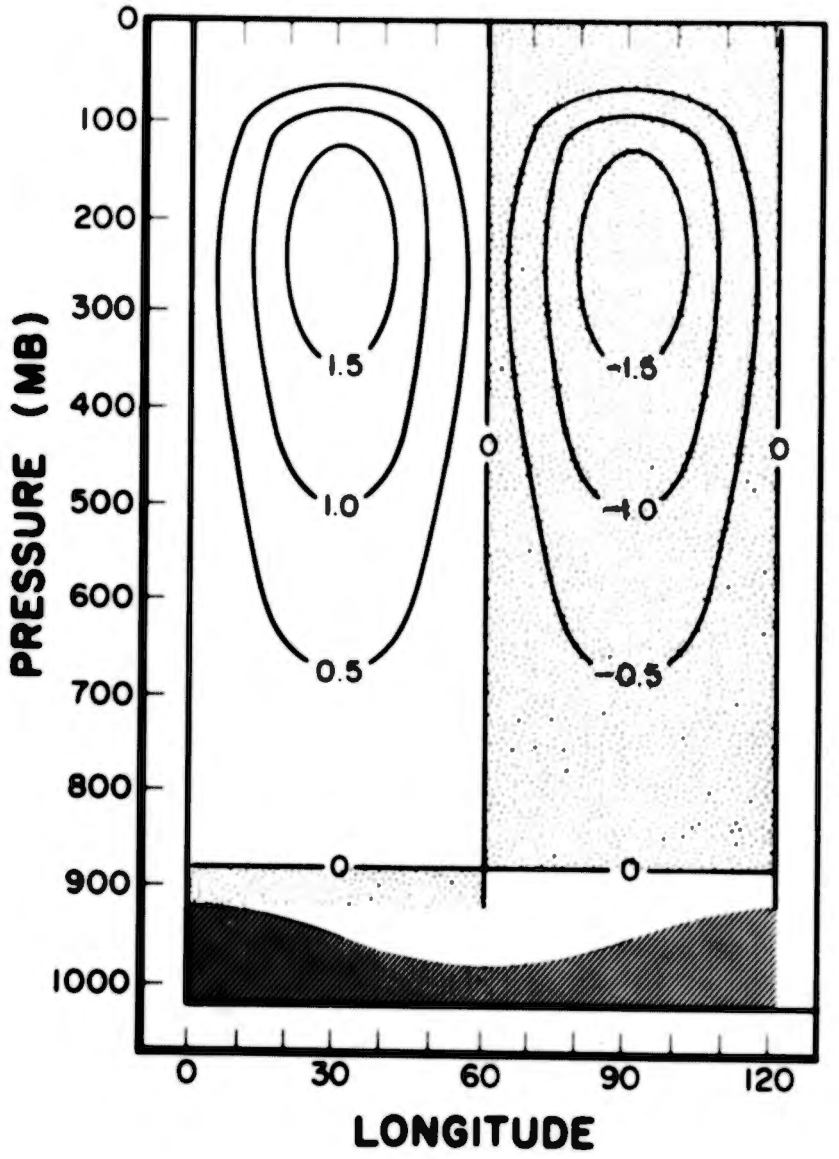

Fig. 14. v_* solution in m sec^{-1} at 45°N for winter. Hypothetical K_0 and other zonal mean profiles taken from Table I. (m,n) = (3,0). Mountain with friction case.

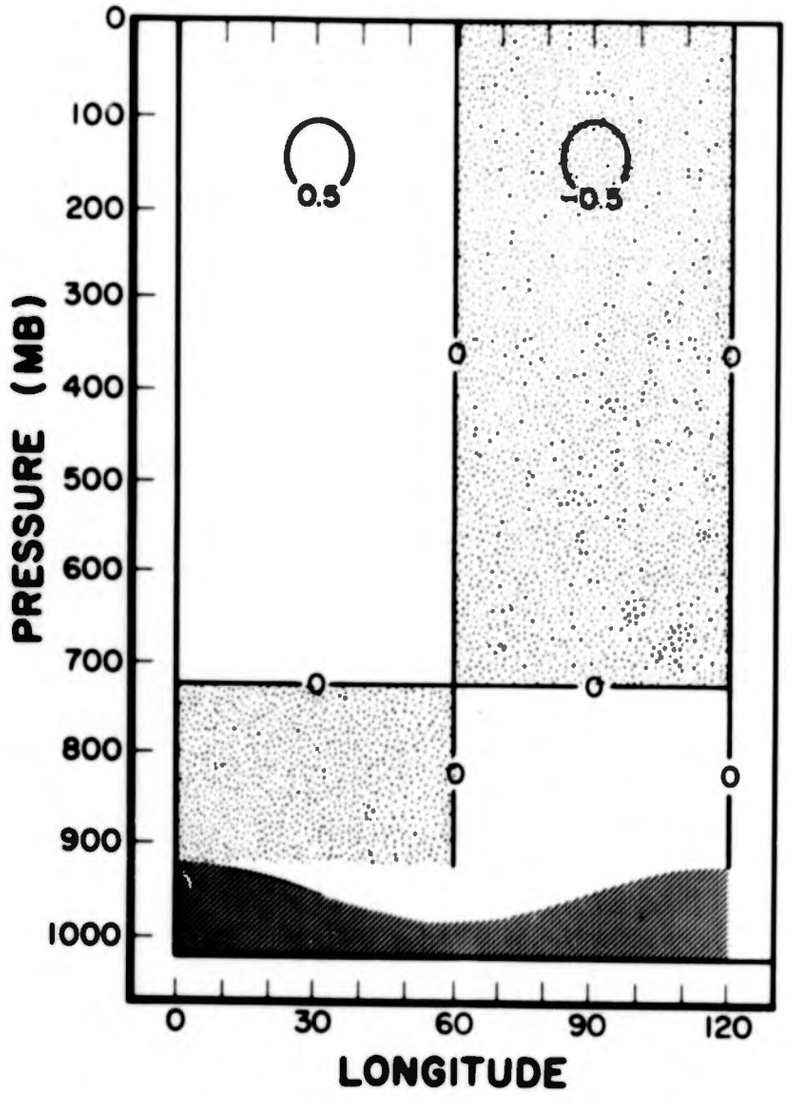

Fig. 15. v_* solution in m sec^{-1} at 60°N for summer. Hypothetical K_0 and other zonal mean profiles taken from Table I. (m,n) = (3,0). Mountain with friction case.

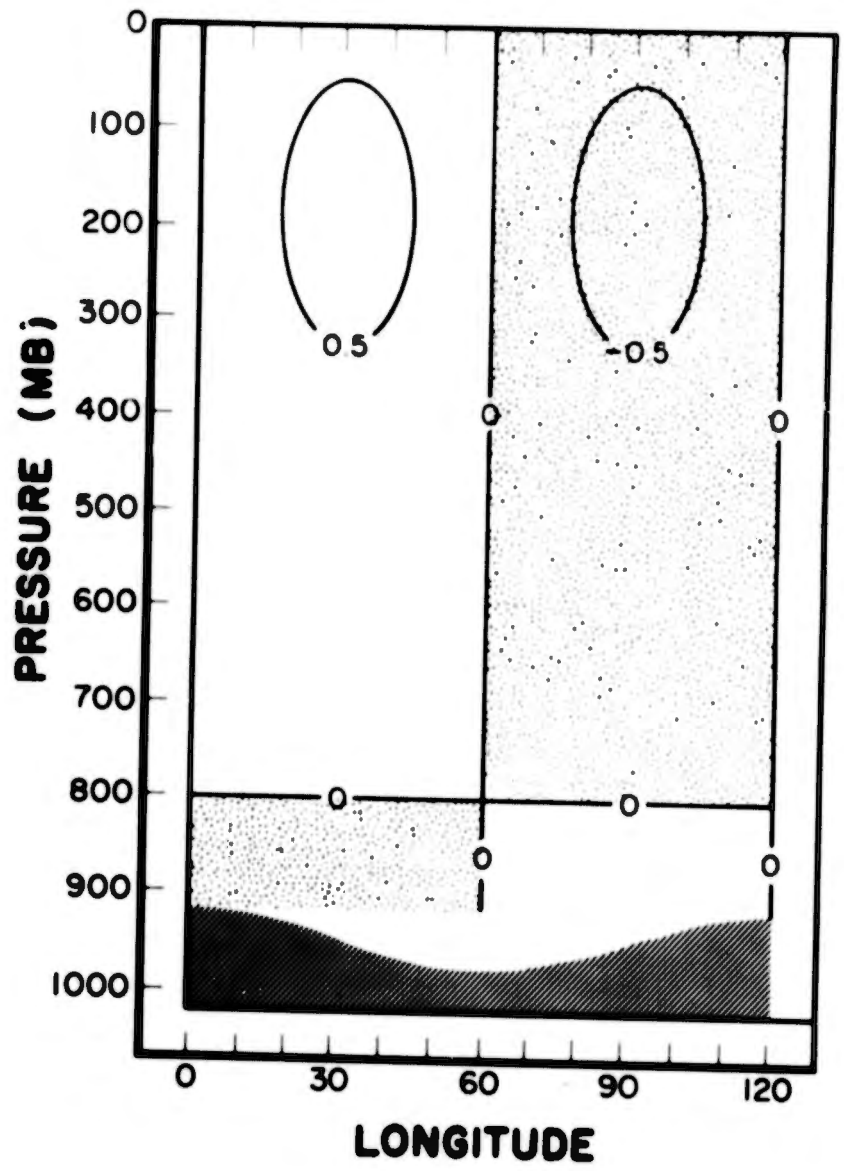

Fig. 16. v_* solution in m sec^{-1} at 60°N for winter. Hypothetical K_0 and other zonal mean profiles taken from Table I. (m,n) = (3,0). Mountain with friction case.

considered as realistically as possible. No claim is made however, that the values used here represent realistic values.

Figures 17 and 18 show the results for $(m,n)=(3,1)$ at 45°N. Significant phase changes from one season to the other at all levels are the interesting feature of these figures. This can happen if the wave number falls on one side of the quasi-resonant frequency in one season and on the other side in another season (c.f., Gilchrist, 1953).

To investigate the acceptability of the barotropic or equivalent barotropic theories, a uniform current, with the 500-mb zonal mean velocity at 45°N, corresponding to the season considered, is introduced. The forcing is kept the same by adjusting the mountain height. The results for $(m,n)=(3,0)$ are given in Figs. 19 and 20. For $(m,n)=(3,1)$, the results are given in Figs. 21 and 22. It can be inferred that the barotropic or equivalent barotropic theories can only give qualitative results even at 500-mb level for $(m,n)=(3,1)$. At least for some important scales, they seem to be incapable of giving acceptable results. Also, from Figs. 21 and 22 we can infer, from the vertical structure of the response, that the wave number $(3,1)$ falls on either side of the quasi-resonant frequency according to the season, giving rise to a 40 degree phase change.

9. Some Concluding Comments

The results here show the importance of the vertical structure of the zonal mean state and the scale of the perturbations and, therefore, have an important bearing on the numerical modeling of the atmosphere. Before trying to construct

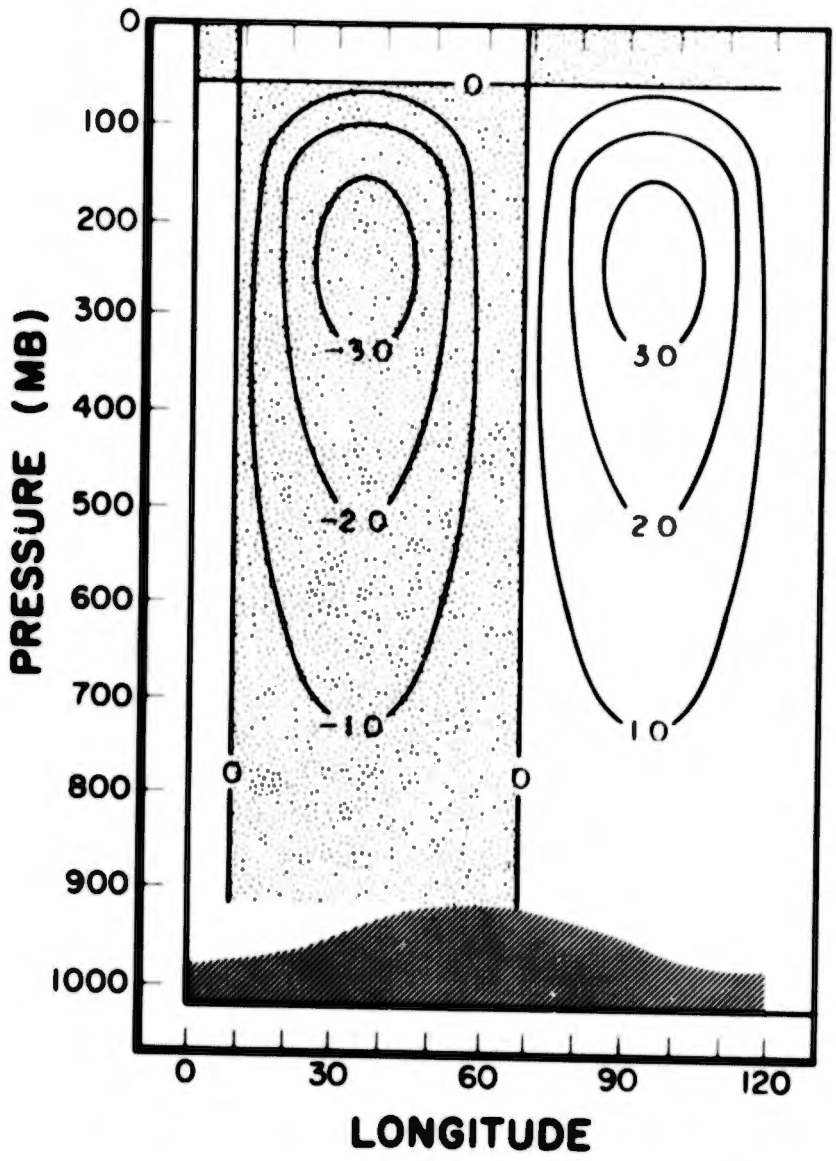

Fig. 17. v_* solution in m sec^{-1} at 45°N for summer. Zonal mean profiles taken from Table I. (m,n) = (3,1). Mountain with friction case.

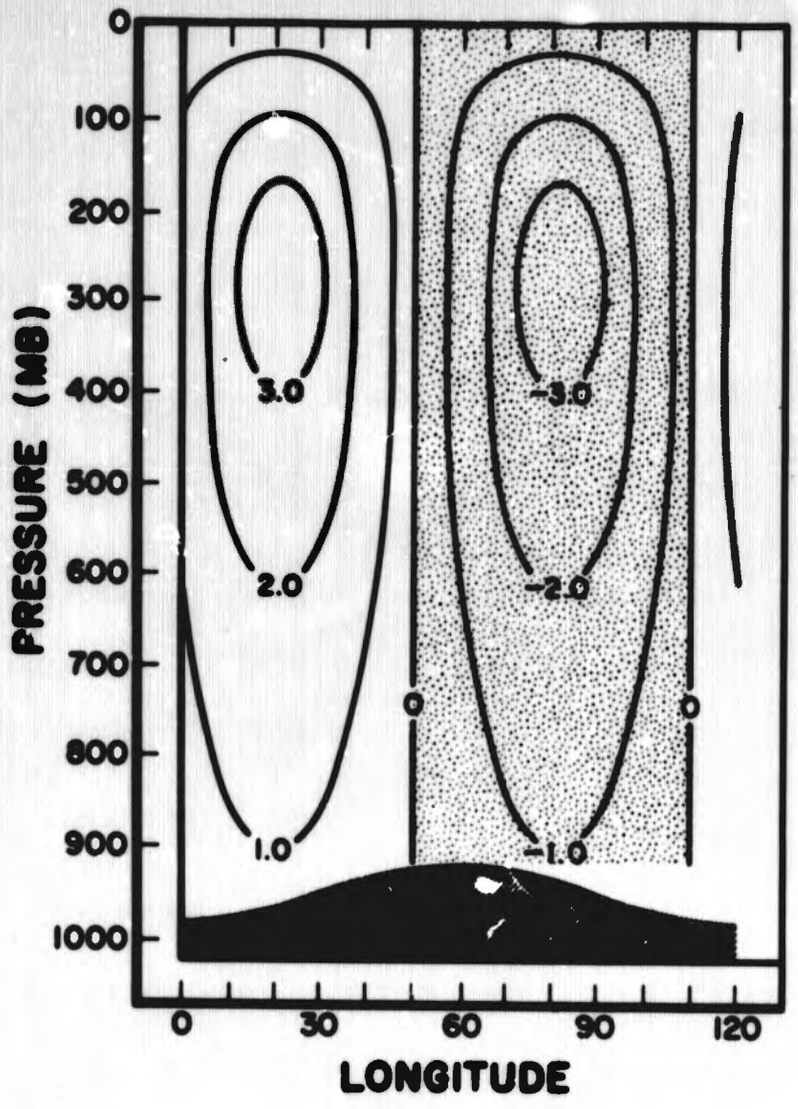

Fig. 18. v_* solution in m sec^{-1} at 45°N for winter. Zonal mean profiles taken from Table 1. (m,n) = (3,1). Mountain with friction case.

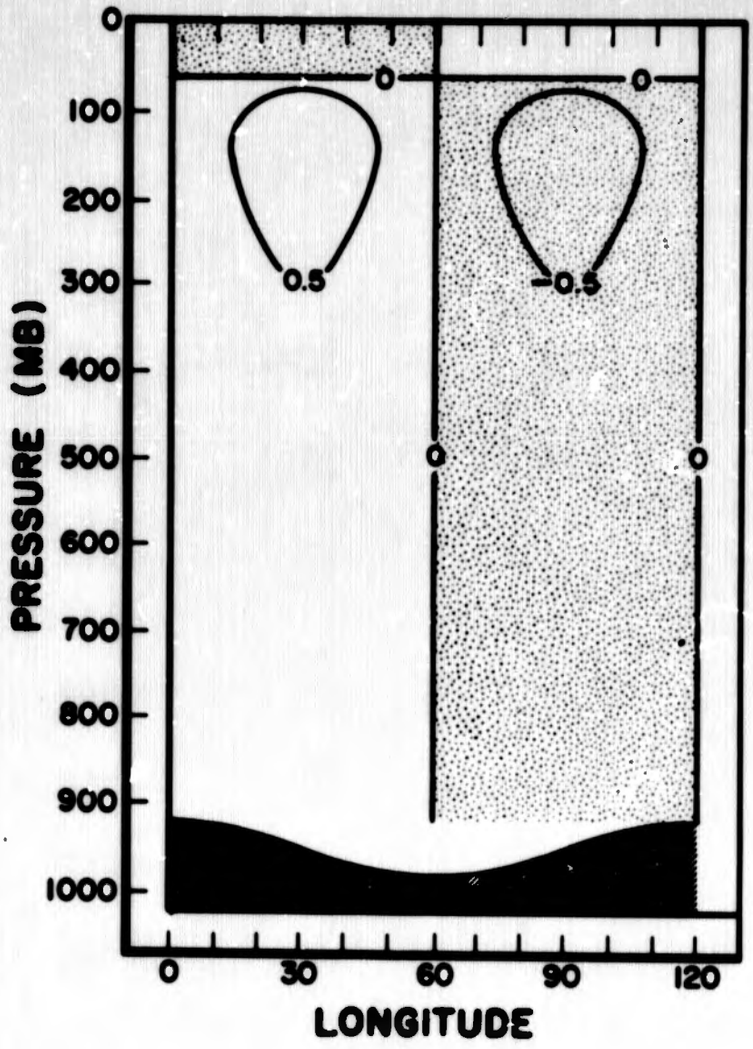

Fig. 19. v_* solution in m sec^{-1} at 45°N for summer. Uniform U_0 equal to that of the 500 mb U_0 given in Table I is used. K_0 values are taken from Table I. (m,n) = (3,0). Mountain with friction case.

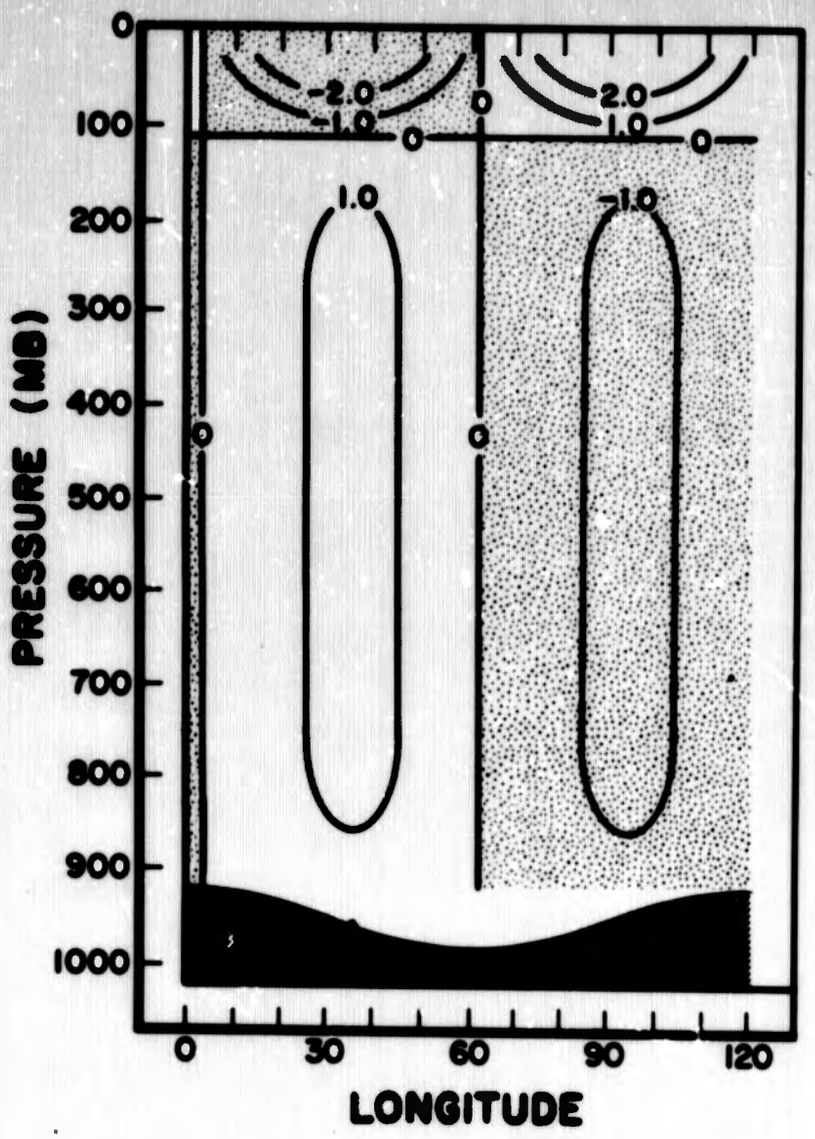

Fig. 20. v_* solution in m sec^{-1} at 45°N for winter. Uniform U_0 equal to that of the 500 mb U_0 given in Table I is used. K_0 values are taken from Table I. (m,n) = (3,0). Mountain with friction case.

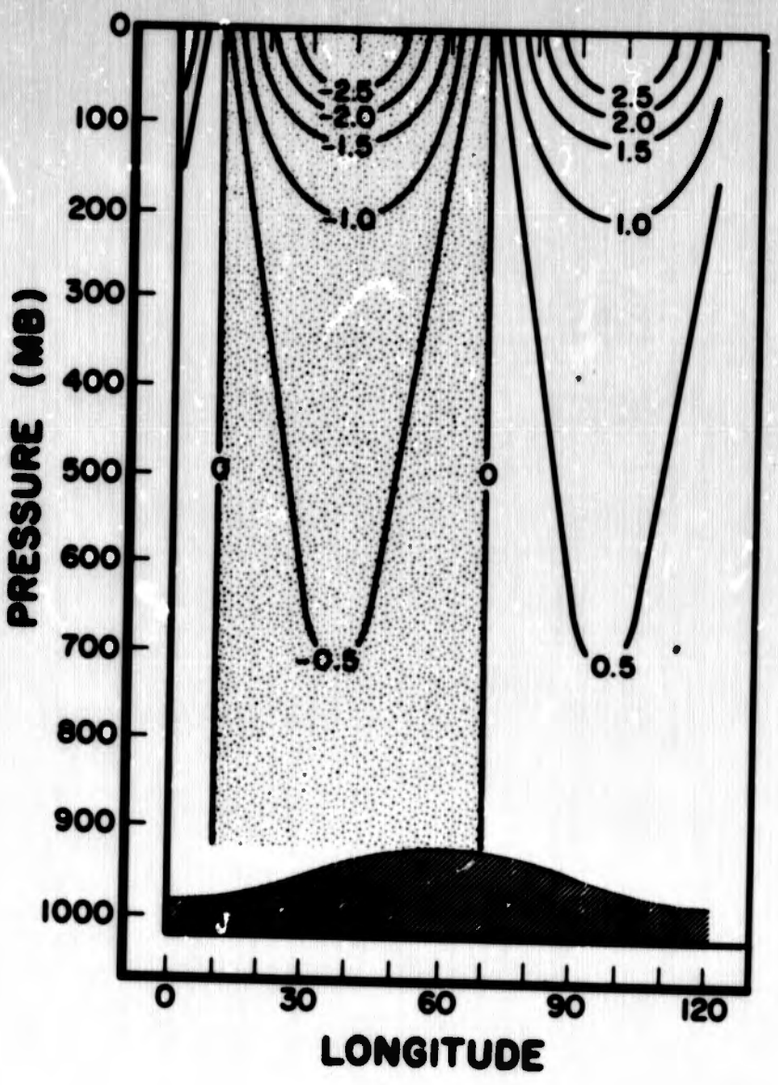

Fig. 21. v_* solution in m sec^{-1} at 45°N for summer. Uniform U_0 equal to that of the 500 mb U_0 given in Table I is used. K_0 values are taken from Table I. (m,n) = (3,1). Mountain with friction case.

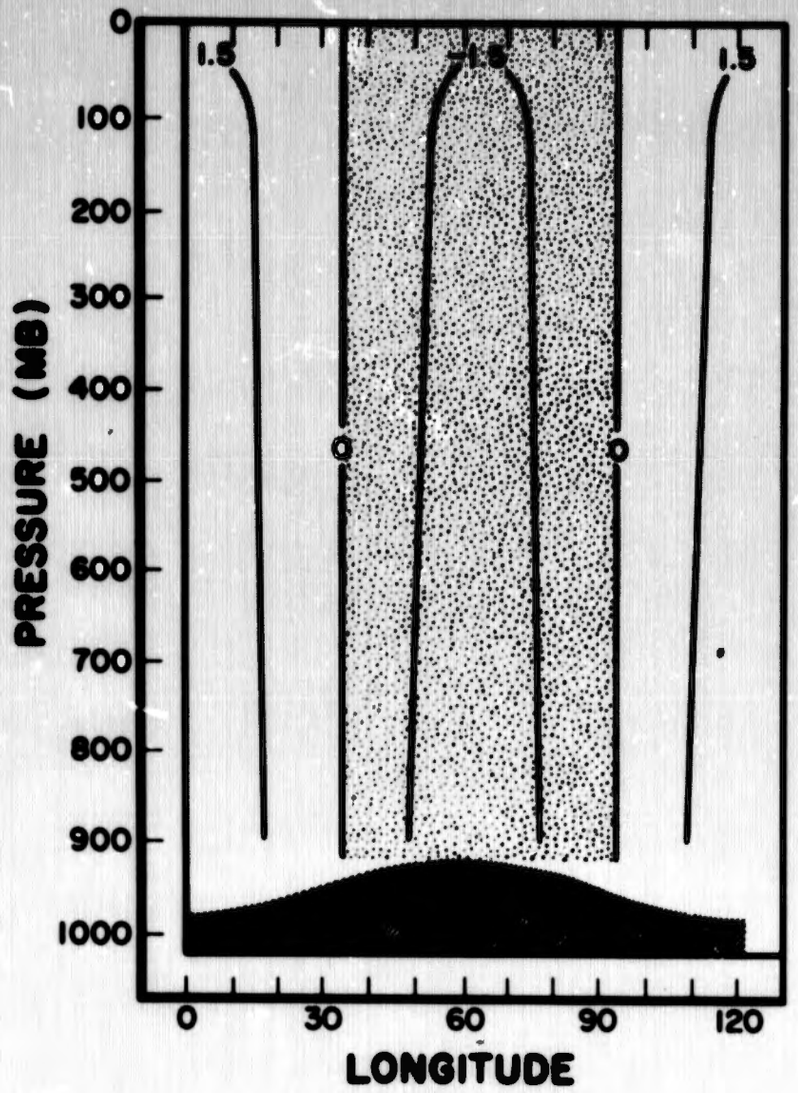

Fig. 22. v_* solution in m sec^{-1} at 45°N for winter. Uniform U_0 equal to that of the 500 mb U_0 given in Table I is used. K_0 values are taken from Table I. (m,n) = (3,1). Mountain with friction case.

a quantitative theory in a spherical geometry, it will be of great interest to experiment with different kinds of heating functions. Above all, we should keep in mind that the nonseparability of (1), the complexity of the lower boundary condition, and our ignorance regarding the vertical structure of the perturbation heating function, are the formidable impediments in the way of constructing a quantitative linear theory.

10. Acknowledgements

With pleasure, I thank Dr. Barry Saltzman for the keen interest he has shown in this work. My thanks are also due to Mr. Charles Gadsden for his aid in map analysis.

This research has been sponsored by the United States Weather Bureau, Department of Commerce, under Contract No. Cwb-10763.

References

Barrett, Earl W., 1961: Some applications of harmonic analysis to the study of the general circulation, III. Beitrage Zue Physik Der Atmospare, Vol. 34.

Bateman, Harry, 1953: Higher Transcendental Functions, MacGraw-Hill Book Co., Inc., Vol. I, pp. 1-302.

Bolin, B., 1950: On the influence of the earth's orography on the general character of the westerlies. Tellus, Vol. 2, pp. 184-195.

Charney, J.G. and A. Eliassen, 1949: A numerical method for predicting the perturbations of the middle latitude westerlies. Tellus, Vol. I, pp. 38-54.

Clapp, Philip F., 1960: Normal heat sources and sinks in the lower troposphere in winter. Mon. Wea. Rev., Vol. 89, pp. 147-162.

Doos, B. R., 1962: The influence of exchange of sensible heat with the earth's surface on the planetary flow. Tellus, Vol. 14, pp. 133-147.

Frenzen, Paul, 1955: Westerly flow past an obstacle in a rotating himispherical shell. Bull. Amer. Meteor. Soc., Vol. 38, pp. 204-210.

Fultz, D., 1961: Developments in controlled experiments on larger scale geophysical problems. Geophys., Vol. 7, pp. 1-103. New York, Academic Press.

Gambo, K., 1956: The topographical effect upon the jet stream in the westerlies. J. Meteor. Soc., Japan, Vol. 34, pp. 24-28.

Gambo, K., 1957: The scale of atmospheric motions and the effect of topography on numerical weather prediction in the lower atmosphere. Papers in Meteor. and Geophys., Vol. 8, pp. 1-24.

Gilchrist, B., 1953: The seasonal phase changes of thermally produced perturbations. Proc. Toronto Meteor. Conf., pp. 129-131.

Haurwitz, B. and Richard A. Craig, 1952: Atmospheric flow patterns and their representation by spherical-surface harmonics. Geophys. Res. Papers, No. 14, pp. 1-78.

Kuo, H.L., 1959: Finite amplitude three-dimensional harmonic waves on spherical earth. J. of Meteor., Vol. 16, pp. 101-111.

Magata, M., 1957: On the topographical effect upon the perturbations of the middle latitude westerlies. Papers in Meteor. and Geophys., Vol. 8, pp. 25-38.

Mintz, Y., 1958: Design of some numerical central circulation experiments. Bull. Res. Council of Israel, Vol. 7G, pp. 67-114.

Queney, P. 1948: The problem of air flow over mountains. A summary of theoretical studies. Bull. Amer. Meteor. Soc., Vol. 29, pp. 16-26.

Rao, Sankar M., 1963: Convergence conditions for relaxation solution of a class of elliptic equations. Final Report, General Circulation Research, U.S.W.B., Contract No. Cwb-10502, pp. 1-8.

Richtmyer, R.D. 1957: Difference Methods for Initial-Value Problems, Interscience Publishers, Inc., New York.

Saltzman, B. and Jose' P. Peixoto, 1957: Harmonic analysis of the mean northern hemisphere wind field for the year 1950. Quart. J. Roy. Meteor. Soc., Vol. 83, pp. 360-364.

Saltzman, B. and A. Fleisher, 1962: Spectral statistics of the wind at 500 mb. J. Atmos. Sci., Vol. 19, pp. 196-204.

Saltzman, B. and M. Sankar Rao, 1963: A diagnostic study of the mean state of the atmosphere. J. Atmos. Sci., Vol. 20, pp. 438-447.

Saltzman, B., 1963: A generalized solution for the large scale time average perturbations in the atmosphere. J. Atmos. Sci., Vol. 20, pp. 226-235 (corrigenda, ibid, 20, 465).

Saltzman, B., 1964: On the theory of the mean perturbations in the atmosphere. (unpublished).

Smagorinsky, J., 1953: The dynamical influence of large scale heat sources and sinks on the quasi-stationary mean motions of the atmosphere. Quart. J. Roy. Meteor. Soc., Vol. 79, pp. 342-366.

Smagorinsky, J., 1964: Some aspects of general circulation. Quart. J. Roy. Meteor. Soc., Vol. 90, pp. 1-14.

Staff Members Academia Sinica, 1958: On the general circulation over eastern Asia, III. Tellus, Vol. 10, pp. 299-312.

Sutcliffe, R.C., 1951: Mean upper contour patterns of the northern hemisphere--Thermal synoptic viewpoint. Quart. J. Roy. Meteor. Soc., Vol. 77, pp. 435-440.

Van Mieghem, J., P. Defrise, J. Van Isacker, 1960: Harmonic analysis of the normal monthly northern hemisphere geostrophic flow at 500 mb. Klasse Der Wetenschappen--Jaargang, 22, Nr 4, 38P.

Wiin-Nielsen, A., 1961: On the distribution of temperature relative to height in stationary planetary waves. Tellus, Vol. 13, pp. 127-139.

PAPER C

Reprint from the Review
PURE AND APPLIED GEOPHYSICS (PAGEOPH)
Formerly 'Geofisica pura e applicata'
Vol. 57, 1964/I BIRKHÄUSER VERLAG BASEL

On the Theory of the Axially-Symmetric, Time-Average, State of the Atmosphere

By BARRY SALTZMAN[1])

Summary – A possible formal approach to a closed steady-state theory of the mean axially-symmetric variables is outlined. The approach involves alternating iterative solutions of the energy and momentum equations. In these equations the effects of transient eddy phenomena of all frequencies are assumed to be parameterized in terms of the mean symmetric variables.

1. Introduction

The time-average distribution of the set of meteorological variables can be expressed as the sum of an axially-symmetric subset obtained by averaging around latitude circles and an axially-asymmetric subset which is the departure from this zonal average. By prescribing one of these two subsets it is possible to develop a separate steady-state theory for the other. On this basis, aspects of the asymmetric theory have been discussed by SMAGORINSKY [14][2]), Staff Members of the Academia Sinica [15], SALTZMAN [11, 12, 13] and DÖÖS [7] for example, and aspects of the symmetric theory have been discussed by ELIASSEN [6], KUO [7] and DAVIES and OAKES [3] for example. In these latter symmetric studies, the mean zonal wind and temperature fields are also prescribed, and in the case of the studies by ELIASSEN and KUO the zonal average effects of the transient asymmetries are given as known 'forcing functions', leaving only the mean toroidal motion as the unknown. In this note I wish to outline schematically a possible formal approach toward a closed steady-state theory for *all* of the symmetric variables without attempting to actually solve any of the detailed problems which would be involved.

2. Fundamental Equations

The 'primitive' equations governing the time-average variables for a spherical earth with pressure as the vertical coordinate are given by the writer (1961) in the

[1]) The Travelers Research Center, Inc., Hartford, Conn., U.S.A.
[2]) Numbers in brackets refer to References, pages 159/160.

form

$$\bar{u}\frac{\partial u}{a\cos\phi\,\partial\lambda}+\bar{v}\frac{\partial\bar{u}}{a\,\partial\phi}+\bar{\omega}\frac{\partial\bar{u}}{\partial p}-\left(f+\frac{\tan\phi}{a}\,\bar{u}\right)\bar{v}+\frac{\partial\bar{\Phi}}{a\cos\phi\,\partial\lambda}-X=0, \tag{1}$$

$$\bar{u}\frac{\partial\bar{v}}{a\cos\phi\,\partial\lambda}+\bar{v}\frac{\partial\bar{v}}{a\,\partial\phi}+\bar{\omega}\frac{\partial\bar{v}}{\partial p}+\left(f+\frac{\tan\phi}{a}\,\bar{u}\right)\bar{u}+\frac{\partial\bar{\Phi}}{a\,\partial\phi}-Y=0, \tag{2}$$

$$\frac{\partial\bar{\Phi}}{\partial p}+\frac{R}{p}\,\bar{T}=0, \tag{3}$$

$$\frac{\partial\bar{\omega}}{\partial p}+\frac{1}{a\cos\phi}\left(\frac{\partial\bar{u}}{\partial\lambda}+\frac{\partial\bar{v}\cos\phi}{\partial\phi}\right)=0, \tag{4}$$

$$\bar{u}\frac{\partial\bar{T}}{a\cos\phi\,\partial\lambda}+\bar{v}\frac{\partial\bar{T}}{a\,\partial\phi}+\bar{\omega}\frac{\partial\bar{T}}{\partial p}-\frac{R}{c_p\,p}\,\bar{\omega}\,\bar{T}-Q=0, \tag{5}$$

where

$$X=\bar{x}+M_x,$$

$$M_x=-\left(\frac{\partial u'^2}{a\cos\phi\,\partial\lambda}+\frac{\partial\overline{u'v'}\cos\phi}{a\cos\phi\,\partial\phi}-\frac{\tan\phi}{a}\,\overline{u'v'}+\frac{\partial\overline{u'\omega'}}{\partial p}\right), \tag{6}$$

$$Y=\bar{y}+M_y,$$

$$M_y=-\left(\frac{\partial u'v'}{a\cos\phi\,\partial\lambda}+\frac{\partial\overline{v'^2}\cos\phi}{a\cos\phi\,\partial\phi}+\frac{\tan\phi}{a}\,\overline{u'^2}+\frac{\partial\overline{v'\omega'}}{\partial p}\right), \tag{7}$$

$$Q=\frac{\bar{\dot{q}}_R+\bar{\dot{q}}_c+\bar{\dot{q}}_e}{c_p}-\left(\frac{\partial\overline{u'T'}}{a\cos\phi\,\partial\lambda}+\frac{\partial\overline{v'T'}\cos\phi}{a\cos\phi\,\partial\phi}+\frac{\partial\overline{\omega'T'}}{\partial p}-\frac{R}{c_p\,p}\,\omega'T'\right). \tag{8}$$

In these equations we have used the following notation:

λ = longitude
ϕ = latitude
p = pressure
t = time
$u = a\cos\phi\,d\lambda/dt$ = eastward wind component
$v = a\,d\phi/dt$ = northward wind component
$\omega = dp/dt$
z = height of an isobaric surface above sea-level
T = temperature
$\dot{q}_R, \dot{q}_c, \dot{q}_e$ = rate of heat addition per unit mass due to radiation, conduction, water phase changes respectively
g = acceleration of gravity
$\Phi = g\,z$
a = radius of the earth
R = gas constant for air

c_p = specific heat at constant pressure
Ω = angular velocity of the earth
$f = 2\Omega \sin\phi$ (the Coriolis parameter)
x = eastward component of the molecular and small scale eddy viscous force per unit mass
y = northward component of the molecular and small scale eddy viscous force per unit mass
$\overline{()}$ = time or ensemble average of () such that $\partial\overline{()}/\partial t = 0$
$()' = () - \overline{()}$.

If we now apply the zonal-averaging operator defined by,

$$()_0 \equiv \frac{1}{2\pi}\int_0^{2\pi} \overline{()}\, d\lambda$$

$$\equiv \overline{()} - ()_1$$

we obtain the following system governing the symmetric variables,

$$\omega_0 \frac{\partial u_0}{\partial p} - \left(f - \frac{\partial u_0 \cos\phi}{a\cos\phi\,\partial\phi}\right) v_0 - X_0 + A_0 = 0, \tag{9}$$

$$v_0 \frac{\partial v_0}{a\,\partial\phi} + \omega_0 \frac{\partial v_0}{\partial p} + \left(f + \frac{\tan\phi}{a} u_0\right) u_0 + \frac{\partial \Phi_0}{a\,\partial\phi} - Y_0 + B_0 = 0, \tag{10}$$

$$\frac{\partial \Phi_0}{\partial p} + \frac{R}{p} T_0 = 0, \tag{11}$$

$$\frac{\partial \omega_0}{\partial p} + \frac{\partial v_0 \cos\phi}{a\cos\phi\,\partial\phi} = 0, \tag{12}$$

$$v_0 \frac{\partial T_0}{a\,\partial\phi} + \left(\frac{\partial T_0}{\partial p} - \frac{R\,T_0}{p}\right)\omega_0 - Q_0 + C_0 = 0, \tag{13}$$

where A_0, B_0, and C_0 are quadratic functions of the asymmetric mean perturbations given by

$$A_0 = \left(u_1 \frac{\partial u_1}{a\cos\phi\,\partial\lambda} + v_1 \frac{\partial u_1}{a\,\partial\phi} + \omega_1 \frac{\partial u_1}{\partial p} - \frac{\tan\phi}{a} u_1 v_1\right)_0,$$

$$B_0 = \left(u_1 \frac{\partial v_1}{a\cos\phi\,\partial\lambda} + v_1 \frac{\partial v_1}{a\,\partial\phi} + \omega_1 \frac{\partial v_1}{\partial p} + \frac{\tan\phi}{a} u_1^2\right)_0,$$

$$C_0 = \left(u_1 \frac{\partial T_1}{a\cos\phi\,\partial\lambda} + v_1 \frac{\partial T_1}{a\,\partial\phi} + \omega_1 \frac{\partial T_1}{\partial p} - \frac{R}{c_p p}\omega_1 T_1\right)_0.$$

We shall assume that these quantities are small enough to be neglected in the first approximation, but that in the higher approximations they can be prescribed from the asymmetric solutions (which, in turn, are based on the specification of a previous symmetric solution). The hope is that the implied iterative process, starting

from a symmetric solution with $A_0 = B_0 = C_0 = 0$, will converge to the true solutions for both the symmetric and asymmetric components of the mean variables. In this discussion we shall be concerned mainly with the problem of achieving the first symmetric solution.

We now make the simplifications (to be verified *a posteriori*) of neglecting $\partial u_0 \cos\phi/a \cos\phi\, \partial\phi$ compared to f in (9) and $\tan\phi\, u_0/a$ compared to f in (10), and further we assume that the toroidal components v_0 and ω_0 are of a second order compared to the other mean zonal variables so that in the first approximation we can neglect terms involving their products, e.g. the first two terms of (10). We then have,

$$\omega_0 \frac{\partial u_0}{\partial p} - f v_0 - X_0 = 0\,, \tag{14}$$

$$f u_0 + \frac{\partial \Phi_0}{a\,\partial\phi} - Y_0 = 0\,, \tag{15}$$

$$\frac{\partial \Phi_0}{\partial p} + \frac{R}{p} T_0 = 0\,, \tag{16}$$

$$\frac{\partial v_0 \cos\phi}{a \cos\phi\, \partial\phi} + \frac{\partial \omega_0}{\partial p} = 0\,, \tag{17}$$

$$v_0 \frac{\partial T_0}{a\,\partial\phi} + \left(\frac{\partial T_0}{\partial p} - \frac{R\,T_0}{p}\right)\omega_0 - Q_0 = 0\,. \tag{18}$$

From (17) we can define a stream function ψ_0 for the mean toroidal motion (c. f., KUO 1956) by the relations,

$$v_0 = \frac{1}{\cos\phi}\frac{\partial \psi_0}{\partial p}\,, \qquad \omega_0 = -\frac{1}{a\cos\phi}\frac{\partial \psi_0}{\partial \phi}\,. \tag{19}$$

In order that the system (14) to (18) be mathematically closed we must introduce some postulates concerning the functional forms of Q_0, X_0 ($\equiv \bar{x} + M_x$) and Y_0 ($\equiv \bar{y} + M_y$). Although a part of Q_0 can probably by prescribed in terms of the spacial distribution of external solar heating, it would appear that a large part of Q_0 (as well as of M_x and M_y) should be related in some way to the mean zonal temperature field T_0. This is because of the relation of radiation and water vapor processes to the temperature and also because the large-scale eddy motions of the atmosphere are basically *convective*, owing their origin to temperature imbalances. The precise form that this relation may take for Q_0 is as yet unknown, though one may be tempted at the outset to look for an Austausch mechanism in regard to the sensible heat transport (e.g., DEFANT [4], ADEM, [1]); we know, however, that this cannot be valid universally since in the lower stratosphere fluxes of heat counter to the mean temperature gradient are observed (e.g., WHITE [17]).

It is even more difficult to use direct physical arguments to arrive at relationships of X_0 and Y_0 to T_0, but here again some speculations have been made (e.g., DAVIES and OAKES [3]). Certainly, the classical Austausch relationships between the momentum transport and shear of the mean zonal current, u_0, cannot be correct for the larger eddies (c.f., STARR [16]), though they probably have some validity for smaller eddy scales (c.f., KUO [7]).

At this time, let us be content to assume that by some combination of empiricism and theory we can postulate general relationship for geophysical fluid systems of the form $Q_\bullet(T_\bullet)$, $X_\bullet(T_\bullet, u_\bullet) = \bar{\chi}(u_\bullet) + M_x(T_\bullet)$ and $Y_\bullet(T_\bullet, v_\bullet) = \bar{y}(v_\bullet) + M_y(T_\bullet)$. With this understanding and using (19), we can proceed formally to reduce (14) to (18) to the following pair of equation which are no more than simplified forms of the energy and momentum equations for the zonal average mean state, respectively:

$$\frac{1}{a\cos\phi}\frac{\partial\psi_\bullet}{\partial p}\frac{\partial T_\bullet}{\partial\phi} - \left(\frac{\partial T_\bullet}{\partial p} - \frac{R\,T_\bullet}{p}\right)\frac{1}{a\cos\phi}\frac{\partial\psi_\bullet}{\partial\phi} - Q_\bullet(T_\bullet) = 0\,, \tag{20}$$

$$\frac{1}{f\,a\cos\phi}\frac{\partial\psi_\bullet}{\partial\phi}\left(\frac{\partial M_y(T_\bullet)}{\partial p} - \frac{R}{p\,a}\frac{\partial T_\bullet}{\partial\phi}\right) - \frac{f}{\cos\phi}\frac{\partial\psi_\bullet}{\partial p} - x(u_\bullet) - M_x(T_\bullet) = 0\,. \tag{21}$$

In principle, by the use of (15) and (16) we can eliminate any linear function $x(u_\bullet)$ from (21) leaving a closed system in the two dependent variables $\psi_\bullet$ and $T_\bullet$, and by specifying appropriate boundary conditions we would then be in a position to solve for the symmetric state. The question now arises concerning a strategy for actually achieving this solution.

3. A proposed method of attack

Let us begin by assuming that a crude first estimate of $T_\bullet$, which we will call $T_\bullet^{(1)}$, can be obtained by neglecting the effects of mean toroidal motions in the energy equation (20)—i.e.,

$$Q_\bullet(T_\bullet^{(1)}) = 0\,. \tag{22}$$

It is imagined that (22) expresses a rough balance between radiative heating, latent heat release and sensible heat transport by eddies, all suitably parameterized in terms of $T_\bullet$ where necessary. In this way the primary non-adiabatic processes can be introduced at the outset to give the most basic elements of the mean zonal temperature distribuation. An interesting attempt at solving this type of problem is given by ADEM [1, 2] whose results show that many of the grosser features of the $T_\bullet$ field can indeed be deduced. An important study regarding the purely radiative effects was made recently by MANABE and MÖLLER [8].

We must now recognize that the same large-scale eddies which transport heat (the effects of which are included in (22)) also have the property of transporting angular momentum in a rotating system. This implies the possibility that mean toroidal motions will be required to effect conservation of the total angular momentum. A first crude solution for these mean toroidal motions which we call $\psi_0^{(1)}$ can be obtained from (21) and appropriate boundary conditions by prescribing $T_\bullet = T_\bullet^{(1)}$. Aspects of this part of the problem have been treated with some success by ELIASSEN [6], KUO [7] and DAVIES and OAKES [3].

Next, by use of this first estimate, $\psi_0^{(1)}$, we are in a position to solve the *complete* energy equation (20) to obtain a presumably better estimate of $T_\bullet$ (i.e., $T_\bullet^{(2)}$). In turn $T_\bullet^{(2)}$ could be prescribed in (21) to solve for a next better estimate of $\psi_\bullet$ (i.e., $\psi_\bullet^{(2)}$), and so forth. We would proceed in the hope that this process of shuttling back and forth between the energy and momentum equations would converge to reasonably accurate values $\psi_\bullet^{(n)}$, $T_\bullet^{(n)}$ for some value of n.

As remarked earlier a similar iterative process involving the solutions of the asymmetric problem would be necessary to further refine the theory by taking into account A_0, B_0 and C_0. In addition, further extensions and refinements should be possible by solving the continuity equations for water vapor and trace substances such as ozone (c.f., e.g., PRABHAKARA [10]), which are of the form,

$$v_0 \frac{\partial \chi_0}{a \partial \phi} + \omega_0 \frac{\partial \chi_0}{\partial p} - H_0 + E_0 = 0 \tag{23}$$

where

χ = mass of water vapor or trace substance per unit mass of air

$$H = \mathcal{S}_\chi - \left(\frac{\partial u' \chi'}{a \cos\phi \, \partial \lambda} + \frac{\partial v' \chi' \cos\phi}{a \cos\phi \, \partial \phi} + \frac{\partial \omega' \chi'}{\partial p} \right)$$

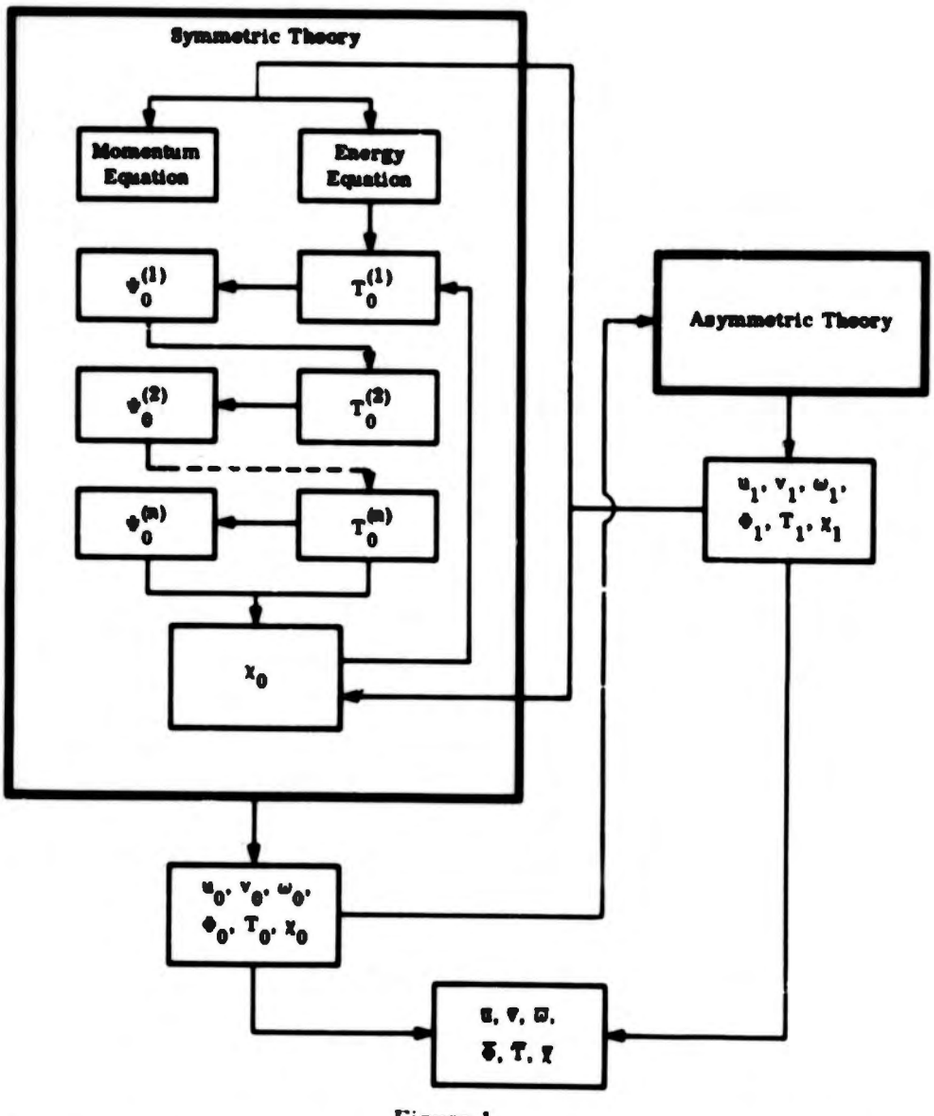

Figure 1
Schematic flow diagram for a diagnostic theory of the mean symmetric state of the atmosphere (see text)

S_χ = source function for χ ($= \bar{q}_e/L$ when χ is specific humidity, ε)

L = latent heat of condensation

and,

$$E = \left(u_1 \frac{\partial \chi_1}{a \cos\phi \, \partial\lambda} + v_1 \frac{\partial \chi_1}{a \, \partial\phi} + \omega_1 \frac{\partial \chi_1}{\partial p} \right).$$

Besides being of interest in their own right, the distributions of χ also play an important role in determining the heating distributions $\dot{q}_R$ and $\dot{q}_e$, and hence, another round of improvements in the theory could be realized in principle if we feed back the information derived from solutions of (23) to the original formulation (22).

The overall scheme proposed here is illustrated in Figure 1. My purpose has been to set this forth as one possible framework in which to work toward a closed theory of the mean state, and in which to show the connection of many diverse contributions, such as those referenced here.

Clearly, the success of the proposed approach will depend critically on our ability to discover valid and dynamically meaningful laws governing the relation between the mean variables and the mean eddy transports of heat, momentum, and trace substances in geophysical (i.e., rotating, thermally-driven) fluid systems. Our ultimate conclusion may, in fact, be that a steady theory founded on such laws is not satisfactory or satisfying or even obtainable (c.f., SALTZMAN [13], Introduction), in which case we must fall back on an initial value approach in which at least the *large*-scale eddy behavior is allowed to develop freely as a consequence of natural instabilities (e.g., PHILLIPS [9]). On the other hand, we must recognize that it would also be somewhat unsatisfying to accept an initial value theory if it turns out that the solution for the mean state is independent of the choice of initial conditions, and hence is determined only by the boundary conditions and system parameters.

Acknowledgement

This research has been sponsored by the U.S.Weather Bureau under Contract Number Cwb-10502.

REFERENCES

[1] J. ADEM, *On the theory of the general circulation of the atmosphere*, Tellus *14* (1962), 102.

[2] J. ADEM, *Preliminary computations on the maintenance and prediction of seasonal temperatures in the troposphere*, Mo. Weath. Rev. *91* (1963), 375.

[3] D. R. DAVIES and M. B. OAKES, *On the problem of formulating a realistic model of the general atmospheric circulation*, J. Geophys. Res. *67* (1962), 3121.

[4] F. DEFANT, *Das mittlere meridionale Temperaturprofil in der Troposphäre als Effekt von vertikalen und horizontalen Austauschvorgängen und Kondensationswärme*, Arch. Meteor., Geophys. und Bioklim. II A *2–3* (1950), 184.

[5] B. R. DÖÖS, *The influence of exchange of sensible heat with the earth's surface on the planetary flow*, Tellus *14* (1962), 133.

[6] A. ELIASSEN, *Slow thermally or frictionally controlled meridional circulations in a circular vortex*, Astrophysica Norwegica *5* (1951), 19.

[7] H.-L. Kuo, *Forced and free meridional circulations in the atmosphere*, J. Meteor. *13* (1956), 561.

[8] S. Manabe and F. Möller, *On the radiative equilibrium and heat balance of the atmosphere*, Mo. Weath. Rev. *89* (1961), 503.

[9] N. Phillips, *The general circulation of the atmosphere: a numerical experiment*, Quart J. Roy. Met. Soc. *82* (1956), 123.

[10] C. Prabhakara, *Effects of non-photochemical processes on the meridional distribution and total amount of ozone in the atmosphere*, Mo. Weath. Rev. *91* (1963), 411.

[11] B. Saltzman, *Perturbation equations for the time-average state of the atmosphere including the effects of transient disturbances*, Geofisica pura e applicata *48* (1961), 143.

[12] B. Saltzman, *Empirical forcing functions for the large-scale mean disturbances in the atmosphere*, Geofisica pura e applicata *52* (1962), 173.

[13] B. Saltzman, *A generalized solution for the large-scale, time-average, perturbations in the atmosphere*, J. Atmos. Sci. *20* (1963), 226.

[14] J. Smagorinsky, *The dynamical influence of large-scale heat sources and sinks on the quasi-stationary mean motions of the atmosphere*, Quart. J. Roy. Met. Soc. 79 (1953), 342.

[15] Staff Members, Academia Sinica, *On the general circulation over eastern Asia* (III), Tellus *10* (1958), 299.

[16] V. P. Starr, *Note concerning the nature of the large-scale eddies in the atmosphere*, Tellus *5* (1953), 494.

[17] R. M. White, *The counter-gradient flux of sensible heat in the lower stratosphere*, Tellus *6* (1954), 177.

(Received 30th November 1963)

PAPER D

FURTHER STATISTICS ON THE EXCHANGE OF KINETIC ENERGY BETWEEN HARMONIC COMPONENTS OF THE ATMOSPHERIC FLOW

Barry Saltzman

Sidney Teweles

ABSTRACT

The transfers of kinetic energy between harmonic components of the 500mb geostrophic flow over the Northern Hemisphere have been measured for an ensemble of daily maps covering a nine year period, based on a truncation at zonal wave number, n = 15. The results show 1) that, in the mean, all waves (n = 1 - 15) transfer their energy to the zonally-averaged motion (n = 0) and, of more physical significance, the aggregate of all waves in the group n = 2 - 15 transfer energy to support the asymmetric polar vortex comprised of wave numbers zero and one, and 2) that, among the waves themselves, waves of n = 2 and 5 - 10 are sources of kinetic energy and all the rest are sinks. The energy source at n = 2 seems to be a significant new result indicating a strong forced conversion of energy on the scale of the major continents and oceans. Seasonal variations are discussed.

Daily measurements of the rates of transfer of kinetic energy to the zonal current from the eddies of different wave number, n (denoted by M) [Saltzman and Fleisher, 1960a], and between the different eddy scales themselves (denoted by L) [Saltzman and Fleisher, 1960b], have now been extended to cover a nine-year period within the years 1955 to 1964.

In view of the longer period of record, we feel enough confidence has been added to the averages to present a resolution into three-month and half- year "seasonal" averages in addition to the annual average, and also into individual wave numbers instead of the groups of wave numbers given previously. The measurements are still only for the 15° to 80°N zonal band at the 500-mb level and for $n = 1 - 15$. They are based on the same assumptions used in the previous studies (e.g., only the horizontal, geostrophic, components of the motion are considered).

The new nine-year averages are given in Table 1 along with probable errors (computed using half the total number of cases) for the ensemble of daily values over the entire year, the warmer and colder half years, and the three-month seasons. The six-month means are also shown graphically in Figure 1, and the annual budget is represented schematically in Figure 2.

From the M values, it can be seen that all waves tend to feed their energy into the zonal current, with maxima at $n = 2$ and 7 in the annual, colder six-month, and winter means. A minimum in M occurs at $n = 4$, as it did in the previous study covering the year 1951. For all wave numbers, the mean values of M appear to be significantly different from zero. The total gain of kinetic energy by the zonal current, measured by $\sum_{n=1}^{15} M(n)$, is given in the last column of Table 1.

Table 1

Mean values of N and L and their probable errors ε,

in units of 10^{-3} ergs/cm^2 sec mb

	n	0	1	2	3	4	5	6	7	8	9	10	11	12	13	14	15	$\sum_{n=1}^{15}$
Year	N		5	26	21	11	14	21	22	15	12	8	5	4	2	2	1	169
	ε (N)$\pm$		3	5	5	4	4	4	3	2	2	1	1	1	1	0	0	12
	L		87	-53	29	12	- 3	-37	-39	-35	-14	-11	4	5	12	17	26	0
	ε (L)$\pm$		21	24	23	23	24	22	23	20	17	14	11	9	8	7	6	---
	Gain	169	82	-79	8	1	-17	-58	-61	-50	-26	-19	- 1	1	10	15	25	
Colder Months (Oct. - Mar.)	N		12	42	27	12	19	23	31	18	14	8	6	4	3	2	1	222
	ε (N)$\pm$		5	9	10	8	7	6	5	4	3	2	2	1	1	1	1	22
	L		148	-107	47	25	- 4	-38	-57	-55	-21	-20	1	4	12	27	38	0
	ε (L)$\pm$		38	43	43	42	44	39	40	36	30	25	20	17	15	12	11	---
	Gain	222	136	-149	20	13	-23	-61	-88	-73	-35	-28	- 5	0	9	25	37	
Warmer Months (Apr. - Sept.)	N		- 2	10	14	11	10	20	14	11	10	7	4	3	2	1	1	116
	ε (N)$\pm$		2	4	4	4	3	3	3	2	2	1	1	1	1	0	0	11
	L		26	1	13	- 1	- 2	-35	-22	-15	- 8	- 3	7	5	12	8	14	0
	ε (L)$\pm$		17	19	19	19	20	20	20	18	16	13	10	8	7	6	5	---
	Gain	116	28	- 9	- 1	-12	-12	-55	-36	-26	-18	-10	3	2	10	7	13	

Table 1 (Continued)

	n	0	1	2	3	4	5	6	7	8	9	10	11	12	13	14	15	$\sum_{n=1}^{15}$
Winter (Dec. - Feb.)	M		15	54	25	11	19	22	28	17	11	7	5	4	2	1	1	222
	ε (M)$\pm$		7	15	17	12	11	9	7	6	4	4	3	2	1	1	1	35
	L		210	-154	61	22	-18	-16	-73	-53	-15	-35	-10	1	9	26	45	0
	ε(L)$\pm$		63	71	68	69	70	61	65	59	49	40	32	27	24	19	18	---
	Gain	222	195	-208	36	11	-37	-38	-101	-70	-26	-42	-15	- 3	7	25	44	
Spring (Mar. - May)	M		2	20	17	21	12	22	27	12	11	8	5	4	2	1	1	165
	ε(M)$\pm$		6	9	9	8	7	7	6	5	3	3	2	1	1	1	1	22
	L		73	-27	14	16	28	-67	-28	-53	-24	- 5	9	9	10	13	32	0
	ε(L)$\pm$		36	45	45	42	46	46	46	41	33	32	23	20	16	15	12	32
	Gain	165	71	-47	- 3	- 5	16	-89	-55	-65	-35	-13	4	5	8	12	31	
Summer (Jun. - Aug.)	M		- 6	9	7	3	4	13	8	10	10	6	3	3	2	1	1	74
	ε(M)$\pm$		2	4	4	4	4	4	3	2	2	1	1	1	1	1	0	11
	L		15	4	9	- 3	- 1	-12	-23	- 8	- 7	- 1	6	3	7	6	5	0
	ε(L)$\pm$		17	17	16	18	18	19	19	18	15	12	10	8	7	6	5	---
	Gain	74	21	- 5	2	- 6	- 5	-25	-31	-18	-17	- 7	3	0	5	5	4	
Autumn (Sep. - Nov.)	M		8	23	35	10	22	28	27	20	16	9	7	4	4	3	1	217
	ε(M)$\pm$		4	8	9	8	8	8	6	5	4	3	2	2	1	1	1	23
	L		54	-37	36	13	-22	-51	-32	-26	-12	- 3	10	5	20	24	21	0
	ε(L)$\pm$		37	39	43	44	43	40	40	33	28	23	20	16	15	11	10	---
	Gain	217	46	-60	1	3	-44	-79	-59	-46	-28	-12	3	1	16	21	20	

The redistribution of kinetic energy among the individual waves, measured by L, shows, in general, a net gain by the long waves $n = 1, 3$, and 4, and the short waves $n = 11 - 15$. The large loss from $n = 2$ appears to be an important new finding that suggests a large forced conversion of potential energy on this scale associated with the continent-ocean structure. The loss from the cyclone band $n = 5 - 10$ is probably compensated by the normal free baroclinic development processes within the troposphere.

From a synoptic viewpoint, we note that the so-called "polar vortex" is no more than the sum of an axially-symmetric component of motion corresponding to $n = 0$ and an axially-asymmetric component corresponding to $n = 1$. Thus, the results here show that the whole polar vortex tends to derive an important part of its energy from the higher wave numbers ($n \geq 2$) by the non-linear transfer processes measured by $\sum_{n=2}^{15} M(n)$ and $L(1)$.

As should be expected from these geostrophic calculations, the results over the spectral region studied are in accord with the theorems on energy transfer in two-dimensional, non-divergent flows presented by Fjortoft [1953]: e.g., the loss of energy from intermediate scales is accompanied by a gain of energy by larger scales as well as by smaller scales. The consistent gain of energy by the higher wave numbers, $n = 11 - 15$, gives the appearance of a Kolmogoroff-type cascade constrained by the truncation at $n = 15$. In this connection, it is important to recognize that the transfer spectrum is a function of the particular truncation point chosen. For example, if we could extend the calculation to include infinitely high wave numbers (and, even more so, if we included <u>vertical</u> transfer processes) we would thereby encompass dissipative energy transfers associated with eddy viscosity, and, as a result, this would markedly affect the entire transfer spectrum. In

our case, we have arbitrarily truncated at $n = 15$ in the belief that this represents a rough limit of the scales describable on hemispheric synoptic charts. Accordingly, we consider the aggregate of all scales $n \geq 16$ as a sort of viscous sink for the surplus energies acquired in the long-time average by eddies in the group $n = 1 - 15$, through the processes measured by L and M and by conversion from potential energy. In truth, however, the region $n \geq 16$ is itself rich in energetical detail involving all sub-synoptic phenomena, and, in fact, certain portions of this region may even be significant sources of kinetic energy for the synoptic motions (e.g., organized cumulus convective motions).

Inspection of the error estimates ($\epsilon = 2\sigma/\sqrt{N/2}$ where σ is the standard deviation and N is the number of days) shows much more variability in L than in M. In fact, for most wave numbers, L varies on a daily or longer period basis between positive and negative values so that, from time to time, the dominant kinetic energy source appears to shift from one wave number to another.

The month-to-month variation in kinetic energy transfer by those waves demonstrating a large and distinct annual cycle is shown in Figure 3. It is interesting to note the degree to which wave numbers 1 and 2 appear to complement each other. The transfer into wave number 1 and the transfer out of wave number 2 both have large values in the colder months and near zero values in the warmer months, wave number 2 in particular having little net transport between April and October. Although there is a similar annual cycle in the transfer into the zonal flow, $\sum_{n=1}^{15} M(n)$, and the transfer out of the group of wave numbers 6-9, the rate of transfer remains substantial even in summer when a minimum rate of transfer appears in July. A unique

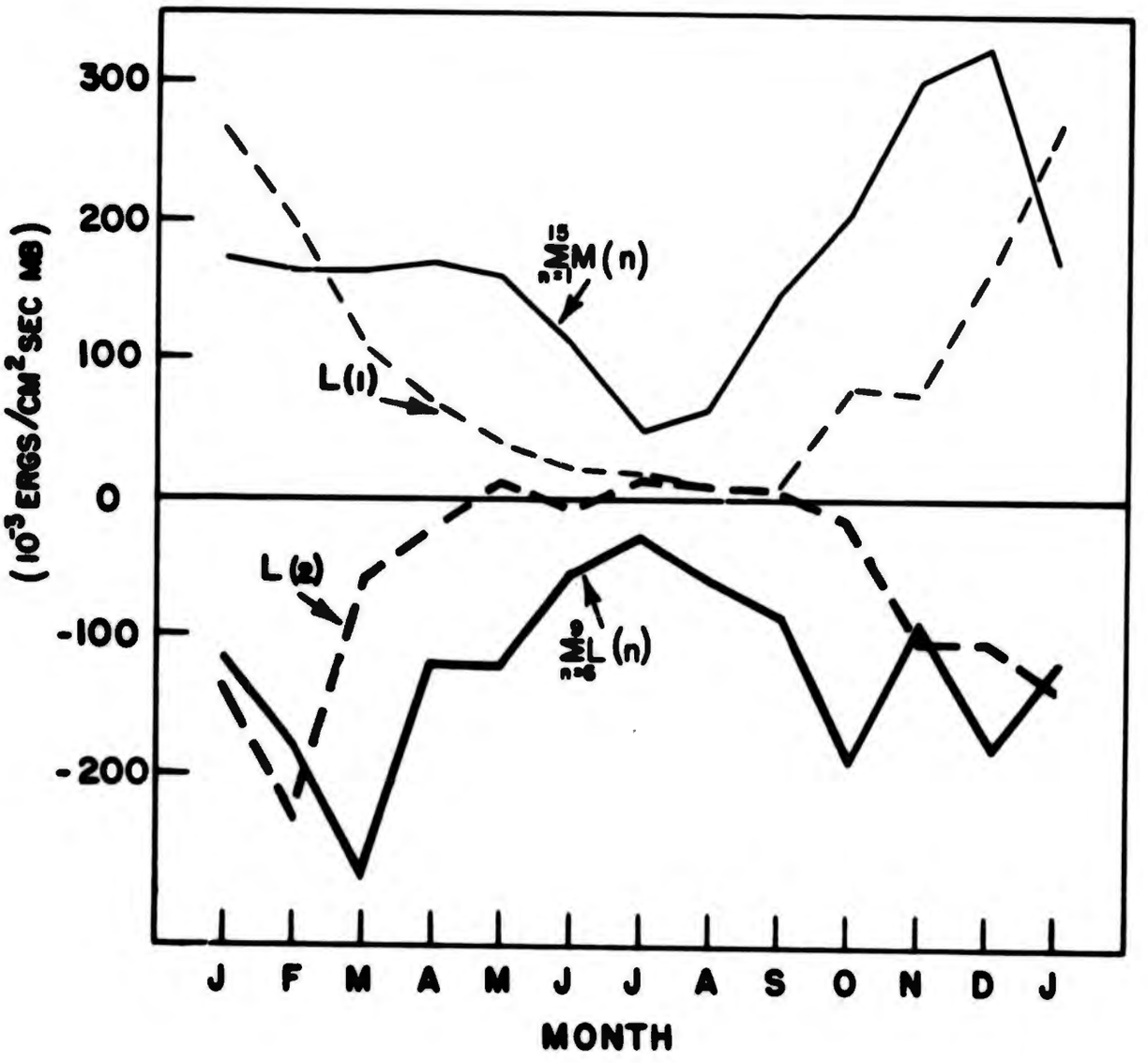

Fig. 3. Monthly means of $\sum_{n=1}^{15} M(n)$, L(1), L(2), and $\sum_{n=6}^{9} L(n)$.

characteristic of the individual month of February, included in the winter statistics, is the tendency for a large positive value of L in wave number four.

Acknowledgements

We are grateful to Professor Aaron Fleisher of MIT for his original work in setting up the numerical formulation and machine program for these calculations, and also to the National Aeronautics and Space Administration for its support in providing computer facilities. Support for this work has been provided by the U. S. Weather Bureau (under Contract No. Cwb-10763), the Atomic Energy Commission, and the U. S. Navy Bureau of Naval Weapons.

References

Fjortoft, R.; On the changes in the spectral distribution of kinetic energy for the two-dimensional, non-divergent flow. Tellus, 5, 225-230, 1953.

Saltzman, B. and A. Fleisher; Spectrum of kinetic energy transfer due to large-scale horizontal Reynolds stresses. Tellus, 12, 110-111, 1960a.

Saltzman, B. and A. Fleisher; The exchange of kinetic energy between larger scales of atmospheric motion. Tellus, 12, 374-377, 1960b.

APPENDIX

JOURNAL OF GEOPHYSICAL RESEARCH VOL. 69, NO. 8 APRIL 15, 1964

Harmonic Analysis of the Topography along Parallels of the Earth

JOSÉ P. PEIXOTO

University of Lisbon and the National Meteorological Service of Portugal, Lisbon

BARRY SALTZMAN

The Travelers Research Center, Hartford, Connecticut

SIDNEY TEWELES

U. S. Weather Bureau, Washington, D. C.

Abstract. The topography along latitude circles for each 5° between the poles has been subjected to harmonic analysis. The amplitude and phase of the first 15 harmonics are presented in tabular form. The first four harmonics are represented on Mercator charts.

Introduction. In previous papers the writers [*Saltzman and Peixoto*, 1957; *Peixoto and Saltzman*, 1958; *Peixoto*, 1963; *Teweles*, 1963] among others [e.g., *Van Mieghem et al.*, 1960] have discussed aspects of the spectral properties of mean fields in the atmosphere. These properties are related to the inhomogeneity of the earth's surface manifested by differences in orography and heating. In order to investigate possible relations of these fields to the orographic influences and in view of the importance that the spectral analysis of the terrestrial topography can assume in many branches of geophysics, it was decided to perform a harmonic analysis of the mean topography along parallels of the entire earth. The results are presented here in tabular form for harmonics up to wave number 15 and in mapped form for the first four wave numbers. Similar computations for the northern hemisphere only have been reported by *Barrett* [1961]. With geodetic rather than meteorological purposes in mind, spherical harmonic analysis of the topography of the lithosphere has been carried to the 16th degree by *Prey* [1922] and, in more recent unpublished analyses, to the 31st degree by G. J. Bruins and U. A. Uotila (information communicated by W. M. Kaula).

TABLE 1. Amplitude Spectrums of the Mean Topography for the Northern Hemisphere, in Meters

	φ, deg N																	
n	0	5	10	15	20	25	30	35	40	45	50	55	60	65	70	75	80	85
1	138	193	252	204	200	316	866	1027	477	269	222	168	249	164	238	449	422	16
2	45	44	125	113	147	222	782	1090	661	391	384	216	112	148	305	425	345	16
3	173	177	179	118	114	204	552	592	193	355	274	224	214	76	305	392	259	16
4	255	257	169	96	151	233	586	692	253	310	167	71	210	272	281	321	176	16
5	82	67	41	83	103	204	372	376	291	286	220	102	177	136	255	314	117	15
6	80	113	112	88	90	57	285	298	124	134	40	166	66	94	270	239	90	15
7	125	122	109	22	113	248	423	347	243	158	125	49	107	139	237	209	104	15
8	88	66	67	61	30	69	292	199	166	90	96	76	73	110	181	181	109	14
9	88	68	107	75	58	129	303	231	156	191	93	85	53	92	144	92	71	14
10	82	95	91	29	71	119	157	80	254	72	64	76	29	119	217	81	65	14
11	40	47	26	68	60	95	270	38	80	87	43	77	8	78	115	19	58	13
12	71	52	69	18	128	134	123	94	198	114	57	45	73	153	106	22	37	12
13	99	104	88	88	94	69	160	130	123	42	31	37	116	103	91	27	13	12
14	39	32	32	57	105	72	43	138	214	32	85	42	17	86	47	27	19	11
15	45	35	11	49	35	49	140	57	115	51	38	58	15	50	20	23	28	11

TABLE 2. Phase Spectrums of the Mean Topography for the Northern Hemisphere, in Degrees Measured Eastward from the Greenwich Meridian

	ϕ, deg N																	
n	0	5	10	15	20	25	30	35	40	45	50	55	60	65	70	75	80	85
1	39	12	23	37	39	66	79	80	71	78	104	142	190	191	309	320	310	289
2	92	67	34	45	58	80	84	81	76	84	90	94	39	154	141	136	128	109
3	26	34	30	26	14	116	92	88	114	118	116	120	117	102	83	80	68	49
4	26	24	26	22	10	8	88	83	84	3	5	34	44	45	47	50	38	19
5	36	22	38	38	32	32	21	17	29	24	26	33	10	16	32	32	24	1
6	40	44	43	36	29	42	32	24	21	16	7	56	43	25	24	21	19	49
7	27	33	85	40	49	0	44	41	39	41	39	37	10	8	13	11	14	32
8	28	25	36	39	36	12	1	42	30	13	16	20	5	3	7	6	8	19
9	36	4	0	34	17	19	12	8	1	9	9	1	20	24	4	0	1	9
10	33	2	2	5	4	1	20	0	35	35	26	19	8	28	32	30	29	1
11	30	32	4	9	3	2	26	21	11	14	17	31	31	18	26	27	22	27
12	6	11	13	17	17	13	30	13	12	11	1	26	17	16	23	4	15	19
13	6	11	14	20	14	11	5	26	20	24	19	16	8	10	16	26	11	12
14	6	13	17	21	25	25	11	24	21	18	11	8	15	9	13	22	20	6
15	12	18	18	3	23	13	13	6	22	5	20	18	9	4	6	19	16	1

Mathematical expressions. The topographic profile of the earth along a given latitude ϕ may be expressed in terms of a one-dimensional (i.e., zonal) Fourier expansion of the form

$$h(\lambda, \phi) = \langle h(\phi) \rangle + \sum_{n=1}^{\infty} |H(n, \phi)| \cos n[\lambda - \epsilon(n, \phi)]$$

where $h(\lambda, \phi)$ = height of the surface above sea level, λ = longitude, $H(n, \phi)$ = amplitude of the harmonic component of wave n, $\epsilon(n, \phi)$ = phase of the harmonic component of wave n, n = wave number, and $\langle h(\phi) \rangle$ = average value of $h(\lambda, \phi)$ around the latitude circle ϕ = constant.

$$\langle h(\phi) \rangle = \frac{1}{2} |H(0, \phi)| = \frac{1}{2\pi} \oint h(\lambda, \phi)\, d\lambda$$

For computational purposes

$$\langle h(\phi) \rangle = \frac{1}{M} \sum_{i=1}^{M} h(\lambda_i, \phi)$$

where M = number of equally spaced data points on a latitude circle.

TABLE 3. Amplitude Spectrums of the Mean Topography for the Southern Hemisphere, in Meters

	ϕ, deg S																
n	5	10	15	20	25	30	35	40	45	50	55	60	65	70	75	80	85
1	129	159	276	229	125	102	44	47	47	41	26	9	234	1287	1540	1568	677
2	60	26	58	102	126	56	78	57	50	43	24	8	240	478	553	606	407
3	245	212	288	249	214	190	106	85	88	44	22	8	91	279	955	664	146
4	204	245	336	322	305	230	86	44	46	39	20	6	140	217	294	136	13
5	39	112	180	191	142	119	102	53	48	43	19	6	51	116	359	221	26
6	161	101	19	63	58	23	31	64	82	38	19	4	92	180	230	121	36
7	130	138	183	136	177	163	83	62	48	38	21	3	67	180	50	9	26
8	41	118	152	146	181	187	103	35	41	38	22	3	45	130	113	43	34
9	112	89	88	142	124	76	59	63	78	34	23	3	124	178	107	67	19
10	166	90	84	22	27	38	68	74	50	36	24	4	53	93	23	35	10
11	20	148	157	107	127	162	60	17	33	31	23	5	38	54	71	24	7
12	4	20	171	176	136	144	98	71	77	33	21	5	56	89	21	29	9
13	110	81	122	145	103	43	64	69	47	31	18	5	52	64	37	37	7
14	28	51	108	82	33	59	16	14	29	27	16	4	33	58	14	40	5
15	22	44	133	148	132	162	84	65	73	32	14	3	32	31	37	32	3

TABLE 4. Phase Spectrums of the Mean Topography for the Southern Hemisphere, in Degrees Measured Eastward from the Greenwich Meridian

	φ, deg S																
n	5	10	15	20	25	30	35	40	45	50	55	60	65	70	75	80	85
1	62	2	336	338	351	357	295	252	259	289	294	315	102	84	56	54	55
2	146	155	126	132	128	134	125	127	123	107	113	135	108	99	70	77	96
3	27	33	42	43	35	33	39	49	48	49	52	74	110	22	18	16	39
4	33	28	26	29	29	27	25	15	12	17	21	44	26	30	14	85	89
5	25	23	15	15	11	13	6	5	5	72	2	25	45	68	1	1	60
6	29	31	46	4	5	27	47	51	49	48	49	11	53	49	45	43	16
7	31	25	30	33	31	30	34	32	28	30	31	51	44	48	41	51	36
8	16	23	22	25	25	24	20	20	21	18	18	36	6	9	9	13	5
9	30	34	13	16	17	20	16	13	9	7	9	24	14	11	39	38	23
10	32	31	33	5	8	33	3	1	34	35	1	16	18	13	13	25	33
11	19	23	25	27	28	26	25	27	29	26	28	10	29	28	27	23	11
12	23	19	19	21	23	24	23	22	19	17	20	6	24	23	14	13	22
13	5	7	13	16	17	16	14	11	9	10	13	2	23	19	23	2	6
14	7	1	6	10	7	3	10	8	8	4	7	24	7	10	5	17	17
15	13	22	1	3	3	2	2	3	1	23	2	20	7	7	16	5	11

The amplitude and phase spectrums were evaluated from the expressions

$$|H(n, \phi)| = [\mathfrak{H}_1^2(n, \phi) + \mathfrak{H}_2^2(n, \phi)]^{1/2}$$

and

$$\epsilon(n, \phi) = \frac{1}{n} \arctan \frac{\mathfrak{H}_2(n, \phi)}{\mathfrak{H}_1(n, \phi)}$$

where $\mathfrak{H}_1(n, \phi)$ and $\mathfrak{H}_2(n, \phi)$ are the real and imaginary parts of the complex Fourier transform of $h(\lambda, \phi)$; i.e.,

$$H(n, \phi) = \frac{1}{\pi} \int_0^{2\pi} h(\lambda, \phi) e^{-in\lambda} \, d\lambda$$

$$= \frac{1}{\pi} \int_0^{2\pi} h(\lambda, \phi) \cos n\lambda \, d\lambda - \frac{i}{\pi} \int_0^{2\pi} h(\lambda, \phi) \sin n\lambda \, d\lambda$$

$$= \mathfrak{H}_1(n, \phi) - i\mathfrak{H}_2(n, \phi)$$

For computational purposes

$$\mathfrak{H}_1(n, \phi) = \frac{2}{M} \sum_{j=1}^{M} h(\lambda_j, \phi) \cos n\lambda_j$$

$$\mathfrak{H}_2(n, \phi) = \frac{2}{M} \sum_{j=1}^{M} h(\lambda_j, \phi) \sin n\lambda_j$$

For all latitudes except those crossing Antarctica, the harmonic analysis is based on topographic heights presented by *Berkofsky and Bertoni* [1955]. The heights presented by them are mean values determined for the 5° × 5° area centered on each 5° latitude-longitude intersection. Values for the topography of Antarctica have been obtained from manuscript maps based on the latest determinations available in 1963. The distributions of the amplitude $H(n, \phi)$ and phase $\epsilon(n, \phi)$ spectrums were computed up to wave number 15, for every 5° latitude circle based on data spaced at 5° inter-

TABLE 5. Zonal Average Topographic Height

Northern Hemisphere		Southern Hemisphere	
φ, deg N	⟨h⟩, m	φ, deg S	⟨h⟩, m
0	169		
5	189	5	195
10	189	10	196
15	158	15	241
20	222	20	234
25	298	25	204
30	586	30	153
35	761	35	76
40	592	40	48
45	438	45	46
50	367	50	23
55	278	55	13
60	314	60	5
65	375	65	172
70	308	70	1071
75	266	75	2118
80	235	80	2431
85	8	85	2744

Fig. 1. Pictorial representation of the first four harmonics of the topography along parallels of the earth (contours at 200-meter intervals are given by solid lines, the 100-meter contour by a dashed line).

vals around each latitude circle (i.e., $M = 72$). These spectrums are discrete line spectrums and hence have meaning only for the discrete integer values of wave number (Tables 1 to 4).

The phase angle $\epsilon(n, \phi)$ indicates the longitude where the first maximum of h, corresponding to n, is located. Additional maximums are located at $\epsilon + 2\pi k/n$ for each integral value of k up to $n - 1$. The reader should note that the harmonic analysis along a latitude having a nonzero height above sea level ($= h$) at only one of the 72 points would result in an equal amplitude ($= 2h/72$) for all harmonics, 1 through 35. For this case, the average height for the latitude would be $h/72$. This situation is approximated at latitudes 85°N, 50°S, 55°S, and 60°S, where land occurs only in one part of the latitude circle.

The zonal average height of the topography above sea level, denoted by $\langle h(\phi) \rangle$, is given in Table 5. There is a marked contrast between the average heights for the primarily oceanic latitudes 50° to 60°S and those for latitudes 75° to 85°S which are dominated by the antarctic ice cap.

The dominant role of the major mountain barriers (Himalayas, Rockies, Alps, Andes) is shown very clearly in Mercator charts of the first four topographic harmonics (Figure 1). For the northern hemisphere, these charts are in essential agreement with those produced by *Van Mieghem et al.* [1960] from spectral values computed by *Barrett* [1961]. The values which he reports were derived for $M = 36$ by means of an analog harmonic analyzer.

Acknowledgment. This work was originally performed at the Massachusetts Institute of Technology in 1956 with the Whirlwind computer; it was subsequently extended in 1963 with an IBM 7094 computer at the Goddard Space Flight Center.

References

Barrett, E. W., Some applications of harmonic analysis to the study of the general circulation, 3, A theory of three-dimensional atmospheric waves, with special reference to topographically-induced perturbations, *Beitr. Phys. Atmosphäre, 34*, 167–197, 1961.

Berkofsky, L., and E. Bertoni, Mean topographic charts for the entire earth, *Bull. Am. Meteorol. Soc., 36*, 350–353, 1955.

Peixoto, J. P., Aplicação da análise espectral ao estudo da circulação planetária da atmosfera, Prof. dissertation, *Rev. Fac. Cien. Univ. Lisboa, 2a Ser., B, 9*, 1963.

Peixoto, J. P., and B. Saltzman, Harmonic analysis of the mean northern hemisphere water vapor distribution for the year 1950, *Geofis. Pura Appl., 41*, 183–188, 1958.

Prey, A., Darstellung der Höhen- und Tiefenverhältnisse der Erde durch eine Entwicklung nach Kugelfunktionen bis zur 16. Ordnung. *Abhandl. König. Gesel. Wiss. Goettingen, Math-Physik Kl., neue Folge, 11*, 1, 1922.

Saltzman, B., and J. Peixoto, Harmonic analysis of the mean northern hemisphere wind field for the year 1950, *Quart. J. Roy. Meteorol. Soc., 83*, 360–364, 1957.

Teweles, S., Spectral aspects of the stratospheric circulation during the IGY, *Planetary Circulations Proj., Rept. 8*, 191 pp., Department of Meteorology, Massachusetts Institute of Technology, Cambridge, 1963.

Van Mieghem, J., P. Defrise, and J. Van Isacker, Harmonic analysis of the normal monthly northern-hemisphere geostrophic flow at 500 mb, *Mededel. Koninkl. Vlaam. Acad. Belg., Kl. Wetenschap., 22*(4), 1–38, 1960.

(Manuscript received November 20, 1963; revised January 27, 1964.)